



Institutt for energi-
og prosessteknikk

Bacheloroppgave

| | |
|-------------------------------------------------------------------------------------------------------------------------------------------------------------------------------------------------------------------------------------------------------------|------------------------------------------------------------------------------------------------------------------------------|
| Oppgavens tittel: Litium-ion-batterier: De lovende batteriteknologiene for energilagring og transport Project title (ENG): Lithium-ion Batteries: The Promising Battery Technologies for Energy Storage and Transport | Gitt dato: 16.10.2023 Innleveringsdato: 22.05.2024 Antall sider rapport / sider vedlagt: 136/1 |
| Gruppedeltakere: Amin Mohamed Tina Høyvik Babiker Maja Farestveit Magnus Vollan Reknes | Veileder: Steven Tyler Boles Prosjektnummer: BIFOREN 24-10 |
| Oppdragsgiver: Beyonder | Kontaktperson hos oppdragsgiver: Julie Pires |

Fritt tilgjengelig:

Tilgjengelig etter avtale med oppdragsgiver:

Rapporten frigitt etter:

Gruppedeltagere signaturer:

Amin Babiker
Tina Høyvik
Maja Farestveit Reknes
Magnus Vollan



Norwegian University of
Science and Technology

FACULTY OF ENGINEERING
DEPARTMENT OF ENERGY AND PROCESS ENGINEERING
STUDY FIELD RENEWABLE ENERGY

FENT2900 - BACHELOR'S THESIS IN RENEWABLE ENERGY

Lithium-ion Batteries: The Promising Battery Technologies for Energy Storage and Transport

Amin Mohamed Babiker

Tina Høyvik

Maja Farestveit Reknes

Magnus Vollan

Trondheim

Spring 2024

Preface

This bachelor's thesis represents the collaborative efforts of four engineering students pursuing a bachelor's degree in Renewable Energy at NTNU in Trondheim. The group consists of three members who specialize in energy storage and one member who specializes in water and wind energy. The project is conducted under the subject code FENT2900 and is equivalent to 20 course credits.

This thesis aims to highlight the benefits and feasibility of promising lithium-ion battery technologies and provide a recommendation to *Beyond* regarding which compositions and technologies are viable to derive further research. In order to limit the task, the group has chosen to focus on energy storage and transport, which are some of *Beyond's* main target market sectors.

We would first like to thank *Beyond* for the opportunity to collaborate and extend our utmost thanks to our external supervisor, Julie Pires, for excellent feedback and availability during the span of our thesis. We would also like to thank our internal supervisor, Steven Tyler Boles, for much helpful guidance and support. Furthermore, we extend our gratitude towards Jacob Joseph Lamb, Odne Stokke Burheim, Ann Mari Svensson, and Ingrid Gullikstad Hallsteinsen from NTNU, as well as Frode Håskjold Fagerli from SINTEF for valuable insight into this field of study.

Lastly, we want to thank each other for the great teamwork and tremendous effort throughout the course of the thesis.

Abstract

This thesis aims to achieve two primary objectives: first, to identify the optimal battery chemistry for energy storage and transportation applications, and second, to evaluate the feasibility of implementing solid and semi-solid state technologies in LIB. The battery technology company *Beyond* asked for an analysis that would look at the current market and evaluate the technology in 5-10 years. As this is a very short time in the battery world, one cannot expect much change to the maturity of the technology within this time. Therefore, this report also makes an estimate of which technologies may be appropriate in 20-30 years.

The rising demand for LIB technology is driven by the growing urgency for clean energy and a green transition. Therefore, enhancing the existing battery technologies is crucial to meet the growing demand within the battery industry. By providing a technical market analysis of existing cathodes, anodes, and electrolytes in terms of cost, sustainability, capacity, and safety, the thesis can identify key areas for improvement and innovation. This is primarily intended to serve as a tool for advising *Beyond*. It involves evaluating both the prospects for near-term utilization and the need for further research, all based on the concept of technology readiness levels for the battery components. Further, *Beyond* is exploring the option of enhancing the standard of conventional LIBs. A common LIB includes liquid electrolytes and solid electrodes, while SSBs consist of an SSE and SSLIBS of a semi-solid electrolyte. In general, higher distributions of solids led to increased safety, mechanical strength, and higher costs, whereas a higher distribution of liquids led to reduced costs and higher ionic conductivities.

The theoretical framework in this thesis provides an in-depth exploration of the general thermodynamics e.g. internal energy and entropy. In addition to general electrochemistry, such as energy, power, and redox reactions, before delving into the fundamental concepts of LIBs. Furthermore, to compare different characteristics of battery technologies, the general battery terminology is presented, to then analyze the various compositions of cathode and anode materials. Moving forward, different electrolytes in LIBs are introduced, liquid, solid state, and semi solid state. Lastly, an analysis is done on the cost of raw, cathode and anode materials. Additionally, the raw materials' carbon footprint and different cathode compositions' recycling ability are addressed.

Methods used during the writing of the theory are then presented, followed by a discussion. This section of the thesis begins by comparing the various cathode and anode materials, looking at properties of cell voltage, specific energy, energy density, thermal stability, and cost, to then

present a summarizing overall performance. Lastly, the potential of SIBs is discussed. Further, the different electrolytes are evaluated, followed by a discussion of manufacturing and sustainability. To give an overall review for *Beyonder*, different recommendations were made. The thesis focused on the application areas for *Beyonder* deemed to be most critical in today's society, energy storage, and transportation. In the recommendations, compatible electrolytes, anodes, and cathodes were matched to their most relevant applications for utilization with regard to *Beyonder*' prospects and TRL.

The conclusion summarises the recommendation to dive into the different battery components in prospects for 5-10 year utilization and the need for further research.

Sammendrag

Denne bacheloroppgaven har to formål. Det første er å identifisere den optimale batterikjemien for energilagrings- og transportapplikasjoner. Det andre er å vurdere muligheten for å implementere solid- og semi-solid teknologier i LIB. Batteri teknologiselskapet *Beyonder* ba om en analyse som skulle se på dagens marked og vurdere teknologien om 5-10 år. Ettersom dette er en svært kort tidsperiode i batteriverdenen, kan man ikke forvente store endringer i teknologiens modenhet i løpet av denne tiden. Derfor gir denne rapporten også et estimat av hvilke teknologier som kan være aktuelle om 20-30 år.

Den økende etterspørselen etter LIB-teknologi er drevet av et voksende behov for ren energi og et grønt skifte. Derfor er det avgjørende å forbedre eksisterende batteriteknologi, i møte med den økende etterspørselen i batteri industrien. Ved å gi en teknisk markedsanalyse av eksisterende katoder, anoder og elektrolytter med hensyn til kostnader, bærekraft, kapasitet og sikkerhet, kan oppgaven identifisere viktige områder for forbedring og innovasjon. Dette er først og fremst ment som et verktøy for å gi råd «Beyonder». Dette innebærer å evaluere både utsiktene for bruk på kort sikt og behovet for videre forskning, alt basert på konseptet med TRL for batterikomponentene. I tillegg undersøker *Beyonder* muligheten for å forbedre standarden på konvensjonelle LIB-batterier. En vanlig LIB består av en LE og faste elektroder, mens SSLIBs eller SSBs består av en semi-solid elektrolytt eller SSE. Generelt sett førte høyere fordelinger av faste stoffer til økt sikkerhet, mekanisk styrke og høyere kostnader, mens en høyere fordeling av væsker førte til reduserte kostnader og høyere ioneledningsevne.

Det teoretiske rammeverket i oppgaven gir en grundig utgreining av generell termodynamikk, som. indre energi og entropi. I tillegg til generell elektrokjemi for eksempel, energi, effekt og redoksreaksjoner, før oppgaven går nærmere inn på de grunnleggende konseptene i LIB. Videre, presenteres den generelle batteri terminologien for å sammenligne ulike egenskaper ved batteri teknologier. Deretter analyseres de ulike sammensetningene av katode- og anodematerialer. Videre introduseres de ulike elektrolyttene i LIB, liquid, solid og semi-solid state. Til slutt, analyseres kostnadene for råmaterialer, katode- og anodematerialer. I tillegg blir råmaterialenes karbonfotavtrykk og ulike katode sammensetninger evne til å resirkulere tatt opp.

Deretter presenteres metoder som er brukt under skrivingen av teorien, etterfulgt av en diskusjon. Denne delen av oppgaven begynner med å sammenligne de ulike katode- og anodematerialene med hensyn til egenskaper som celledspenning, spesifikk energi, energitetthet, termisk stabilitet og kostnader, for deretter å presentere en oppsummering av den totale ytelsen. Til slutt

diskuteres potensialet til SIB. Videre evalueres de ulike elektrolyttene, etterfulgt av en diskusjon om produksjon og bærekraft. For å gi en samlet oversikt til *Beyonders*, ble det gitt ulike anbefalinger. Avhandlingen fokuserte på de applikasjonsområdene til *Beyonders* som anses som mest kritiske i dagens samfunn, nemlig energilagring og transport. I anbefalingene ble kompatible elektrolytter, anoder og katoder tilpasset de mest relevante bruksområdene for utnyttelse med hensyn til *Beyonders* fremtidsutsikter og TRL.

Konklusjonen oppsummerer anbefalingene for de ulike batterikomponentene med tanke på 5-10 års bruk og behovet for videre forskning.

Contents

| | |
|--------------------------------------------------|-------------|
| Preface | i |
| Abstract | ii |
| Sammendrag | iv |
| List of Figures | x |
| List of Tables | xiv |
| Abbreviations | xv |
| Nomenclature | xvii |
| 1 Introduction | 1 |
| 1.1 Aim of Work | 2 |
| 2 Theory | 3 |
| 2.1 General Thermodynamics | 3 |
| 2.1.1 The first law of thermodynamics | 3 |
| 2.1.2 Internal energy | 3 |
| 2.1.3 Entropy | 4 |
| 2.1.4 The second law of thermodynamics | 4 |
| 2.1.5 Gibbs free energy | 4 |
| 2.1.6 Pressure and volume | 5 |
| 2.2 General Electrochemistry | 5 |
| 2.2.1 Energy and power | 5 |
| 2.2.2 Electrochemical equilibrium | 6 |
| 2.2.3 Redox reactions | 6 |
| 2.2.4 Oxidation numbers | 6 |
| 2.2.5 Chemical potential | 7 |
| 2.2.6 Electronegativity | 7 |
| 2.2.7 Overpotentials | 7 |
| 2.2.8 Reversible Potential | 9 |
| 2.2.9 Capacity | 9 |
| 2.2.10 Efficiency | 10 |

| | | |
|-------|-----------------------------------------------------|----|
| 2.3 | The Fundamentals of Lithium-Ion Batteries | 11 |
| 2.3.1 | Electrodes | 11 |
| 2.3.2 | Electrolyte | 13 |
| 2.3.3 | Solid Electrolyte Interphase | 14 |
| 2.3.4 | Separator | 15 |
| 2.3.5 | Current Collectors | 15 |
| 2.3.6 | Casing | 15 |
| 2.3.7 | Terminals | 16 |
| 2.3.8 | A battery cycle | 16 |
| 2.3.9 | Manufacturing | 18 |
| 2.4 | General Battery Terminology | 23 |
| 2.4.1 | Ionic Conductivity | 23 |
| 2.4.2 | C-rate | 23 |
| 2.4.3 | Thermal stability | 23 |
| 2.4.4 | State of Charge | 24 |
| 2.4.5 | Depth of Discharge | 25 |
| 2.4.6 | State of Health | 25 |
| 2.4.7 | Degradation | 25 |
| 2.4.8 | Battery Cell Classifications | 32 |
| 2.4.9 | Technology Readiness Level | 35 |
| 2.5 | Cathode materials | 36 |
| 2.5.1 | LCO | 37 |
| 2.5.2 | NMC | 39 |
| 2.5.3 | LFP | 40 |
| 2.5.4 | LMFP | 43 |
| 2.5.5 | LNMO | 45 |
| 2.5.6 | Summarising values | 46 |
| 2.6 | Anode materials | 48 |
| 2.6.1 | Graphite | 49 |
| 2.6.2 | Graphite doped with silicon | 50 |
| 2.6.3 | Hard carbon | 51 |
| 2.6.4 | LTO | 52 |
| 2.6.5 | Summarising values | 54 |
| 2.6.6 | Sodium-ion Batteries | 55 |

| | | |
|----------|----------------------------------------------------|-----------|
| 2.7 | Liquid-State Batteries | 55 |
| 2.7.1 | LIBs Compared to Other Batteries | 55 |
| 2.7.2 | Liquid Electrolytes | 56 |
| 2.8 | Solid State Lithium-ion Batteries | 58 |
| 2.8.1 | Definitions and Basic Principles of SSBs | 58 |
| 2.8.2 | Inorganic Solid-State Electrolytes | 62 |
| 2.8.3 | Solid Polymer Electrolytes | 64 |
| 2.8.4 | Hybrid Solid-State Electrolytes | 66 |
| 2.8.5 | Manufacturing | 67 |
| 2.9 | Semi Solid State Lithium-ion Batteries | 72 |
| 2.9.1 | Manufacturing | 72 |
| 2.9.2 | Semi-Solid State Electrolytes | 74 |
| 2.10 | Economy | 76 |
| 2.10.1 | Liquid State | 82 |
| 2.11 | Sustainability | 83 |
| 3 | Methods | 87 |
| 4 | Discussion | 88 |
| 4.1 | Comparison of the cathode materials | 88 |
| 4.1.1 | Cell voltage | 88 |
| 4.1.2 | Specific energy | 88 |
| 4.1.3 | Energy density | 89 |
| 4.1.4 | Thermal stability | 90 |
| 4.1.5 | Cycle life and Degradation | 91 |
| 4.1.6 | Cost | 92 |
| 4.1.7 | Overall performance | 94 |
| 4.2 | Comparison of the anode materials | 95 |
| 4.2.1 | Cell voltage | 95 |
| 4.2.2 | Specific energy | 96 |
| 4.2.3 | Energy density | 96 |
| 4.2.4 | Cycle life and degradation | 97 |
| 4.2.5 | Cost | 97 |
| 4.2.6 | Overall performance | 98 |
| 4.2.7 | Sodium-ion Batteries | 99 |

| | | |
|----------|----------------------------------|------------|
| 4.3 | Electrolytes | 99 |
| 4.3.1 | Ionic Conductivity | 99 |
| 4.3.2 | Safety | 99 |
| 4.3.3 | Mechanical Strength | 100 |
| 4.3.4 | Costs | 100 |
| 4.3.5 | Li-metal compatibility | 100 |
| 4.3.6 | Summary | 101 |
| 4.4 | Manufacturing | 102 |
| 4.5 | Sustainability | 104 |
| 4.6 | Recommendation | 105 |
| 4.6.1 | Energy storage | 105 |
| 4.6.2 | Transportation | 106 |
| 5 | Conclusion | 109 |
| 5.1 | Further Research | 110 |
| A | KI deklarasjon | i |

List of Figures

| | | |
|------|---------------------------------------------------------------------------------------------------------------------------------------------------------------------------------------|----|
| 1.1 | Cumulative Lithium-Ion Battery Demand For Electric Vehicles / Energy Storage Applications [GWh]. Reprinted from Statista. [1]. | 1 |
| 2.1 | The ranking rules for the oxidation numbers in the periodic table of elements. Reprinted from Odne Stokke Burheim. [3] | 7 |
| 2.2 | Charge and discharge efficiency in a battery. Reprinted from Hrvoje et al. [20] . . | 10 |
| 2.3 | Sketch of the primary components in a battery. Edited from Gregory L. Plett. [22] | 11 |
| 2.4 | The periodic table of elements. Reprinted from NTNU. [25] | 12 |
| 2.5 | The table of standard reduction potential. Reprinted from Nagpal. [29] | 13 |
| 2.6 | Illustration and schematic of the SEI-structure. Reprinted from Stephan Leuthner.[45] | 15 |
| 2.7 | LIB Composition showing the terminals and the metal casing. Edited from EV FireSafe. [51] | 16 |
| 2.8 | Processes present during manufacturing of a LIB pouch cell. Edited from Beck et al. [54] | 18 |
| 2.9 | Different electrode stacking methods, a) Single sheet stacking, b) Z-Stacking, c) Cylindrical winding, d) Prismatic winding. Edited from Deng et al. [58] | 20 |
| 2.10 | Illustration of a C6/LiFePO4 battery showing the formation of the inner and outer SEI layers when charged (a) and stored in open circuit (b). Reprinted from Li et al. [33] | 28 |
| 2.11 | Illustration of the equivalent circuit of how the resistance in the SEI layer works. Reprinted from Osaka et al. [88] | 29 |
| 2.12 | Illustration of the formation of lithium metal plating in three different scenarios. Reprinted from Lin et al. [89] | 31 |
| 2.13 | Dendrite formation in LIBs. Edited from Babu et al. [95] | 32 |
| 2.14 | Sketch of a Cylindrical Cell. Reprinted from Abbas et al. [100] | 33 |
| 2.15 | Illustration of a Pouch Cell. Reprinted from Abbas et al. [100] | 34 |
| 2.16 | Illustration of a Prismatic Cell. Reprinted from Abbas et al. [100] | 35 |
| 2.17 | Performance overview comparing A) LCO, B) NMC and C) LFP. Reprinted from Kostandi and Wadsworth. [108] | 37 |
| 2.18 | Illustration of the layered structure of LCO. Published by The University of Liverpool. [115] | 38 |

| | | |
|------|-------------------------------------------------------------------------------------------------------------------------------------------------------------------------------------------------------------------------|----|
| 2.19 | Illustration of the crystal structure of NMC as a cathode material. Reprinted from Garcia et al. [118] | 39 |
| 2.20 | Graphic illustration of how NMC811 stores more Li-ions than LCO. Reprinted from Marie and Gifford. [120] | 40 |
| 2.21 | Illustration of the crystal structure for LFP. Reprinted from Hu et al. [121] | 41 |
| 2.22 | Illustration of the rate of charge for LFP. Reprinted from Gunnarshaug et al. [123] | 42 |
| 2.23 | Graphic illustration comparing LFP batteries to NMC/NCM. Reprinted from Bhandari et al. [125] | 43 |
| 2.24 | Illustration (d) shows the crystal structure for LMFP while illustration (e) demonstrates the presence of channels oriented along the [010] axis, facilitating the diffusion of Li-ions. Reprinted from Li et al. [128] | 44 |
| 2.25 | Performance Overview of LMFP Based On Data From Table 2.4 | 45 |
| 2.26 | Illustration of the crystal structure of LNMO. Reprinted from He et al. [133] | 45 |
| 2.27 | The chart displays an overview of anode characteristics. Reprinted from Xinghao Lu. [142] | 48 |
| 2.28 | Illustration of carbon based anode materials different crystal structure during phase change used in LIBs, a) Graphite b) soft carbon c) HC. Reprinted from Crabtree et al. [143] | 49 |
| 2.29 | Illustration of the crystal structure of graphite. Reprinted from Katja Kretschmer. [146] | 49 |
| 2.30 | Illustration of the crystal structure of graphite doped with silicon. Reprinted from Nguyen et al. [148] | 50 |
| 2.31 | Illustration displays the pulverization of silicon when its volume expands during swelling. Reprinted from Choi and Aurbach. [150] | 51 |
| 2.32 | The atomic structure of HC in various years. Reprinted from Dou et al. [153] | 52 |
| 2.33 | (a) Illustration of the spinel crystal structure of LTO (b) Illustration of rock-salt-LTO after intercalation of Li-ions and phase change. Reprinted from Katja Kretschmer. [154] | 53 |
| 2.34 | Illustration of energy densities in Wh/L and Wh/kg for different batteries. Reprinted from Da Deng. [159] | 56 |
| 2.35 | Schematic of an SSB cell. Reprinted from Famprakis et al. [168] | 58 |
| 2.36 | Thin-film SSB. Reprinted from Huang et al. [167] | 59 |
| 2.37 | Three-dimensional SSB. Edited from Huang et al. [167] | 59 |
| 2.38 | Bulk-type SSB. Edited from Huang et al. [167] | 60 |

| | | |
|------|------------------------------------------------------------------------------------------------------------------------------------------------------------------------------------------------------|----|
| 2.39 | Comparison of the cell stacks in a conventional series connection and in an SSB stack. Reprinted from Placke et al. [177] | 61 |
| 2.40 | Comparing an SSE (a) with an LE (b). Reprinted from Huang et al. [167] . . . | 62 |
| 2.41 | The components of an SSB with an ISE. Reprinted from Sen et al. [180] | 63 |
| 2.42 | Illustration of an SSB with an SPE. Reprinted from Liu et a. [188] | 65 |
| 2.43 | Comparison of ISEs and SPEs in LMBs. Reprinted from Song et al. [193] | 65 |
| 2.44 | Illustration of a hybrid SSE in a battery. Reprinted from Yang et al. [185] | 66 |
| 2.45 | Illustration of anode-less SSB structure. Reprinted from Kerman et al. [201] . . . | 69 |
| 2.46 | The different approaches to Li-metal anode processing. Reprinted from Schmaltz et al. [163] | 70 |
| 2.47 | SSB cell assembly process. Reprinted from Schnell et al. [172] | 71 |
| 2.48 | Comparing conventional LIB, SSB and SSLIB in operation. Edited from Chang et al. [178] | 73 |
| 2.49 | Conventional (left) and a type of SSLIB (right) cell structure. Reprinted from Bryntesen et al. [208] | 73 |
| 2.50 | Schematic diagram of lithium batteries using (a) LE; and (b) gel polymer electrolyte. Reprinted from Chae et al. [211] | 75 |
| 2.51 | Overview of three bar charts showing the following: 1) breakdown of the cell cost, 2) the cost share of materials in a cell, 3) breakdown of the cell mass. Reprinted from Li et al. [219] | 77 |
| 2.52 | Overview of different cathode chemistries mass distribution of raw materials. Reprinted from COBRA. [139] | 77 |
| 2.53 | Graphic illustration of predicted anode mix advancements over a time period of 7 years. Reprinted from Bhandary et al. [125]. | 78 |
| 2.54 | The graph illustrate the battery material prices for a 6 year period for different metals. Reprinted from Bhandari et al. [125] | 79 |
| 2.55 | The graphs illustrate projected materials prices for cobalt, nickel, manganese and lithium in USD/kg from 2010-2030. Reprinted from Orangi et al. [124] | 80 |
| 2.56 | Compares different costs of cathode chemistries. Reprinted from Snowdon et al. [224] | 81 |
| 2.57 | Compares LMFP and LFP costs over two years. Reprinted from Jinga et al. [147] | 81 |
| 2.58 | The bar chart illustrates the distribution of the battery supply chain across countries. Reprinted from Bhandari et al. [125] | 82 |

| | | |
|------|---------------------------------------------------------------------------------------------------------------------------------------------------------------------------------------------------------------------------------------------------------------|----|
| 2.59 | The graphs illustrate different costs in USD/kWh for cathode battery packs for different demands. One curve is from 2021, while the other two are projected graphs from 2025, both with and without recycling. Reprinted from Bhandari et al. [125] | 83 |
| 2.60 | Criticality and environmental impact quadrant matrix. Reprinted Manjong et al. [230] | 85 |
| 2.61 | Characteristics of the different recycling methods. D = Pyrometallurgy, E = Hydrometallurgy, F = Direct Recycling. Reprinted from Mao et al. [236] | 86 |

List of Tables

| | | |
|-----|----------------------------------------------------------------------------------------------------------------------------------|----|
| 2.1 | Manufacturing costs per year of a LIB manufacturing process. Values retrieved from Liu et al. [59] | 21 |
| 2.2 | Energy consumption and duration normalized per unit of a LIB manufacturing process. Values taken from Yuan et al. [60] | 22 |
| 2.3 | Table showing the reversible electrochemical reaction for LCO and graphite. [3] . | 37 |
| 2.4 | Table of the properties of different cathode materials | 47 |
| 2.5 | Table of the properties of different anode materials. | 54 |
| 2.6 | Table of Li-metal properties | 61 |
| 2.7 | The Table below shows cost per USD/kg of various anodes. Values obtained from Hettessheimer et al. [222] | 79 |

Abbreviations

| | |
|---------|------------------------------------------------|
| ASSB | All-Solid State Battery |
| BMS | Battery Management System |
| CED | Cumulative Energy Demand |
| DoD | Depth of Discharge |
| EMF | Electromotive Force |
| EV | Electric Vehicle |
| GDIP | Green Deal Industrial Plan |
| GHE | Gel Polymer-ceramic Hybrid Electrolytes |
| GPE | Gel Polymer Electrolyte |
| GWP | Global Warming Potential |
| HC | Hard Carbon |
| HCP | Hexagonal Close Packed |
| ISE | Inorganic Solid Electrolyte |
| IL | Ionic Liquid |
| LAM | Loss of Active Material |
| LATP | Lithium Aluminium Titanium Phosphate |
| LCA | Life Cycle Assessment |
| LCO | Lithium Cobalt Oxide |
| LE | Liquid Electrolyte |
| LFP | Lithium Iron Phosphate |
| LIB | Lithium-ion Battery |
| LMFP | Lithium Manganese Iron Phosphate |
| LNMO | Lithium Nickel Manganese Oxide |
| LTO | Lithium Titanate Oxide |
| MOF | Metal Organic Framework |
| NASICON | Sodium Super Ionic Conductor |
| NG | Natural Graphite |
| NMC | Nickel Manganese Cobalt |
| NMP | N-Methyl-2-Pyrrolidone |
| NTNU | Norwegian University of Science and Technology |
| PHEV | Plug-in Hybrid Electric Vehicle |
| PVDF | Polyvinylidene Fluoride |
| SBR | Styrene-butadiene Rubber |

| | |
|-------|----------------------------------------|
| SDG | Sustainable Development Goals |
| SEI | Solid Electrolyte Interphase |
| SG | Synthetic Graphite |
| SHE | Standard Hydrogen Electrode |
| SIB | Sodium-ion Battery |
| SICSE | Single-Ion Conducting Soft Electrolyte |
| SIL | Solvent Ionic Liquid |
| SPE | Solid Polymer Electrolyte |
| SR | Silicon Rubber |
| SSB | Solid State Battery |
| SSE | Solid State Electrolyte |
| SSLIB | Semi-Solid State Lithium-ion Battery |
| SoC | State of Charge |
| SoH | State of Health |
| TRL | Technology Readiness Level |

Nomenclature

| | |
|--------------|--------------------------------|
| ∇C_i | Concentration gradient |
| c_{bulk} | Bulk electrolyte concentration |
| c_{surf} | Surface concentration |
| D_i | Diffusion coefficient |
| E | Actual potential |
| E^0 | Equilibrium potential |
| E^{rev} | Reversible potential |
| ϵ | Efficiency |
| F | Faraday constant |
| G | Gibbs free energy |
| \bar{g} | Molar gibbs free energy |
| H | Enthalpy |
| I | Current |
| I_+ | Ionic current |
| I_t | Total current |
| J_i | Mass flux rate |
| j | Current density |
| j_0 | Exchange current density |
| η | Total overpotential |
| η_a | Activation overpotential |
| η_c | Concentration overpotential |
| η_0 | Ohmic overpotential |
| η_r | Reaction overpotential |
| P | Power |
| Q | Heat |
| S | Entropy |
| ΔS | Change in entropy |
| σ | Produced entropy |
| s | Seconds |
| T | Temperature |
| t_+ | Ion transference number |
| U | Internal energy |
| W | Work |

1 Introduction

The demand for sustainable energy storage solutions and low carbon production methods has grown exponentially in parallel with the world's increased awareness of climate change and global warming. As a result of the rising demand for a green energy transition, the necessity for batteries has become the key source for powering mobility applications and stationary storage. The advent of electric vehicles and other high-voltage applications has led to an exponential increase in lithium-ion battery demand. An important factor for the significant increase in demand has been driven by the electrification of the energy market. This is visualized in Figure 1.1, illustrating the global exponential increase.

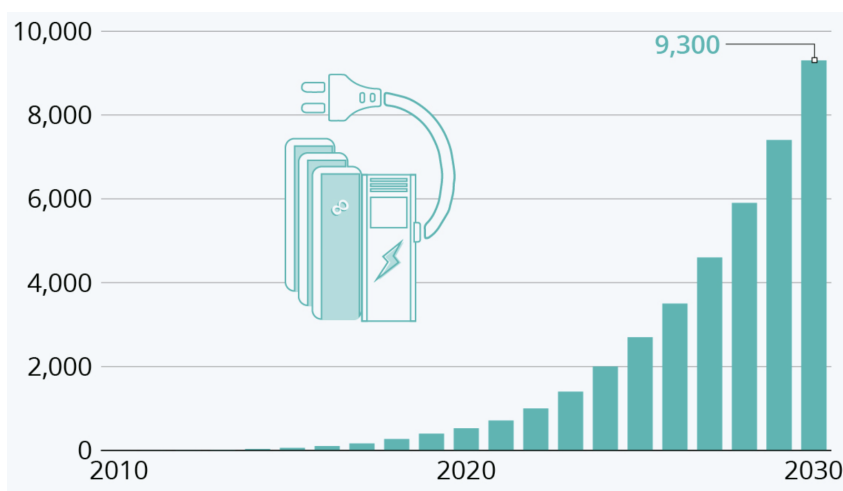


Figure 1.1: Cumulative Lithium-Ion Battery Demand For Electric Vehicles / Energy Storage Applications [GWh]. Reprinted from Statista. [1].

Batteries have come a long way since it was first conceptualized and further developed by Volta in the early 1800s, which then became what is today known as a voltaic pile [2]. The lithium-ion battery is the oldest and currently most widely used battery. It can be used in a wide range of different applications, including the storage of renewable energy and the powering of electric vehicles and portable consumer electronics.

In order to adapt lithium batteries for diverse applications, there has been a significant focus on modifying the various components within the battery in recent years. This will enable the specific properties and behavior of the batteries to be altered. Common approaches include modifying the composition of the anode, cathode, and electrolyte.

1.1 Aim of Work

The objective of this assignment is to conduct a feasibility analysis to identify the different battery technologies currently available on the market and to find out which of them is the most promising for the *Beyonders* marked segments. Initially, the fundamental principles of battery technology, the various components and their respective functions will be presented. The respective components to be analysed are the anode, cathode and electrolytes. Subsequently, the paper will examine the different components in greater depth, identifying the reasons behind the distinctive properties of the various technologies. Finally, the various components that complement each other for specific applications will be discussed.

This analysis will assist the battery supplier Beyonder in its future decision-making regarding the type of battery that the company should prioritize in the future. Overall, the assignment will examine both established and emerging technologies. For Beyonder, this thesis will inform their approach to the battery industry. It will assess the potential benefits of investing in newer materials and technologies or the merits of maintaining reliance on more mature technologies. To inform this decision, we will consider a range of factors, including economics, production, sustainability, and technology readiness level.

2 Theory

The following chapter will first give an overview of general thermodynamics and electrochemistry. After that, the underlying theory regarding traditional *Lithium-ion Batteries (LIBs)*, *Solid-State-Batteries (SSBs)* and *Semi-Solid State Lithium-ion Batteries (SSLIBs)* is covered.

2.1 General Thermodynamics

Thermodynamics is a very useful tool to analyze and understand different processes and factors that affects the process [3]. This chapter will therefor give a brief summary of some introductory thermodynamics.

2.1.1 The first law of thermodynamics

The first law of thermodynamics is a conservation law, witch says that energy can neither be created or destroyed [4].

$$\Delta E_{pot} + \Delta E_{kin} = Q - W \quad (2.1)$$

Another way to explain the first law of thermodynamics is that added heat (Q) minus work extracted (W) must be equal to any change of kinetic energy (E_{kin}) and potential energy (E_{pot}), as shown in Equation 2.1. [3]

2.1.2 Internal energy

The internal energy (U) is the energy that is left in a system after the kinetic energy and the potential energy. [3]

$$U = E - E_{kin} - E_{pot} \quad (2.2)$$

$$\Delta U = Q - W - \Delta E_{kin} - \Delta E_{pot} \quad (2.3)$$

The definition of internal energy is shown in Equation 2.2, while Equation 2.3 shows the change in internal energy in a closed system. [5]

2.1.3 Entropy

Entropy is, in microscopic scale, defined as the level of disorganization. When a substance is added heat, the molecules of the substance will start to move more because of the added thermal energy. This movement is called entropy [6, 7].

There are different forms of entropy: transported, Q/T , changed, ΔS , and produced, σ .

$$\Delta S = \frac{\Delta Q}{T} \quad (2.4)$$

If a system has a constant temperature (T) and is added heat (Q), the change of entropy is defined as Equation 2.4. [3]

2.1.4 The second law of thermodynamics

The second law of thermodynamics says that any process causes the total entropy of a system to either increase or remain constant. [6]

One of the definition of the second law of thermodynamics is that entropy production can not be negative because of the first law of thermodynamics 2.1.1. This is shown in Equation 2.6 [3].

$$S \geq 0 \quad (2.5)$$

$$\sigma \geq 0 \quad (2.6)$$

The first law of thermodynamics states that all energy is conserved. However, it does not provide insight into the direction of a process or the equilibrium state. If this law can be applied to the entire universe, it implies that the universe is evolving towards greater disorder. The definition of the second law of thermodynamics indicates that entropy losses occur during a process and that efficiency rarely reaches 100%. [3]

2.1.5 Gibbs free energy

Gibbs free energy represents the potential energy in a chemical reaction. Equation 2.7 shows the definition of Gibbs free energy. This is hence only for closed systems. [3]

$$G = H - TS \tag{2.7}$$

In batteries there are a number of electrochemical reaction. Gibbs free energy is a property that show us if a reaction is spontaneous or not. If $\Delta G < 0$ for a reaction, then it is spontaneous and do not need any external energy to occur. If $\Delta G > 0$ the reaction is not spontaneous and is in need of external energy to occur. If $\Delta G = 0$ the reaction is at equilibrium. [8]

2.1.6 Pressure and volume

The entropy change for a process where we first change the temperature and then later the volume is defined as Equation 2.8. [3]

$$dS = C_v d\ln T - mE d\ln V \tag{2.8}$$

2.2 General Electrochemistry

A battery is an energy storage technology that is able to convert chemical energy to electrical energy [3]. In this chapter, the fundamentals of electrochemistry are presented. Understanding the principles allows for battery optimization.

2.2.1 Energy and power

In the field of energy storage, it is important to know the difference between energy and power. To get a comprehensive understanding of energy there also needs to be an understanding of power. The standard unit for energy is joule (J) and the unit for power (P) is watt (W). [3, 9]

The two properties are independent due to their conceptual relationship in physics. A system can, for example, offer a lot of power but low energy. This means that the system only supplies the power in a short period of time. When designing an energy storage system, one has to find the balance between the energy capacity and the power capacity needed. Often, there is a need for a combination of the two. The high power capacity is needed for a short period of time, for example, to start a machine or drive up a hill, while the high energy capacity is needed to operate electrical devices for a longer period of time. [3]

For energy applications, the properties of specific energy, energy density, and specific power are important. Specific energy is defined as energy per mass, energy density is defined as energy per volume, and specific power is defined as power per mass. [3]

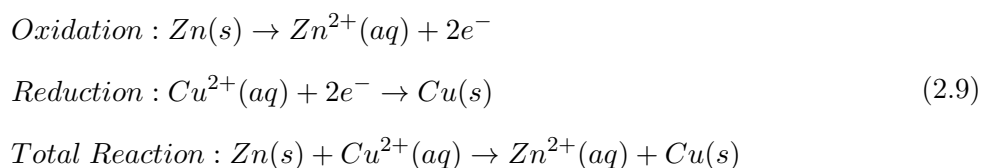
2.2.2 Electrochemical equilibrium

Nature will always aim to achieve equilibrium, meaning something is equal on each side. If a membrane is between two different concentrations, nature will try to minimize the differences between the two sides. [10]

A battery works with a concentration difference. When the battery is charged, lithium-ions (Li-ions) accumulate on the anode, which forms a concentration difference with the cathode. When the battery is discharged, the ions are free to move and will seek an equilibrium. The ions will go to the cathode with a low concentration. [3]

2.2.3 Redox reactions

A redox reaction is a chemical reaction where electrons move between substances. If a substance gives away an electron, it is reduced. If it receives an electron, it is oxidised. A typical example is the reaction in electrolysis shown in Equation 2.9, where the copper (Cu) is reduced, and the zinc is oxidized. [11]



These reactions always happen simultaneously, and the substances involved are called a reduction pair [12, 11]. Reducing potential (ΔE) is a measure of the strength and direction of electrons moving between substances [12, 13] and is measured in millivolts (mV) [12]. This redox reaction is not observable, but one can calculate what happens by using oxidation numbers that represent how many electrons a substance has gained or reduced [11, 14].

2.2.4 Oxidation numbers

As the main reaction in a battery is the redox reaction, the oxidation numbers are a good measure to consider. The different oxidation numbers show how many electrons are being oxidised and reduced of the different elements in a redox reaction. The change in oxidation number in a battery determines the battery type. These oxidation numbers are written in Roman numerals. The ranking rules for the oxidation numbers in the periodic table of elements are shown in Figure 2.1. [3]

Oxidation number ranking rules. Lower numbered rule outrank higher numbered ones

| | |
|---|------------------------------------------------------------------------------------------------------------------------------------------------------------------------------------------|
| 1 | The oxidation number of any pure element is always 0. |
| 2 | The oxidation number of hydrogen is always plus one $+I$. |
| 3 | The oxidation numbers of alkaline elements are always $+I$. |
| 4 | The oxidation numbers of earth alkaline elements are always $+II$. |
| 5 | The oxidation numbers of halogen elements are always $-I$. |
| 6 | The charge of the compound or ion determines the remaining oxidation number. |
| 7 | The oxidation number of oxygen is always $-II$. |
| 8 | Nondiscrete oxidation numbers are expressed with fractal Roman numbers. |
| 9 | Elements to the right and above in the periodic table of elements will win negative charge, for example, K gives electrons to Na, Na gives electrons to Al, and Cl gives electrons to F. |

Figure 2.1: The ranking rules for the oxidation numbers in the periodic table of elements. Reprinted from Odne Stokke Burheim. [3]

2.2.5 Chemical potential

The chemical potential can be used to define the potential effect of a chemical reaction. This is defined as the partial derivative of the Gibbs free energy with respect to the number of moles of a component at constant temperature and pressure, as shown in Equation 2.10. [3, 15]

$$\mu_i = \left(\frac{\partial G}{\partial n_i} \right)_{T,p,n_j \neq i} \quad (2.10)$$

2.2.6 Electronegativity

The electronegativity of an atom signifies its tendency to attract electrons. The values used for electronegativity were derived by Linus Pauling, and they range from less than one for the alkali metals to four for fluorine. Large values indicate a stronger attraction for electrons than lower values. [16]

2.2.7 Overpotentials

When a battery is in operation, the cell potential will differ from the equilibrium. This is due to various irreversible losses that limit the reactions from the ideal and are present in all electrochemical cells to varying degrees. These losses add to the equilibrium potential, E^0 , and give the actual cell potential, which can be expressed as E . This added potential is called an overpotential and can be expressed as η , thus giving Equation 2.11 below. [17]

$$E = E^0 + \eta \quad (2.11)$$

There are several reasons why losses occur in a cell, such as the mass transfer of the reactant, friction from surface conversions and electron transfer. As a whole, overpotentials can be divided into three categories:

- Ohmic overpotential (η_o)
- Activation overpotential (η_a)
- Concentration overpotential (η_c)

The total overpotential can be expressed as the summation of the different types as shown in Equation 2.12. [17]

$$\eta = \eta_o + \eta_a + \eta_c \quad (2.12)$$

Ohmic overpotential

The ohmic overpotential, here expressed as η_o , occurs due to the internal resistance of an electrochemical cell and follows Ohm's law, $\eta_o = rj$. When ions travel through the electrolyte, they meet friction, which causes the ohmic losses [3]. There is also friction involved in the electron movement, but the ionic resistance is often higher. However, in the case of semiconducting materials, the electronic resistance may be higher [17].

Activation overpotential

The added potential required to overcome the activation energy of the cell reaction to produce a specified current is called the activation overpotential. It is also called the surface overpotential, expressed as η_a . The activation overpotential is more specifically related to the surface reactions and conversions before, during and after electron transfer. [17]

Concentration Overpotential

When the reactant or product is transported through the electrolyte and into the surface, some losses occur due to the flux of mass, which causes a concentration overpotential η_c . Depending on the cell reaction and mass diffusion rate, the reactant does not reach the electrode surface

and the product accumulates. The reactant concentration then becomes lower at the electrode surface than at the bulk electrolyte. [3]

When the electron transfer reaction is fast, the surface concentration of the reactant decreases as the current increases due to the reactants being consumed at a faster rate until it eventually reaches zero. The reactants are consumed the moment they reach the surface, and the concentration gradient cannot increase. The current, in this instance, is called the limiting current j_{lim} . To increase the current further, the thickness of the boundary needs to be lowered. [3]

2.2.8 Reversible Potential

The free energy is a potential of work. This potential is measured as reversible potential E^{rev} and is also known as electromotive force (EMF) [3]. This force allows one electron to move from one place to another [18]. By definition, the reversible potential can only be measured between two separate locations. In batteries, this would typically correspond to the anode and cathode.

The reversible potential is given by the Nernst equation shown in Equation 2.13, where z is the number of electrons exchanged per mole of the product components, F is the Faraday constant, and \bar{g} is the molar Gibbs free energy.

$$EMF = E^{rev} = -\frac{\Delta\bar{g}}{zF} \quad (2.13)$$

At standard state, EMF is defined as shown in Equation 2.14.

$$EMF^\circ = E^\circ = -\frac{\Delta\bar{g}^\circ}{zF} \quad (2.14)$$

If one changes the concentrations in a reaction (z), the EMF will also change. Equation 2.15 is used to calculate the EMF when the concentration changes.

$$E^{rev} = E^\circ - \frac{\bar{R}T}{zF} \ln[K] \quad (2.15)$$

2.2.9 Capacity

The capacity of a battery is defined as the total amount of electric charge any given battery can hold due to the chemical reactions present. Electric charge is gathered during the charging phase

and released during the discharge phase [19]. Battery capacity is calculated utilizing Equation 2.16 below.

$$Q_t = I \cdot t \quad (2.16)$$

Capacity is most commonly expressed in [Ah] but can in other suitable scenarios be expressed in [Wh] under the handle “energy”. This unit of capacity describes the amount of current the battery can deliver during a single hour of use. [19]

2.2.10 Efficiency

By definition, efficiency is what comes out of a process compared to what goes in. In batteries, the discharge and charge efficiencies are important. Discharge measures a measure of how much of the stored chemical energy is converted into usable electrical energy, whilst charging efficiency governs how much external electrical energy can be stored as chemical energy [3]. Figure 2.2 illustrates this.

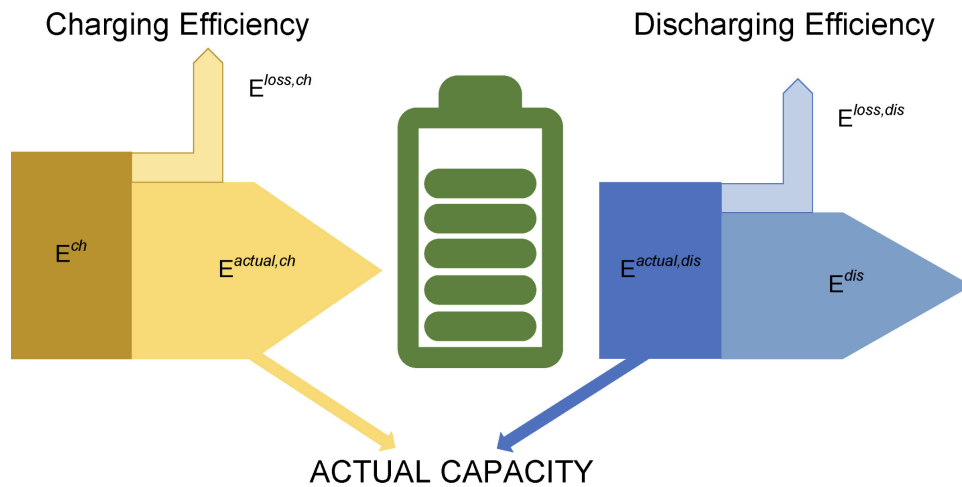


Figure 2.2: Charge and discharge efficiency in a battery. Reprinted from Hrovje et al. [20]

Efficiency can be applied to many variables, including heat, power and energy. The work efficiency equation is shown in Equation 2.17. [3]

$$\epsilon = \frac{W_{out}}{W_{in}} \quad (2.17)$$

Suppose there is a process with several energy storage units. In that case, one can obtain the energy efficiency for the entire system by multiplying the different efficiencies with each other, as shown in Equation 2.18.

$$\epsilon_n = \prod_{i=1}^n \epsilon_i \quad (2.18)$$

2.3 The Fundamentals of Lithium-Ion Batteries

LIBs are crucial energy storage devices that power several aspects of modern life, from household electronics to electric vehicles (EVs) and large-scale energy storage systems. This overview will explore the foundational principles that underlay LIB operation, including the components LIBs consist of and the different technologies used within battery construction. It is important to note that the polarization of the electrodes is dependent on which cycle the battery is under. During charging, the anode is the positive electrode, and the cathode is the negative electrode. Under discharging, these polarization values are reversed. They primarily consist of an anode, a cathode, an electrode, a separator, an electrolyte and a casing [21]. Figure 2.3 is a schematic of a conventional LIB.

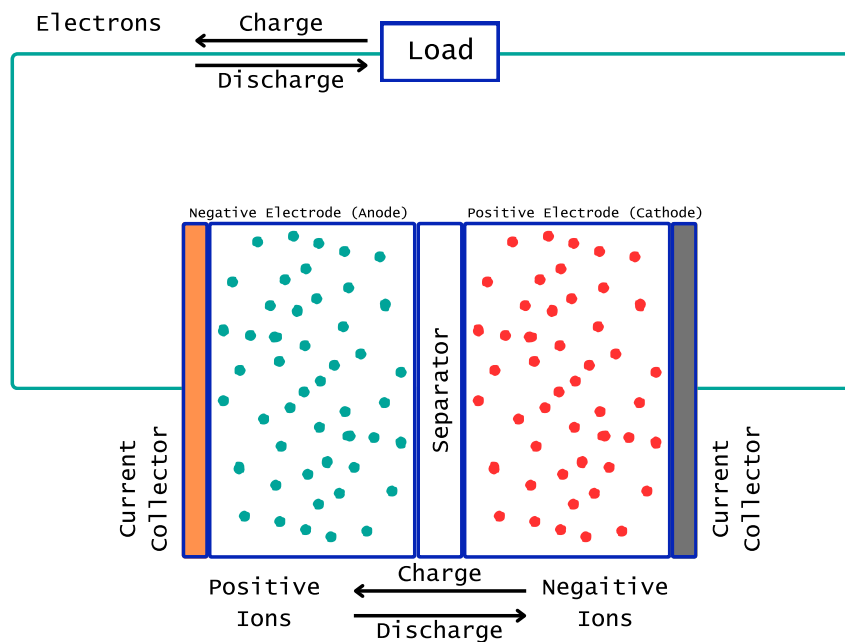


Figure 2.3: Sketch of the primary components in a battery. Edited from Gregory L. Plett. [22]

2.3.1 Electrodes

Electrodes are the components that facilitate the electrochemical redox reactions that occur during the charge and discharge of a battery. These components are divided into anodes and cathodes. During discharge, the electrons are oxidised at the anode and are reduced at the cathode. By standard convention, they represent the positive and negative electrodes respectively during charge, and the inverse during discharge. [23]

The different compositions of materials give the electrodes its properties. The ideal composition of a LIB includes Li, which has a single electron in its outer orbit, and a substance that is only missing electrons in its outer orbit. Li is the lightest alkali metal, meaning it is the smallest metal of group 1 and possesses a single electron in its outer orbit. However, Li cannot go with a halogen in group number 17 in the periodic table, shown in Figure 2.4. This is because the halogens only miss one electron to get a full outer shell. When it reacts with Li, which only has one electron in its outer shell, the halogen would take the outer electron of the Li, and the halogens would achieve a full outer shell. The intermolecular forces that bind the Li and halogen together would be too strong, making the Li unable to deintercalate. Hence, using elements in the chalcogen group (group 16) is a solution. These elements are highly reactive with Li because they lack two electrons in the outer shell, and Li has one to give. When a chalcogen atom reacts with Li, the bonds formed are not as strong, making it easier to discharge. Group numbers 15, 14 and 13 in the periodic table are also commonly used. [3, 24]

| Group→ | 1 | 2 | 3 | 4 | 5 | 6 | 7 | 8 | 9 | 10 | 11 | 12 | 13 | 14 | 15 | 16 | 17 | 18 |
|---------|----------|----------|----------|--------------|-----------|-----------|-----------|-----------|-----------|-----------|-----------|-----------|-----------|-----------|-----------|-----------|-----------|-----------|
| ↓Period | | | | | | | | | | | | | | | | | | |
| 1 | 1 H | | | | | | | | | | | | | | | | | 2 He |
| 2 | 3 Li | 4 Be | | | | | | | | | | | 5 B | 6 C | 7 N | 8 O | 9 F | 10 Ne |
| 3 | 11 Na | 12 Mg | | | | | | | | | | | 13 Al | 14 Si | 15 P | 16 S | 17 Cl | 18 Ar |
| 4 | 19 K | 20 Ca | 21 Sc | 22 Ti | 23 V | 24 Cr | 25 Mn | 26 Fe | 27 Co | 28 Ni | 29 Cu | 30 Zn | 31 Ga | 32 Ge | 33 As | 34 Se | 35 Br | 36 Kr |
| 5 | 37 Rb | 38 Sr | 39 Y | 40 Zr | 41 Nb | 42 Mo | 43 Tc | 44 Ru | 45 Rh | 46 Pd | 47 Ag | 48 Cd | 49 In | 50 Sn | 51 Sb | 52 Te | 53 I | 54 Xe |
| 6 | 55 Cs | 56 Ba | 57 La | * 72 Hf | 73 Ta | 74 W | 75 Re | 76 Os | 77 Ir | 78 Pt | 79 Au | 80 Hg | 81 Tl | 82 Pb | 83 Bi | 84 Po | 85 At | 86 Rn |
| 7 | 87 Fr | 88 Ra | 89 Ac | ** 104 Rf | 105 Db | 106 Sg | 107 Bh | 108 Hs | 109 Mt | 110 Ds | 111 Rg | 112 Cn | 113 Nh | 114 Fl | 115 Mc | 116 Lv | 117 Ts | 118 Og |
| | | | | * 58 Ce | 59 Pr | 60 Nd | 61 Pm | 62 Sm | 63 Eu | 64 Gd | 65 Tb | 66 Dy | 67 Ho | 68 Er | 69 Tm | 70 Yb | 71 Lu | |
| | | | | ** 90 Th | 91 Pa | 92 U | 93 Np | 94 Pu | 95 Am | 96 Cm | 97 Bk | 98 Cf | 99 Es | 100 Fm | 101 Md | 102 No | 103 Lr | |

Figure 2.4: The periodic table of elements. Reprinted from NTNU. [25]

To determine which elements are the best fit with lithium (Li), one must also consider the reduction potential of the elements relative to the standard hydrogen electrode (SHE), which is assigned to 0 for all temperatures [26, 27]. This indicates the standard reduction potential of the different elements, and it is illustrated in Figure 2.5. The reduction potential in voltage is shown on the right-hand side. It indicates how much voltage can be released during a reduction reaction [28]. One of the main goals for LIBs is for the voltage difference between the anode and the cathode material to be as great as possible. This difference makes up the cell voltage. The difference in potential between the anode and cathode determines the cell potential of the battery.

This is because the total reaction in a LIB is a redox reaction. It is also important to ensure that the difference in standard cell potential between the anode and cathode is as great as possible, as this will result in a high cell voltage. As with the cathode materials, the anode materials employed in LIBs must possess optimal properties for both electrochemical intercalation and deintercalation. The composition of the different anode materials also contributes to a battery's properties/characteristics. These affect their performance, cost, safety and sustainability. [3]



| | | | |
|-----------------------------------------------------------------------------------------------------------------------------------------------------------|-----------------------------------------------------------------------------------|-------|-----------------------------------------------------------------------------------------------------------------------------------------------------------|
|  <p style="color: red; font-weight: bold;">Stronger oxidizing agent</p> | $F_2(g) + 2 e^- \longrightarrow 2 F^-(aq)$ | 2.87 |  <p style="color: blue; font-weight: bold;">Weaker reducing agent</p> |
| | $H_2O_2(aq) + 2 H^+(aq) + 2 e^- \longrightarrow 2 H_2O(l)$ | 1.78 | |
| | $MnO_4^-(aq) + 8 H^+(aq) + 5 e^- \longrightarrow Mn^{2+}(aq) + 4 H_2O(l)$ | 1.51 | |
| | $Cl_2(g) + 2 e^- \longrightarrow 2 Cl^-(aq)$ | 1.36 | |
| | $Cr_2O_7^{2-}(aq) + 14 H^+(aq) + 6 e^- \longrightarrow 2 Cr^{3+}(aq) + 7 H_2O(l)$ | 1.33 | |
| | $O_2(g) + 4 H^+(aq) + 4 e^- \longrightarrow 2 H_2O(l)$ | 1.23 | |
| | $Br_2(l) + 2 e^- \longrightarrow 2 Br^-(aq)$ | 1.09 | |
| | $Ag^+(aq) + e^- \longrightarrow Ag(s)$ | 0.80 | |
| | $Fe^{3+}(aq) + e^- \longrightarrow Fe^{2+}(aq)$ | 0.77 | |
| | $O_2(g) + 2 H^+(aq) + 2 e^- \longrightarrow H_2O_2(aq)$ | 0.70 | |
| | $I_2(s) + 2 e^- \longrightarrow 2 I^-(aq)$ | 0.54 | |
| | $O_2(g) + 2 H_2O(l) + 4 e^- \longrightarrow 4 OH^-(aq)$ | 0.40 | |
| | $Cu^{2+}(aq) + 2 e^- \longrightarrow Cu(s)$ | 0.34 | |
| | $Sn^{4+}(aq) + 2 e^- \longrightarrow Sn^{2+}(aq)$ | 0.15 | |
| | $2 H^+(aq) + 2 e^- \longrightarrow H_2(g)$ | 0 | |
| | $Pb^{2+}(aq) + 2 e^- \longrightarrow Pb(s)$ | -0.13 | |
| | $Ni^{2+}(aq) + 2 e^- \longrightarrow Ni(s)$ | -0.26 | |
| | $Cd^{2+}(aq) + 2 e^- \longrightarrow Cd(s)$ | -0.40 | |
| | $Fe^{2+}(aq) + 2 e^- \longrightarrow Fe(s)$ | -0.45 | |
| | $Zn^{2+}(aq) + 2 e^- \longrightarrow Zn(s)$ | -0.76 | |
| $2 H_2O(l) + 2 e^- \longrightarrow H_2(g) + 2 OH^-(aq)$ | -0.83 | | |
| $Al^{3+}(aq) + 3 e^- \longrightarrow Al(s)$ | -1.66 | | |
| $Mg^{2+}(aq) + 2 e^- \longrightarrow Mg(s)$ | -2.37 | | |
| $Na^+(aq) + e^- \longrightarrow Na(s)$ | -2.71 | | |
| $Li^+(aq) + e^- \longrightarrow Li(s)$ | -3.04 | | |
| <p style="color: blue; font-weight: bold;">Stronger reducing agent</p> | | | |

Figure 2.5: The table of standard reduction potential. Reprinted from Nagpal. [29]

Finding the standard potential involves combining the different materials and examining the different half-reactions. This is a complicated process that is outside the scope of this thesis [30]. Thus, only the various individual redox reactions for the different elements are considered. Oxygen (O) has, for example, a reduction potential of 1.23V while Li has a reduction potential of $-3.04V$. Together, this makes a cell potential of 4.27V. In addition to the high cell voltage, O is a relatively light and highly reactive element. These are some of the main reasons O exists in many conventional cathode materials. [29, 31]

2.3.2 Electrolyte

Electrolytes are a major component in a battery and are used to facilitate the movement of ions between the electrodes of the battery. This enables the battery to convert stored chemical energy into electrical energy [32]. The different types of electrolytes will be explored further in

upcoming sections.

2.3.3 Solid Electrolyte Interphase

During the first cycle of a battery, a passivation layer called a solid electrolyte interphase layer (SEI) is made from the electrolyte and the anode. The SEI layer is a very important part for the function of the battery, as it allows the transportation of Li-ions between the electrolyte and the anode [3, 33]. In primary batteries, it has an impact on the safety, the performance, the self discharge, the low temperature performance and the faradaic efficiency of the cell. It also determines the faradaic charge efficiency, cycle life and Li deposition morphology in secondary batteries. In the case of LIBs, it also determines the irreversible loss of capacity (Q) during the first cycle of charging [34].

The electrolyte contains additives such as vinylene-carbonate. Initially, when the anode absorbs Li-ions, the Li-ions, the solvent and the additives are reacting with the outer layer of the anode. This reaction creates the SEI layer that protects the anode and extends the battery life to thousands of cycles. [35]

The reaction that creates this film consumes 5-10% of the Li that is in the battery. This reduces the capacity of the battery by 5-10% [33, 35]. To avoid customers noticing this relatively big reduction in capacity, the battery companies run some battery cycles in the factory before they are shipped out [35].

The fine structure of the SEI layer has not yet been found [36, 37, 38]. Experimental studies demonstrate that the SEI both consists of a porous outer layer and a compact inner layer, which mainly consists of inorganic and organic Li-salts. Li-ions are able to go through both layers, while the solvent from the electrolyte can only pass through the outer porous layer before being stopped at the interface between the outer and inner SEI layer. The inner layer works as an insulator for both the solvent in the electrolyte and the electrons in the anode [33] [39] [40] [41] [42]. It is also found that the formation of SEI is highly dependent on the composition of the electrolyte, the electrode voltage and electrode surface morphology, as the SEI layer is partly made up of the solvent in the electrolyte [33]. Over time, the SEI layer continues to grow, making a complex mosaic-type of structure [34] and decreasing the battery's capacity and limiting its performance [43, 44], this is illustrated in Figure 2.6.

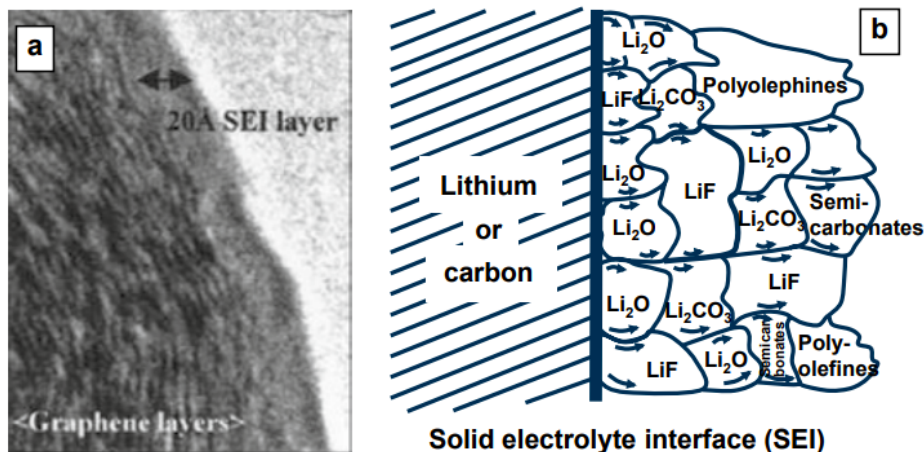


Figure 2.6: Illustration and schematic of the SEI-structure. Reprinted from Stephan Leuthner.[45]

2.3.4 Separator

The separator creates a physical barrier between the anode and cathode, allowing Li-ions to pass, but not electrons, preventing them from short-circuiting the battery. Instead, they are compelled to go through an external circuit. If the anode and cathode are in contact, there would be no potential difference between them, and no electrons would go from one side to the other. [35]

The separators are commercially made of a polymer-based material such as polyolefins, which can be divided into two sub-classes: polyethylene and polypropylene. These conventional separators suffer from shrinkage at higher temperatures, which leads to safety concerns during high temperature operations. However, recent advancements in the use of natural minerals have presented additional options to solve this issue. [46]

2.3.5 Current Collectors

Current collectors are crucial parts of any battery, serving as a bridge between the current generated at the electrodes and the external circuit [47]. Cu is frequently used for the anode current collector, while aluminium (Al) is often used for the cathode [35]. Since Al forms an alloy with Li, Cu is instead used for the anode [47, 48].

2.3.6 Casing

The casing or enclosure on the outside of a battery helps protect the cells from harsh environments such as extreme temperatures, humidity, movement and vibrations. [49]

2.3.7 Terminals

In a battery, the terminals function as the electrical contacts between the battery and an external load. Electrons gather in the negative terminal and flow to the positive terminal during discharge [50]. Figure 2.7 illustrates the negative and positive terminals as well as the casing for a type of LIB.

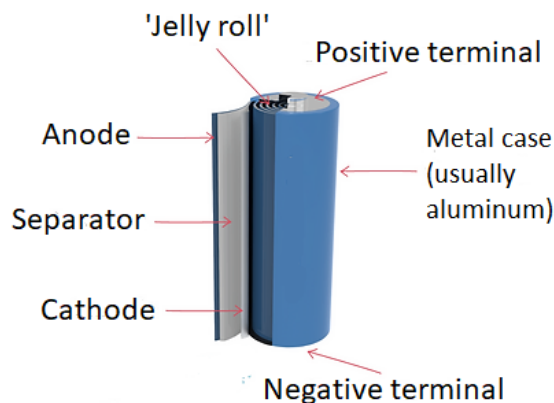


Figure 2.7: LIB Composition showing the terminals and the metal casing. Edited from EV FireSafe. [51]

2.3.8 A battery cycle

When the battery is charging, an electric pulse is given to the cathode, which in this example is made of LFP. This liberates a Li-ion and an electron from the LiFePO_4 cathode [33]. The Li-ion goes into the electrolyte while the electron conducts to the anode through an external circuit. As the FePO_4^- loses an electron and becomes FePO_4 , the cathode becomes more and more electronegative. This means that its urge to borrow an electron becomes greater, which explains why all the Li-ions and electrons are not released at the same time [35, 24].

The electron that goes through the external circuit does not move far. The metal atoms in the wire are combined with metallic bonds, where all the metal cores stand still and share the outer electrons that make up a sea of electrons. When the electron from the anode and cathode goes to the wire, the electron pushes the other electrons and creates a domino effect in the wire. This push works similar to a wave in the ocean. A wave mostly pushes the water molecules in a vertical direction and only a little in the horizontal direction. When the wave breaks on the shore, a lot of water molecules get washed up on the beach. Similarly, the wave of electrons piles up, causing a lot of electrons to enter the cathode. This is why the electrons travel between the anode and cathode at the speed of light. [35, 52]

After the Li-ions have deintercalated from the cathode, they go into the electrolyte by conduction. The electrolyte is attracted to the positive charge of the Li-ions and forms a protective shell around the Li-ion. This is called a solvation shell, and it allows the Li-ions to move freely in the electrolyte. In the cathode, this reaction occurs at millions of different places at each instant. [35]

Due to nature always seeking equilibrium, the electrolyte will always try to maintain a neutral charge with the amount of positive and negative ions it contains. The electron moves from the cathode to the anode almost immediately compared to the Li-ion. Therefore, when a Li-ion is conducted from the cathode to the electrolyte, the electrolyte will give up another Li-ion from the mixture of positive and negative ions. [35]

When the electron that was conducted from the cathode through the wire enters the anode, it bonds with a Li-ion that was conducted through the electrolyte. This creates a Li atom that sits between the layers of graphene and is held in place by the electrostatic force. This is called an intercalation. [35]

When the battery is fully charged, the anode consists of highly reactive Li with nowhere to send the electrons. The graphite does not want to absorb more electrons, and the electrolyte does not want to conduct more Li-ions. [35]

When the battery is discharging, the voltage that was set over the battery when charging is released. This means that the same force that made the Li-ions deintercalate from the cathode makes the Li-ions deintercalate from the anode through the electrolyte and back to the cathode. This intercalation process within the cathode facilitates the movement of ions and opens up an electronic pathway between the anode and cathode because of the imbalance of electrons and charge. With an imbalance of ions in the electrolyte, new Li-ions must be added from the anode. Li releases an electron to the graphite to become an ion. The electron then travels to the current collector and onto the wire. [35, 53]

Parallel to electrons taking the electrical pathway, the Li-ions take the ionic pathway through the electrolyte the same way as before. In the cathode, the FePO_4^- crystal structure intercalates the electron with the Li-ion to form a Li atom, returning the cathode to its original state of LiFePO_4 . [35]

At the beginning of the discharge, the difference in ion concentration between the anode and cathode is large. The difference in charge will decrease as the Li goes from the anode to the

cathode, and so will the voltage. When the voltage drops, the discharge cycle is considered complete, and the battery is ready to repeat the cycle. [35]

2.3.9 Manufacturing

This section focuses on the manufacturing of a pouch cell as this is the format that *Beyonder* uses. It consists of three main steps: (1) electrode manufacturing, (2) cell assembly, and (3) cell finishing, also known as formation. In each of these three main steps lies several smaller processes, each essential to the completion of a battery cell. This section will account for these processes for a conventional pouch cell. Figure 2.8 shows the different steps.

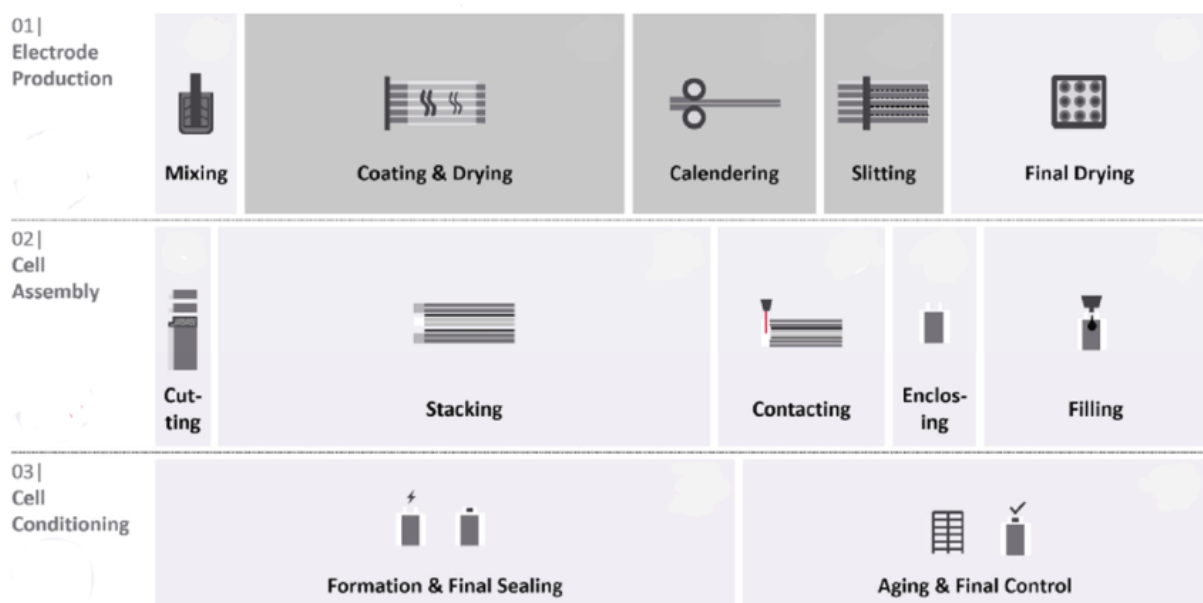


Figure 2.8: Processes present during manufacturing of a LIB pouch cell. Edited from Beck et al. [54]

Electrode Manufacturing

The electrode manufacturing step of the cell is divided into six distinct processes: mixing, drying, coating, calendering, slitting and final drying.

During the mixing process, different materials are combined depending on the batteries' cathode and anode chemistries. This process then mixes the slurry for a long time to ensure homogeneity.

The slurry for the cathode materials typically contains active materials such as NMC, a binder, a solvent and conductive additives. In almost 90% of cases, the binder is made up of a Poly(vinylidene fluoride)

The slurry for cathode materials typically contains an active material like NMC, a polymer binder

which is in 90% of cases Poly(vinylidene fluoride) (PVDF), a solvent like water or N-Methyl-2-Pyrrolidone (NMP), which is considered toxic [55], and conductive additives such as carbon. The anode slurry usually contains an active material like graphite, graphite-silicon, or HC, a conductive material like carbon black, and a polymer binder such as carboxymethyl cellulose [56, 57].

After mixing the cathode and anode slurries, they are then coated onto individual current collectors in a continuous coating process. The cathode and anode slurries binds to an Al and Cu current collector respectively, after which the electrode compounds are placed into a dry room to remove the solvents used in the slurry. [56, 57]

When the electrode compounds have finished drying, they are passed through a calendaring process, which involves the use of rollers. These rollers will “flatten” the compound into the required thickness and increase the density. [56, 57]

With the required thickness, the electrodes also have to be slitted, which means cutting them to achieve the width required by the cell enclosure. Subsequently, it is subjugated to a final drying process to remove any residual moisture that might be present. When this is completed, the electrodes are ready for the cell assembly process. [56, 57]

Cell Assembly

When the finished slitted electrodes are completed, they are cut one final time to have the proper dimensions in length for their given cell, after which they are put through a process called “electrode stacking”, where the cathodes, separators and anodes are stacked on top of each other. This can be done through single sheet stacking, z-stacking or windings, depending on the cell type, as shown in Figure 2.9 below. [56, 57]

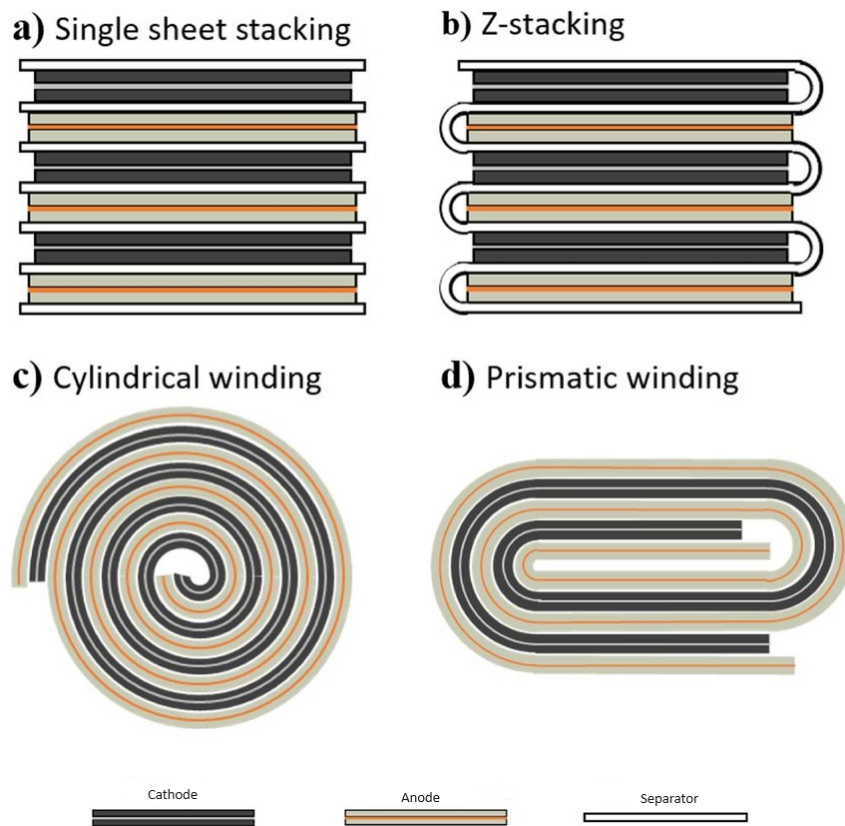


Figure 2.9: Different electrode stacking methods, a) Single sheet stacking, b) Z-Stacking, c) Cylindrical winding, d) Prismatic winding. Edited from Deng et al. [58]

When the electrode stacking is completed, the electrical contacting tabs are welded to the electrode current collectors. After this, the stacks are placed inside a pouch foil, sealed and excess material is trimmed and filled with the LE under a partial vacuum. [56, 57]

Cell Finishing

After the cells are finished, they are put through a formation process where they are subjected to their first charge and discharge cycle. This is where the SEI layer is developed and can take up to three weeks. During this process, certain gases are developed, swelling the battery cell. These gases are then released, and the cell undergoes its final sealing process. [56, 57]

When the battery has been completely sealed, it is placed in storage for its ageing process, in which the cell completes the chemical reactions that were started during the formation process to stabilize the performance of the cell. The final step before the cells are ready for shipping is to conduct quality controls regarding performance and safety. [56, 57]

As can be seen in Table 2.1 and 2.2, certain points far exceeds others in different categories. The manufacturing process's coating, drying and solvent recovery phases are prevalent in all three categories: costs, time and energy consumption. These processes account for almost 20% of the yearly costs of the production line, close to 50% of the energy consumption and well over 60% of the total manufacturing time. Note that this is for the production of conventional batteries and not with other cutting-edge technologies. [59, 60]

Table 2.1: Manufacturing costs per year of a LIB manufacturing process. Values retrieved from Liu et al. [59]

| Manufacturing Process | Costs per year [USD] | Percentage [%] |
|-----------------------|-------------------------|-------------------|
| Slurry mixing | 7,396,000 | 7.91 |
| Coating / Drying | 13,984,000 | 14.96 |
| Solvent recovery | 4,296,000 | 4.60 |
| Calendering | 4,849,000 | 5.19 |
| Slitting | 2,891,000 | 3.09 |
| Vacuum drying | 2,990,000 | 3.20 |
| Stacking | 8,086,000 | 8.65 |
| Welding | 6,864,000 | 7.34 |
| Enclosing | 11,636,000 | 12.45 |
| Formation / aging | 30,482,750 | 32.61 |

Table 2.2: Energy consumption and duration normalized per unit of a LIB manufacturing process. Values taken from Yuan et al. [60]

| Manufacturing process | Energy [$\frac{kWh}{cell}$] | Percentage [%] | Time [min] | Percentage [%] |
|---------------------------|----------------------------------|-------------------|---------------|-------------------|
| Slurry Mixing | 0.11 | 0.83 | 1.0 | 0.32 |
| Coating | 0.18 | 1.36 | 0.3 | 0.096 |
| Drying / Solvent recovery | 6.22 | 46.84 | 192 | 61.26 |
| Calendering | 0.38 | 2.86 | 1.2 | 0.38 |
| Slitting | 0.71 | 5.35 | 3.0 | 0.96 |
| Stacking | 0.77 | 5.80 | 3.0 | 0.96 |
| Welding | 0.25 | 1.88 | 1.2 | 0.38 |
| Enclosing | 0.69 | 5.20 | 4.8 | 1.53 |
| Formation / aging | 0.07 | 0.53 | 93.7 | 29.90 |
| Dry Room | 3.90 | 29.37 | 13.2 | 4.21 |

2.4 General Battery Terminology

For a better understanding of the analysis, this section explains the general battery terminology.

2.4.1 Ionic Conductivity

Ionic conductivity is the electrical conductivity caused by the motion of ionic charge in a substance [61, 62]. One method of measurement is called the ion transference number or ion transport number. This measures the ratio of the total current carried by that ion in an electrolyte [63]. The expression is shown in Equation 2.19, where t_+ is the transference number, I_+ is the current carried by the ion, and I_{tot} is the total current [64].

$$t_+ = \frac{I_+}{I_{tot}} \quad (2.19)$$

This means that if the transference number of an ion is close to 1, most of the total current is carried by that ion. When the transference number is large, the concentration polarization decreases, yielding a higher power density in a cell. Note that not every study uses ion transference numbers to refer to the transfer and conductivity of ions. Many of the currently existing LE technologies have a transference number that is less than 0.5. [65]

2.4.2 C-rate

A battery's C-rate describes its charge and discharge rates [66]. In other words, it measures the rate at which a battery is charged or discharged relative to its capacity. For example, a 1C rate means that a battery can provide 1A for 1 hour, during which the battery goes from 100% SoC to 0% SoC. A 2C rate would mean a charge/discharge time of 30 minutes, while a 0.5C rate corresponds to a charge/discharge time of 2 hours. Losses during charging and discharging affect the C-rate, especially in fast charges and discharges. Another term often used is the depth of discharge DoD. The terms SoC and DoD sums up 100% as shown in Equation 2.20. [3]

$$SoC = 100\% - DoD \quad (2.20)$$

2.4.3 Thermal stability

Temperature operates as a capacity indicator for batteries. Most batteries operate fairly similarly at different temperatures. At lower temperatures, batteries tend to have a lower capacity because

of the exponential relationship between conductivity and temperature. On the other hand, most batteries operate irreversibly at high temperatures, lowering their cycle life. [3]

The production of heat during the charging and discharging of a battery can be divided into two categories: reversible and irreversible. The irreversible heat depends on the C-rate, with higher C-rates resulting in greater heat release. In contrast, the reversible heat represents a smaller factor and is therefore less significant. However, the irreversible heat is of greater importance. The aforementioned heat can be quantified by examining the following equation, which illustrates the relationship between heat and the current and resistance within the battery. As the heat generated increases, the temperature of the battery rises. As previously stated, this will result in an acceleration of the battery's chemical processes. [67]

$$Q_{irr} = R \cdot I^2 \quad (2.21)$$

Thermal runaway is also an important factor in the thermal stability of a material. This is the maximum temperature a material can withstand before it triggers an exothermic reaction, producing heat faster than the battery can cool down. This rapid temperature rise can trigger further reactions and eventually lead to an aggressive fire. [3]

2.4.4 State of Charge

State of charge (SoC) is an important part of battery management systems (BMS), which are used to manage a battery. The SoC is used to assess rechargeable storage solutions' operational status and longevity. [68]

SoC refers to the battery's charge level and denotes the difference between a fully charged battery and the available energy stored in the same battery. This indicates the percentage of charge remaining in the battery, and it is used to determine the immediate usability and the estimated remaining runtime of the battery at any given moment. SoC is calculated using Equation 2.22 below. [68, 69]

$$SoC [\%] = \frac{Q(t) [Ah]}{Q_n [Ah]} \cdot 100\% \quad (2.22)$$

There are several techniques used to estimate the SoC of a battery, from utilizing simple current and voltage measurements, to conducting algorithms that incorporate thermal and internal resistance. [69]

2.4.5 Depth of Discharge

Depth of discharge (DoD) is a term used to indicate the percentage of the battery that has been discharged compared to the original capacity of the battery. It is considered to be complementary to SoC, meaning that whilst one increases, the other decreases and vice versa. An example of this can be that a battery with a SoC of 90% will have a DoD of 10%. Whilst this example will add up to 100%, there are cases where the percentage will go beyond this value. This can happen if the battery's capacity is higher than its nominal rating. Equation 2.23 below presents a method for calculating DoD. [70]

$$DoD = 1 - SoC \quad (2.23)$$

2.4.6 State of Health

State of health (SoH) reflects on the general condition and performance degradation of a battery during its operational lifespan. SoH incorporates factors such as capacity fade, increases in internal resistance and changes in charge acceptance, which are result cycling, ageing and external elemental factors [68]. State of health is calculated using Equation 2.24 below.

$$SoH [\%] = \frac{Current\ Capacity\ [Ah]}{Design\ Capacity\ [Ah]} \cdot 100\% \quad (2.24)$$

Various diagnostic techniques, including capacity testing and electrochemical impedance spectroscopy, are employed to evaluate SoH accurately. These methods provide insight into the battery's internal condition, mechanisms of degradation and tendency for failure, enabling proactive measures and maintenance. [68, 69]

To maintain the SoH of a battery, it is recommended that the operation of the battery is held between 20% and 80% of its capacity. If the battery is operated outside of this range, it may initiate unintentional chemical reactions, resulting in accelerated degradation and an increased likelihood of several safety concerns. [3, 71]

2.4.7 Degradation

Degradation in batteries is a term for the progressive loss of battery performance and storage capacity over time. This is a common phenomenon that will happen to all batteries, and no matter what preemptive measures are taken, it is bound to happen to some degree. This section will

account for and provide an overview of the different kinds of degradation types and mechanisms for general LIBs. [72]

There are three main causes of battery degradation: operational, environmental and time. Operational causes are factors that relate to how the battery is used and maintained. Charging habits are one of the most common user-caused degradation factors along with deep-discharging, which is where the battery reaches its maximum DoD before being recharged. [73]

Environmental causes encompass the surroundings of the battery is either stored or operates in. This can for example be the climate, temperature or humidity. Temperature extremes can in particular be damaging to the battery, with cold temperatures seizing functionality and warm temperatures speeding up degradation. [73]

Lastly, time based degradation occurs independently of other external factors and refers to the natural degradation of the battery, even when not in use. This type of degradation is often known as calendar degradation. Although this happens regardless of external factors, the severity is often influenced by the SoC the battery is stored at, with higher SoC usually leading to more degradation. [72, 73]

As there are several causes of battery degradation, there are also several underlying mechanisms that influence this process. In general, the degradation mechanisms can be divided into three distinct categories: particle cracking and loss of active materials, lithium plating and dendrites, and SEI growth.

Particle Cracking and Loss of Active Materials

One mechanism involves the loss of active materials (LAM) due to particle cracking which leads to a decreased volume fraction of active materials. Particle cracking is a phenomenon that occurs when the electrode materials contract and expand during the intercalation and deintercalation of Li-ions. This results in mechanical wear between the active materials and leads to fractures and stress within the material. This will ultimately lead to a degradation in capacity but can be mitigated by controlling the SEI-growth. [74, 75]

SEI Growth

As mentioned, the SEI layer is made of Li-ions, the solvent and the additive in the electrolyte during the first cycles of the battery. The SEI layer is vital for many reasons, however its continued growth and intake of Li-ions causes the battery to slightly degrade during each cycle it runs through. [76]

There has been a lot of research on the SEI layer, [33, 77, 78, 79, 80, 81, 82, 83, 84, 85, 86], but its behaviour is still being discussed [36, 37, 38]. For SEI growth in graphite anodes, one model assumes electron tunneling to be the rate determining step for the capacity losses and that can predict the calendar life and cycle life of a Li-battery [33]. Tunneling is a phenomenon whereby electrons that lack sufficient energy are unable to move between two locations with too much of a force barrier. The electrons then use a quantum-mechanical (de Broglie) wave, accumulate where the wave is growing and thin out where the wave is diminishing [87]. Since the SEI is conductive, some electrons will also go from the anode to the SEI layer. Therefore, some electrons will also go from the anode to the SEI layers. These electrons then count as losses. This is illustrated in Figure 2.10 (a) and explains that a solvent reduction is assumed to occur at the interface between the inner and outer SEI layers. As the solvent is halted, the velocity of Li-ions is reduced. This is facilitated by electron tunneling from the graphite anode through the inner SEI layer to the Lowest Unoccupied Molecular Orbital of the solvent [33].

The SEI layer also blocks most electrons from further decomposing the electrolyte and ensuring long-term electrochemical stability [33, 37, 43]. However, when the battery is not charging and is under open circuit conditions, the SEI layer can still be formed. Electrons can tunnel through the inner layer and reduce the solvent molecules at the inner and outer SEI interface when a battery is stored at an SoC above 0%. During the flow of electrons, the Li-ions will parallel diffuse through the inner SEI layer. This process results in capacity losses and is illustrated in Figure 2.10 (b) [33]. Over time, the SEI layer continues to grow, making a complex mosaic-type structure [34], which decreases the battery's capacity and limits its performance [43, 44].

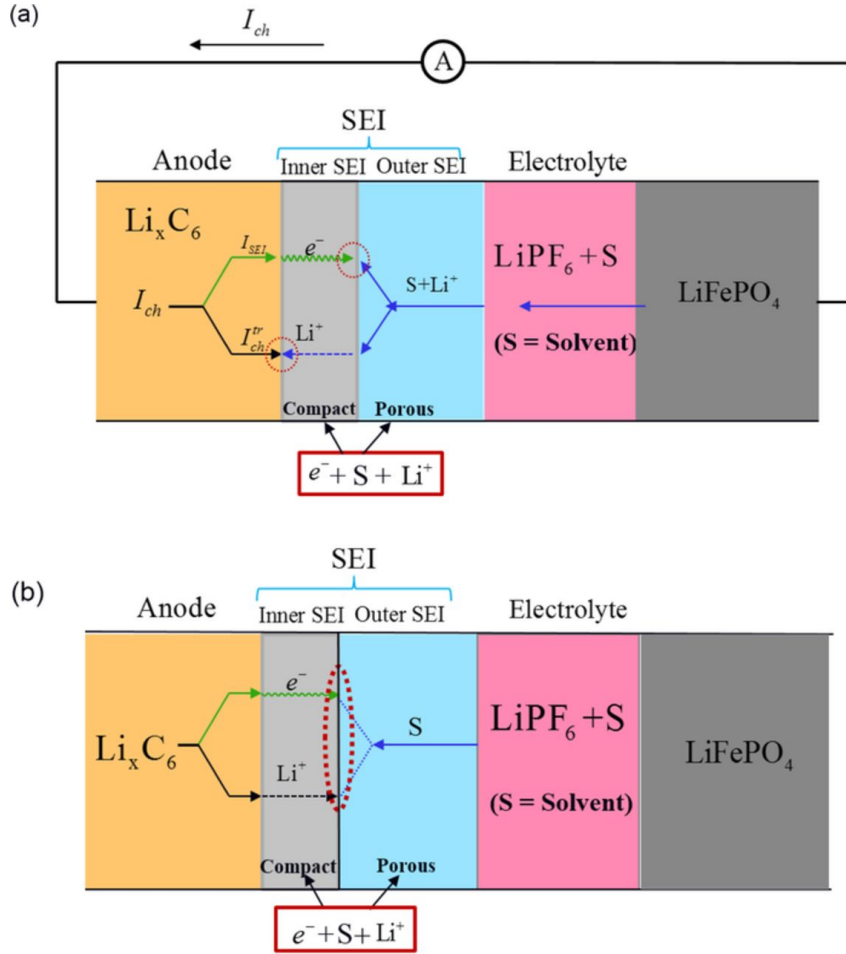


Figure 2.10: Illustration of a $\text{C6}/\text{LiFePO}_4$ battery showing the formation of the inner and outer SEI layers when charged (a) and stored in open circuit (b). Reprinted from Li et al. [33]

When the battery is being charged and discharged, the anode expands and contracts as Li-ions enter and exit. On the other hand, the SEI layer is solid and does not move fluidly. The rubbing leads to mechanical stress between the layers, which causes loss of active material and particle cracking. This results in the anode not being completely covered with SEI. The solvent becomes again exposed to the anode, forming a new layer of SEI. In this manner, SEI is expanding, and the volumetric changes create capacity losses upon cycling [33]. As the surface area of the SEI layer increases, the battery's internal resistance also rises. When the Li-ions go through the SEI layer, they meet more resistance, resulting in the Li-ions moving at a slower rate [3, 76]. This resistance is illustrated by an electrical circuit in Figure 2.11 [88].

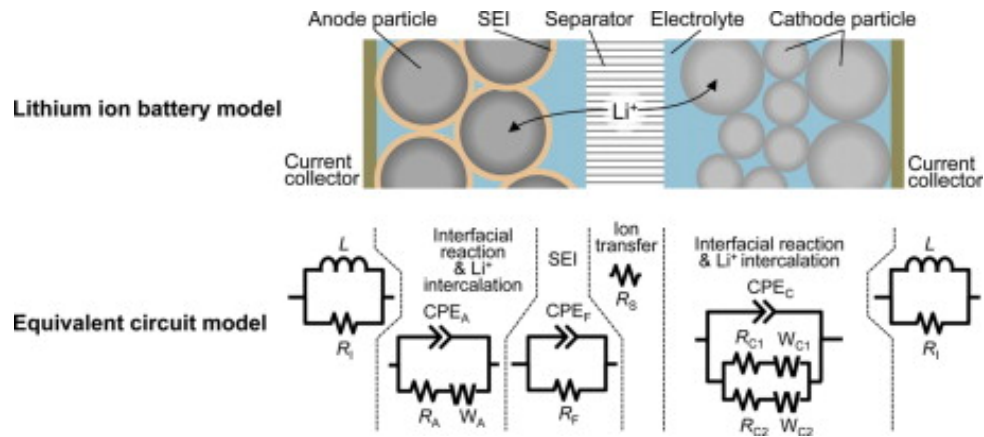


Figure 2.11: Illustration of the equivalent circuit of how the resistance in the SEI layer works. Reprinted from Osaka et al. [88]

The reduction reaction, which is responsible for the creation of the SEI layer, is exothermic and exhibits a distinctive energy profile. This energy can be released at high temperatures under the battery cycle. The fact that the reaction that forms the SEI layer is exothermic means that heat is released and entropy is increased, leading to greater general instability. This is supported by the standard entropy values for the SEI components. An increase in C-rate can also contribute to increase the level of entropy and stress. The entropy increase is a part of the SEI structure's evolution towards a maximum entropy state. This is often associated with equilibrium, stability and improved battery performance. If the levels of entropy on the other hand is too low or too high, it may have negative effects on the adaptiveness and structural integrity of the SEI. The double-layered structure of SEI, which both consists of organic and inorganic components, makes the thermodynamical aspect even more complicated. Factors such as the electrochemical double layer, surface tension, form and structure all contributes to the energy gradient in the SEI layer. In order to optimize the performance and lifetime of a LIB, it is essential to understand these thermodynamic aspects of SEI formation. [36]

The increased temperature also enhances the Li-ion diffusion. This makes the particles more prone to cracking and can lead to battery failure after extended cycling. If the temperature of the battery becomes too high, the electrolyte can also start to decompose and the SEI layer, especially the outer organic layer will destabilize. When the organic layer decomposes, new inorganic substances with low entropy are formed. Gas with high entropy and irreversible heat are released as byproducts. This process leads to the addition of new high entropy structures within the SEI. These structures eventually degrade and potentially initiate thermal runaway. In contrast, low temperatures slow down the SEI formation. This results in a more stable SEI layer, but the consumption of Li becomes high. [36]

Lithium Plating and dendrites

Lithium plating is a common phenomenon which occurs in Li-based batteries and can significantly alter the performance, capacity and safety of the batteries. Lithium plating occurs when Li-ions in the battery electrodes form an uneven metallic Li deposit on the anode. For lithium plating to occur, the battery has to either operate outside its intended temperature range or be exposed to unintentional usage behaviour. These scenarios are shown in Figure 2.12. When the battery is operating at a lower temperature than the batteries preferred temperature range, the chemical reactions and the intercalation of the Li-ions occur at a slower rate. Some of the ions are therefore not able to intercalate into the anode. Instead, they accumulate outside of the anode. As electrons are lost from the anode, they react with the Li-ions to form Li-metal atoms. As these Li-atoms accumulate, they form lithium plating. This is shown in Figure 2.12 (D). The ions not being able to intercalate also happens if the C-rate of the battery is higher than the ionic conductivity rate of the anode. As the Li-ions will not have time to intercalate into the anode material, shown in 2.12 (E). The same reaction happens when the battery operates at a high SoC, where the anode simply is too full of Li-ions to absorb more. This is shown in Figure 2.12 (F). [89]

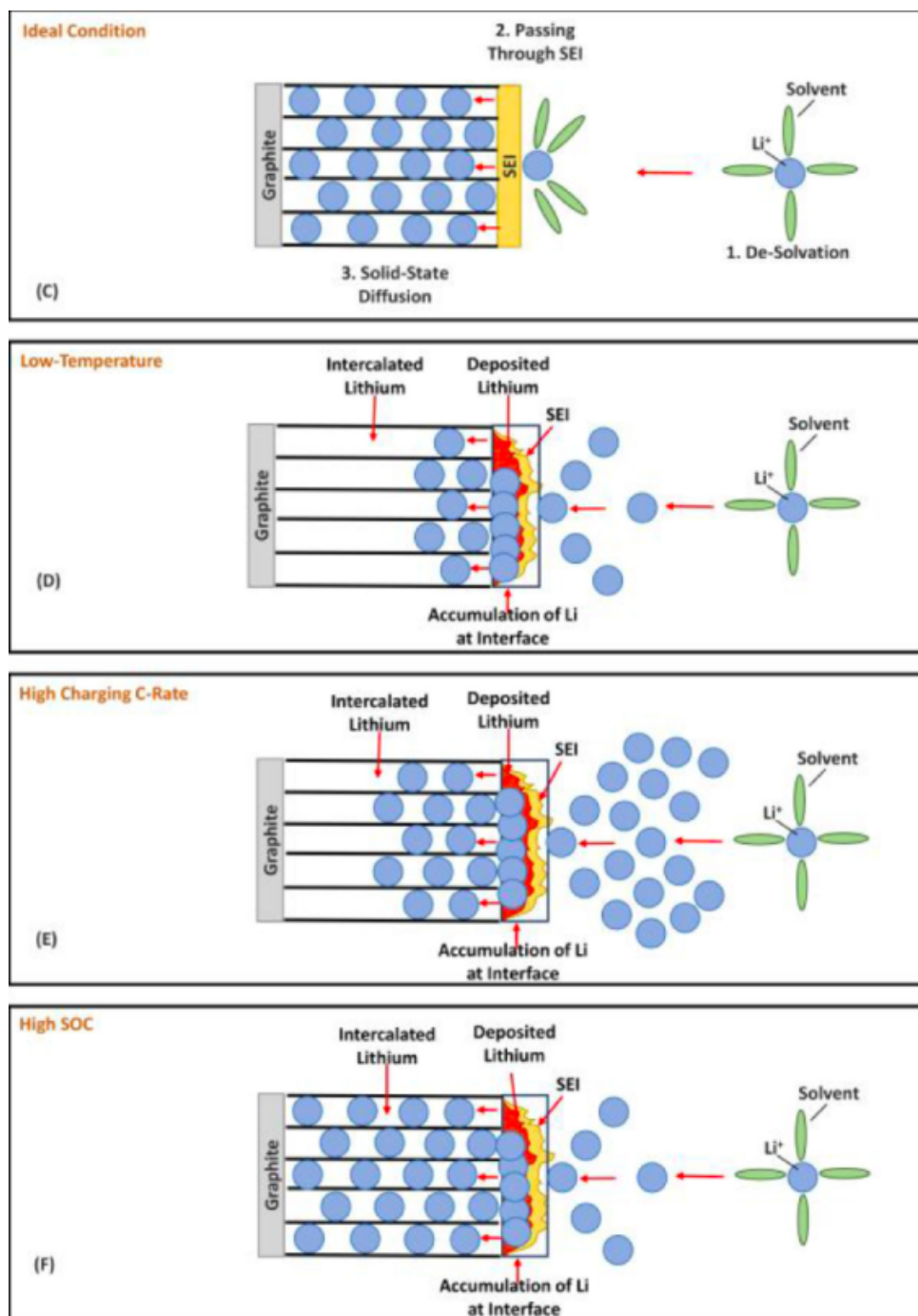


Figure 2.12: Illustration of the formation of lithium metal plating in three different scenarios. Reprinted from Lin et al. [89]

This plating of Li-metal can continue to grow under the same conditions mentioned above. The Li-metal will then start to grow filaments, called dendrites, through the electrolyte. This reduces structural stability and triggers thermal runaway, which is a process that increases the temperature uncontrollably [90]. Dendrites can grow through a structure's interstitial voids [91], which are empty spaces in a close packed crystal structure [92]. When the dendrite grows and

reaches the cathode, the battery is short-circuited, leading to the battery bursting into flames or in an explosion [93, 94]. A schematic is shown in Figure 2.13.

Despite the high Li-ion transference number, dendrite growth can occur through in the structure interstitial voids [91]. Interstitial voids are empty spaces in a close packed crystal structure [92].

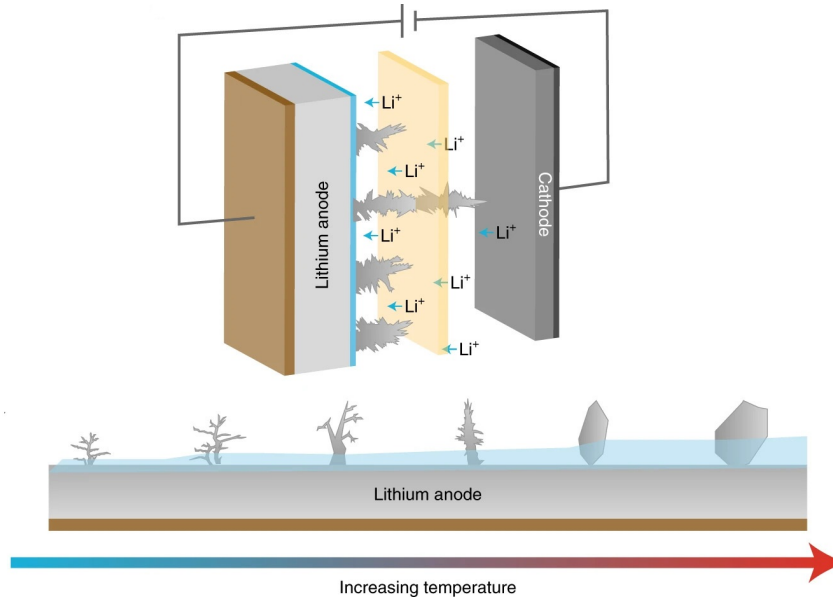


Figure 2.13: Dendrite formation in LIBs. Edited from Babu et al. [95]

2.4.8 Battery Cell Classifications

Batteries play a pivotal role in powering different systems and devices, providing a portable energy source for both smaller electronic and larger-scale applications. Primary and secondary batteries represent two energy storage technologies, each with distinct attributes. In this subsection, an explanation of both these technologies will be conducted, accounting for their advantages and disadvantages.

Primary Cells

Primary cells, often referred to as disposable batteries, are single-use batteries that are incapable of recharge. They convert chemical energy into electrical energy through an irreversible chemical reaction. When the reactants in the battery are depleted, the batteries become unusable and must either be disposed or recycled.

Secondary Cells

Secondary cells, also known as rechargeable cells, are designed and intended to be used multiple times, unlike primary cells. They store and release energy through a reversible chemical reaction,

allowing them to be recharged multiple times during their lifespan by applying an external current. This recharging process restores the chemical reactants, enabling the battery to be reused after depletion.

Secondary cells are generally lower in energy density than primary batteries but make up for it by being able to recharge. This makes them ideal for applications where the powered equipment is used frequently, or where external energy is abundant. Initially, the cost of secondary cells is much higher than with primary cells, but with an increasing number of charging cycles they offer significant cost savings over time as they can be recharged and reused, reducing the need for battery replacement. [96]

These cells are generally more environmentally friendly than primary cells due to their reusability. However, the production and disposal of these batteries still have environmental impacts, particularly in terms of raw materials extraction. Recycling options for secondary cells are more developed and effective compared to primary cells [97]. More on this in section 2.11.

Cylindrical Cells

Cylindrical cells were the earliest type of commercially produced cell in the early 1900s and have until recently been the most widely used packaging style for both primary and secondary cells. The cylindrical design is considered to be the most structurally sound design and can withstand tremendous internal pressures in comparison to cells with square designs [98, 99]. Figure 2.14 shows a cylindrical cell.

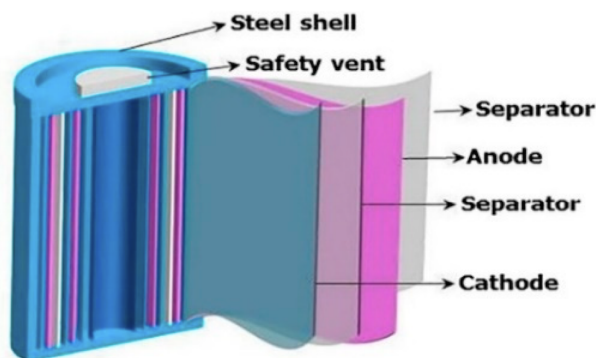


Figure 2.14: Sketch of a Cylindrical Cell. Reprinted from Abbas et al. [100]

During cell assembly, the anode, cathode and electrolytes are layered on top of each other and rolled up to fit inside the cylindrical compartment. This process makes these types of electrolytes crack because of their limited flexibility. In addition to this, their design makes the packaging density less desirable in comparison to the pouch and prismatic cells. [98, 99]

Companies such as Tesla primarily utilized cylindrical cells when making their EVs but have, in recent years, started transitioning to more space-efficient prismatic cells. However, they have sworn off pouch cells because of concerns of fires and thermal runaway. [101]

Pouch Cells

Pouch cells are typically used for Li-based batteries as an alternative to conventional cylindrical and prismatic cells. Unlike these traditional cell types, pouch cells offer unique attributes such as a reduction in weight and size and shape flexibility. In more recent years, they have become a widely used cell type for the automotive industry and for certain portable electronic devices. [102]

A pouch cell consists of all the typical battery components. In contrast to traditional cells, the internal components are stacked on top of each other in layers, enabling a flat design that works well in applications where space is limited. These layers are usually enclosed in a soft, flexible laminate which is vacuum sealed to minimize waste of space found in other cell types, often reaching a packing efficiency between 90 - 95%. The enclosure being both flexible and thin makes it vulnerable to punctures compared to a “hard-shelled” prismatic or cylindrical cell. A simple illustration of what a typical pouch cell looks like is presented in Figure 2.15 [102, 103]

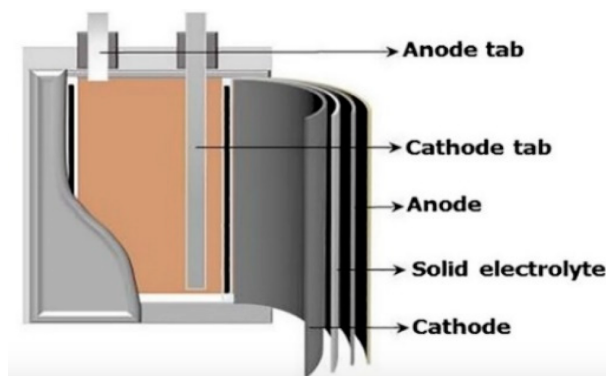


Figure 2.15: Illustration of a Pouch Cell. Reprinted from Abbas et al. [100]

Pouch cells are prone to a shorter service life when exposed to high temperatures and humidity. Furthermore, pouch swelling is a common occurrence. This is when gases that develop inside the battery expand the volume of the enclosure, which is typically a manufacturing error. It is accounted for by providing a designated pocket for gas expansion, which is removed before the cells leave the factory. Some swelling will inevitably occur regardless, but with a relatively low expansion rate of around 5% of its original volume. This is why pouch cells are stacked next to each other as opposed to on top of each other. [102, 103]

Prismatic Cells

Prismatic cells partially resemble pouch cells. The primary difference is the enclosure in a rigid rectangular box that allows for efficient and structured stacking of multiple cells into energy modules for scalability. Due to their usually larger size, fewer weld connections between cells are needed when scaling the modules for use in high-energy applications. These are especially good properties in, for example, the automotive industry, where energy density and specific energy are paramount. An illustration of the internal components of a prismatic cell is presented in Figure 2.16. [98, 103]

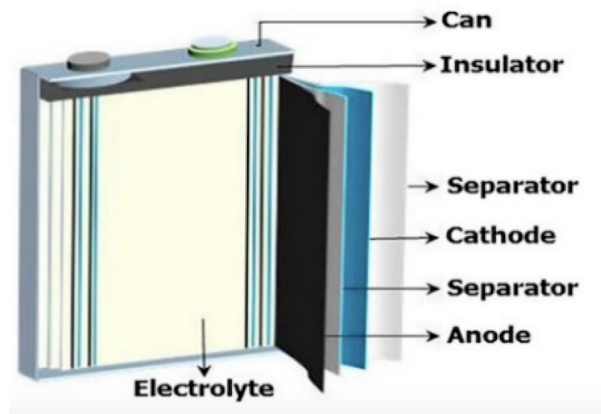


Figure 2.16: Illustration of a Prismatic Cell. Reprinted from Abbas et al. [100]

The format restricts shape variations, and the larger size of these batteries makes them unsuitable for applications with limited space. Because of their general shape and material selection, they are often more expensive than other cell types. [98, 103]

2.4.9 Technology Readiness Level

The Technology Readiness Level (TRL) is the most widely used scale for assessing the maturity of a technology. It enables the consistent comparison of maturity between different types of technologies. However, it lacks a clear definition, particularly in the field of renewable energy technologies [104]. This thesis uses the European Commission's categorization of TRLs from Horizon 2020. The Commission defines TRLs as follows: [105]

- TRL 1 - Basic principles observed
- TRL 2 - Technology concept formulated
- TRL 3 - Experimental proof of concept
- TRL 4 - Technology validated in lab

- TRL 5 - Technology validated in relevant environment
- TRL 6 - Technology demonstrated in relevant environment
- TRL 7 - System prototype demonstration in operational environment
- TRL 8 - System complete and qualified
- TRL 9 - Actual system proven in operational environment

2.5 Cathode materials

For a battery to successfully charge, it is important that the cathode material is able to intercalate, which implies for a lattice structure of the polycrystalline particles to host a guest atom [106, 107]. In a LIB, the guest atoms are Li-ions, while the structure of the cathodes changes depending on the composition of the mineral [107].

The combination of Li and O has a high cell potential and is highly reactive, as mentioned in 2.3.1. The high reactivity causes the elements to want to react with each other. At the same time, it means that reactions can occur with other unintended materials. This means that it is necessary to provide additional protection for the battery in order to prevent the occurrence of unwanted reactions, which is why the cathode is in need of other elements that are not as reactive. The cathode in LIBs consists of a “Li-ion donor”, which tells the primary properties of cell characteristics. The name of these LIBs are determined by what sort of donor or transition metal oxides the cathode consists of. Generally, the cathode composition of LIBs includes metals combined with Li. These metals often have partially filled up d-orbitals such as iron (Fe), manganese (Mn), nickel (Ni) and cobalt (Co), which are very flexible in terms of oxidation number [3]. This has led to the cathode materials that will be presented in this chapter: lithium cobalt oxide (LCO), nickel manganese cobalt oxide (NMC), lithium iron phosphate (LFP), lithium manganese iron phosphate (LMFP) and lithium nickel manganese oxide (LNMO).

The usage of transition metals is common due to their varying stages and structures, which can change depending on the quantity of electrons. When the different ratios of the transition metals react with O, various metal oxides are produced. This ability helps to stabilize the cathode material. Additionally, the change in compositions also gives the cathode material greater malleability. [3]

The variations in the chemical composition of LIBs result in distinct performance characteristics as shown in Figure 2.17. The greater the colors extend within a given metric, the greater the

performance in the given category [108]. All three LIBs presented are widely considered as common and in high demand in the commercialized market.

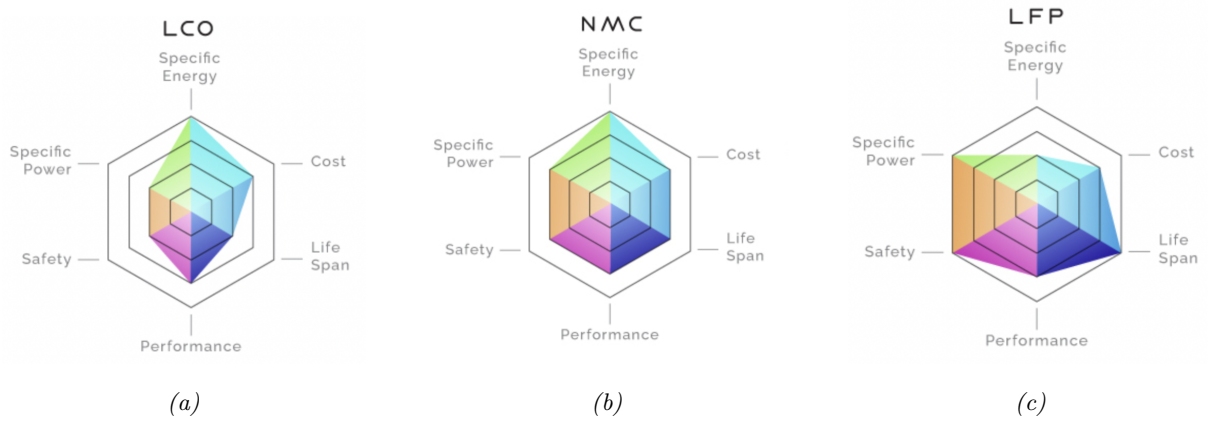


Figure 2.17: Performance overview comparing A) LCO, B) NMC and C) LFP. Reprinted from Kostandi and Wadsworth. [108]

2.5.1 LCO

LCO (LiCoO_2) became the first Li-ion chemistry to be commercialized in the early 1990s by John B. Goodenough, placing LIBs on the market [109]. Therefore, the standard LCO cathode serves as the foundation in the landscape of LIBs. [3]. LCO consists of a cathode layered with Li, Co and O components [110]. In this chemical composition, the transitional metal Co is used to stabilize the chemical composition in addition to increasing the cell voltage.

The reduction reactions happening in an LCO reaction is shown in Table 2.3. It shows that the LCO cathode has a cell voltage of 3.5-4.3 V. In Table 2.3, the x in $\text{Li}_{(1-x)}\text{CoO}_2$ is restricted to 55% to ensure the optimal quantity of depleted Li ions [3]. When the Co oxidizes from Co(III) to Co(IV), the cell voltage is reduced during discharge from 4.2 to 3.0 V [111].

Table 2.3: Table showing the reversible electrochemical reaction for LCO and graphite. [3]

| | Battery discharge reaction for LCO | E°/V |
|---------|-----------------------------------------------------------------------------------------------|--------------------|
| Anode | $\text{Li}_x\text{C} \rightarrow \text{C} + x\text{Li}_{diss.} + xe^-$ | 3.04 |
| Cathode | $\text{Li}_{1-x}\text{CoO}_{2,s} + x\text{Li}_{diss.}^+ + e^- \rightarrow \text{LiCoO}_{2,s}$ | 1 - 1.3 V |
| Total | $\text{Li}_{1-x}\text{CoO}_{2,s} + \text{Li}_xC_s \rightarrow \text{LiCoO}_{2,s}$ | 4 - 4.3 V |

The Co present in the cathode also determines the crystal structure, which is layered. This means that the atoms are chemically bonded in plain layers with relatively weak forces between

the atoms in adjacent layers [112]. These weak bonds are more flexible than other structures as the layers can slide from side to side [107]. The weak intermolecular forces between the layers also make the crystalline structure unstable. The Li-ions situated between the layers serve to reinforce the structure. As a consequence, about 55% of the Li can be deintercalated from the structure, otherwise the structure itself will collapse [3]. The layers consist of Co-centered octahedra, which give the Li-ions 2D mobility through the “tunnels” of the structure [111]. This layered crystal structure is illustrated in Figure 2.18. Each CoO_2 molecule occupies an interstitial hole, with a plane of O at both the top and the bottom, which forms the metal oxide. The Li-ions will again be located between the metal oxide layers. The layered structure gives the cathode material relatively open access, leading to easy pathways for the ions to intercalate. This attribute increases the material’s ionic conductivity [113]. The mobility of Li-ions within the layered cathode active material varies with their state of charge [114].

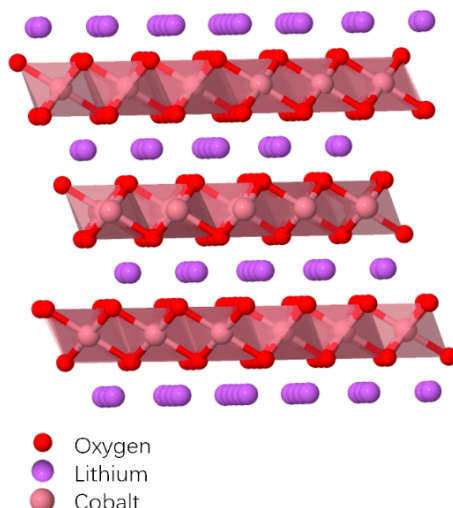


Figure 2.18: Illustration of the layered structure of LCO. Published by The University of Liverpool. [115]

Conventional LCO batteries are in high demand within the market of portable electronics such as mobile devices, computers and other digital tools. Despite LCO batteries possessing a high specific energy and energy density, they are declining in popularity compared to other LIBs, such as NMC. This shift can be attributed to several factors, including financial, environmental and political considerations. More on this in sections 2.11 and 2.10. Additionally, LCO batteries rely on a rate of Li-ions at only 0.55, resulting in a relatively limited life span of 500-1000 cycles, short specific power and poor thermal durability. Nevertheless, LCO batteries have paved the way for experimenting with other cathode mixtures in order to achieve lower costs and higher density in terms of energy and power. [110, 116]

2.5.2 NMC

The NMC (LiNiMnCoO_2) cathode consists of various mineral ratios of Ni, Mn and CoO_2 . In contrast to the LCO battery, the NMC battery was first introduced to the commercial market in 2004. In two decades it has become one of the most thriving conventional LIBs within the EV and plug-in hybrid electric vehicle (PHEV) sectors used by companies such as Toyota, Volkswagen, Audi, Ford and many more. Its success lies in the combination of the transition metals Ni and Mn with Co in the cathode. [109]

These layered materials in an NMC cathode have a structure like rocksalt, with alternating layers of Li and metal ions in a cubic close-packed O array with an ABCABC stacking sequence. This structure, shown in Figure 2.19, makes it easy to move Li-ions during intercalation, thereby increasing the ionic conductivity. This is because the practical capacity of layered materials depends on how many different ions can be added and taken away. The key is the ratio of Ni:Mn:Co. In particular, the exchange of Li for Ni between the layers, helped by Co, can have a big effect. Irreversible changes to the surface can also affect performance, causing impedance to rise and capacity to decrease. [117]

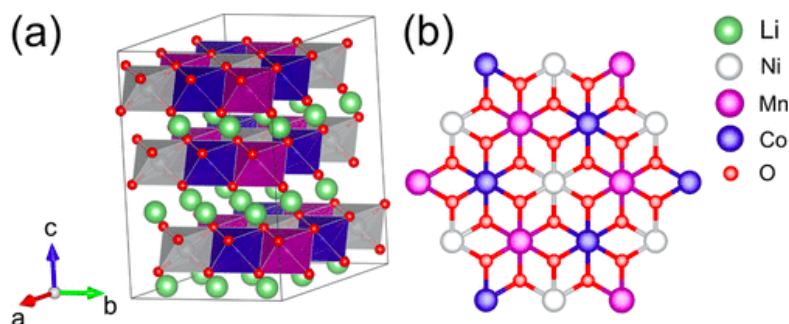


Figure 2.19: Illustration of the crystal structure of NMC as a cathode material. Reprinted from Garcia et al. [118]

Ni contributes largely to increasing the overall cell voltage of the composition because of its high reduction potential [119]. The Co stabilizes and makes up the layered structure of the composition. The Mn also contributes to stabilizing the structure and furthermore strengthens the bonds between the different layers. Due to this, the layers do not need as much support to keep the structure in place, which increases the flow of ions compared to LCO, as shown in Figure 2.20. This enhances both the capacity and the ionic conductivity of the cathode material. Nickel, together with cobalt, acts as an amplifier, enabling higher capacities. Increasing the amount of nickel to cobalt allows NMCs to achieve higher energy densities at the same voltage as

LCO. In addition to nickel being slightly lighter than cobalt and capable of holding more Li-ions, resulting in higher specific energy [25]. This enables NMC structures with a high nickel ratio to achieve higher energy densities, as depicted in Figure 2.52 [120].

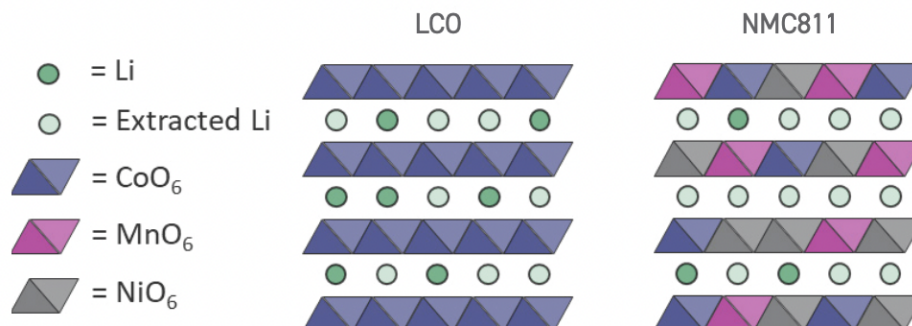


Figure 2.20: Graphic illustration of how NMC811 stores more Li-ions than LCO. Reprinted from Marie and Gifford. [120]

As shown in Figure 2.5, Ni offers a high potential cell voltage. Mn, on the other hand, is low on specific energy but exhibits higher thermal stability. When combined, the metals achieve a complementary interaction, playing on each other's strengths. The ratios of Mn, Ni, and Co are usually based on one-third of each metal, known as the 1-1-1 ratio. However, due to a Co bottleneck, various combinations with less Co, such as the 8-1-1 or the 9-5-5 ratio, are being viewed as promising for the future of the EV market. [109, 116]

The NMC metric in Figure 2.17 shows that it has a high specific energy, meaning it enables EVs to achieve a greater range in a single charge. Additionally, it has a relatively long life span and high safety. Greater cycle life means NMC cells can undergo more charge-discharge cycles before deteriorating. [109]

2.5.3 LFP

Another common cathode material for LIBs is LFP (LiFePO_4). The (Fe^{2+}) and phosphate (PO_4^{-3}) are strongly bonded together to form iron phosphate (FePO_4) inhabiting seven electrons in the outer orbit [33]. This means that FePO_4 takes the outer electron from the Li to reach a more steady state. The components then become charged as FePO_4^- and Li-ions [33, 35, 24]. The LFP uses the transition metal iron (Fe) to stabilize the compound. The phosphorus (P) is used to increase the reactivity and to create stronger bonds in the crystal structure.

It is the olivine crystal structure for LFP that determines the batteries' electrochemical prop-

erties, the diffusion coefficient of Li-ions, the thermal stability and the electrochemical stability. The crystal structure of LFP is illustrated in Figure 2.21. The structure consists of FeO_6 octahedra, which share an edge with an LiO_6 octahedra, which are in turn connected by a PO_4 tetrahedra. Collectively, this forms a three-dimensional spatial network structure called $\alpha - \text{LiFePO}_4$. As the Li-ions deintercalates from the cathode, the FePO_4 is formed in a crystal which is almost identical to the LiFePO_4 , as shown in Figure 2.21. During the deintercalation, there is a relatively small volumetric change of 6.81%. This translates to a lower degree of degradation as mechanical wear within the battery and promotes/prompts good cyclability and longevity. [121]

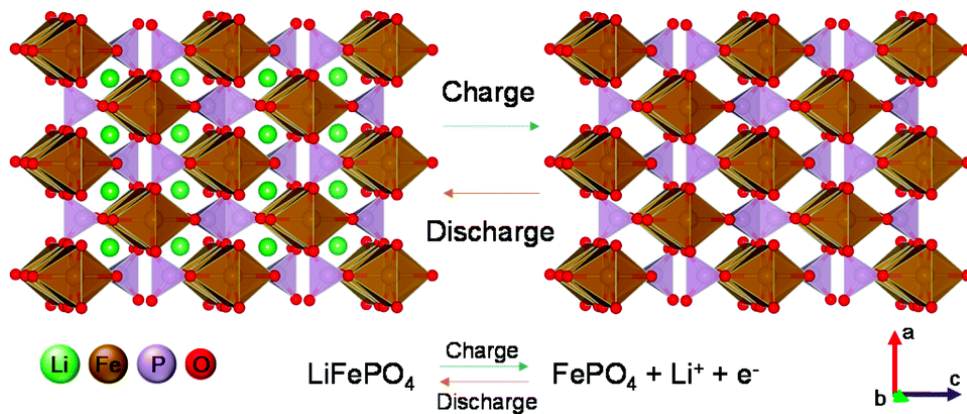


Figure 2.21: Illustration of the crystal structure for LFP. Reprinted from Hu et al. [121]

The strong covalent bond between the P and the O in the LFP also contributes to good thermal stability, cyclability, and safety [121]. The strength or “stiffness” of these bonds makes the rate for the phase change of the cathode material increase. The longer it takes for the cathode to intercalate Li-ions, the longer it takes for the material to charge and discharge. This means that the C-rate and specific power of LFP is longer than other cathode materials [122].

The size and weight of the cathode material is relatively large, both due to the olivine crystal structure and the weight of Fe. The olivine structure has a larger volume than for example the layered structure. This means that the specific energy and energy density is reduced. [121, 122]

The poor ionic conductivity in LFP comes from both the olivine structure and the redox reactions of iron. Despite this, LFPs are capable of using smaller particles which increases the surface area per unit volume, subsequently increasing the active sites where Li-ions can attach. As a result, the LFPs ability to take up more Li-ions is enhanced, which increases the ionic conductivity and capacity. [121]

A distinctive feature of LFPs is that the cathode material initially intercalates the Li-ions in the

outermost core of the cathode. Consequently, during the discharge process, a shell of FePO_4 will form with a shrinking core of LiFePO_4 . This implies that the LFP cathode does not undergo a completely uniform phase transformation. When the cathode material is charged, both the start and end of the phase transformation has a uniform change in oxidation state. However, during the middle of the charge when the battery has reached a certain state of charge, the battery reaches an almost stationary state where virtually no Li-ions deintercalate out of the cathode. Towards the end of the charge, the potential changes rapidly until a single phase region is reached. This is illustrated in Figure 2.22. [123]

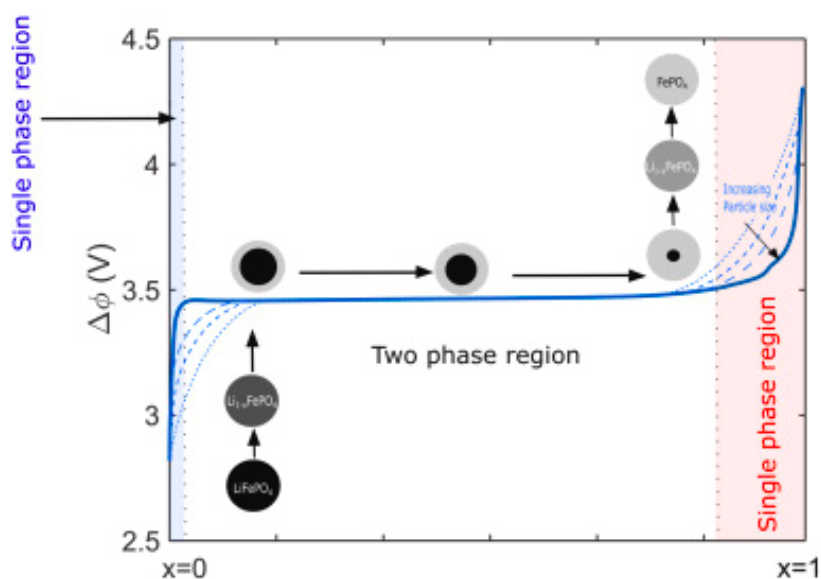
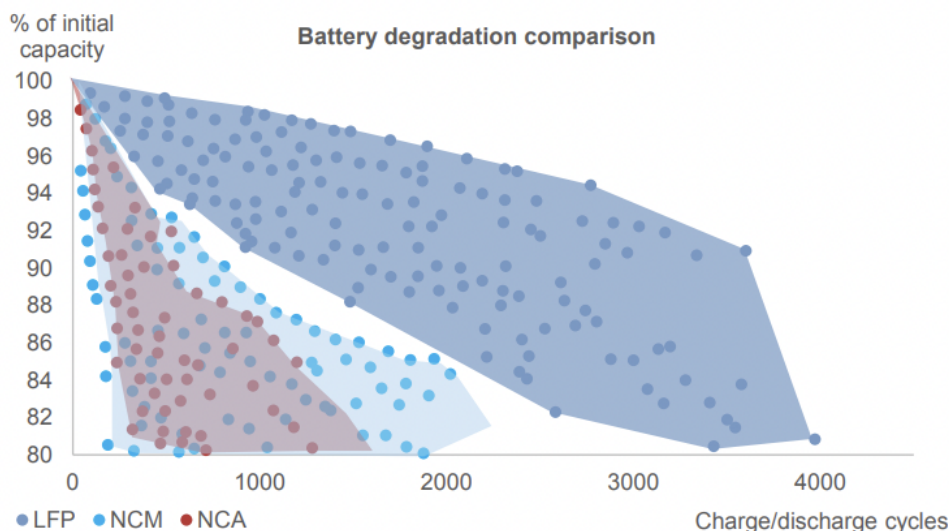


Figure 2.22: Illustration of the rate of charge for LFP. Reprinted from Gunnarshaug et al. [123]

This phenomenon presents a challenge to the utilization of LFP cathodes in systems. The small differences in the curve make it difficult for systems to know what the state of charge is for the battery between 20% and 80% state of charge. The system can, for example, think it has a 40% rate of charge while it actually has 20%. When this happens, the battery has to be fully charged for the battery to calibrate the state of charge. This is critical for the transportation, as the driver has to know the distance one can overcome without charging the battery. [123]

Although the LFP battery was introduced to the market in 1999, prior to NMC, it did not experience the same rapid adoption. A fundamental pillar of LIB development, especially within the EV market, is specific energy, as illustrated in Figure 2.17, where LFP exhibits the lowest characteristic/feature among the three batteries. LFPs continue to be regarded as a highly promising cathode material in the future due to their overall performance as it has great specific power, life span, and inherent safety. Figure 2.23 displays how LFP batteries exhibit excellent durability and extended life cycles at around 2000 complete charge and discharge cycles. [124,

109, 116]



Source: Preger et al. (2020)

Figure 2.23: Graphic illustration comparing LFP batteries to NMC/NCM. Reprinted from Bhandari et al. [125]

2.5.4 LMFP

LMFP (LiMnFePO_4) is a type of LIB whose cathode is constructed on the basis of LFP cathode chemistries and is considered to be a promising successor due to their enhanced electrochemical properties, such as an increase in specific energy by 20-40% [120, 45]. While still maintaining the safety and production costs of regular LFPs [71]. LMFP is different from LFPs because of the introduction of Mn as a partial replacement for a portion of the iron found in LFPs. These kinds of batteries are not conceptually new but have only recently become a viable option, meaning limited data is available. A resurfaced interest from *Gotion* and LMFP production expansion from other Chinese companies shows that there is potential for mass production of LMFPs for automotive applications [126, 127].

LMFP has the same crystal structure as LFP. The difference is that LMFP has partially switched out some of the Fe atoms with Mn atoms. This makes the two crystal structures slightly different, but they are both still in the olivine family of crystal structures. Olivine has the structural formula AB_2O_4 , where A and B occupy the tetrahedral and octahedral cavities of an hexagonal close packed (HCP) O network. In the case of LMFP, there is a significant difference in the distribution of Li-ions compared to other similar compounds. Li-ions are arranged in chains,

sharing edges and running parallel to the $[010]$ direction. In contrast to the distribution of $(\text{Mn}, \text{Fe})\text{O}_6$ octahedra, which share corners with four other $(\text{Mn}, \text{Fe})\text{O}_6$ octahedra and with four PO_4 tetrahedra, one of them via one edge. The structure reveals the existence of tunnels that can be used to remove Li-ion cations along $[010]$, as illustrated in Figure 2.24. [128]

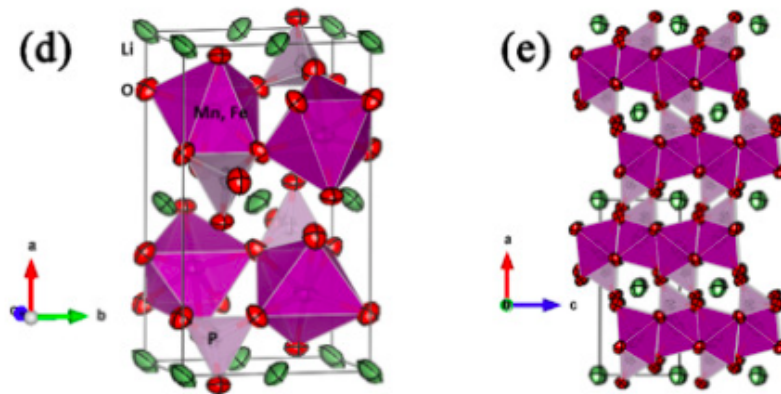


Figure 2.24: Illustration (d) shows the crystal structure for LMFP while illustration (e) demonstrates the presence of channels oriented along the $[010]$ axis, facilitating the diffusion of Li-ions. Reprinted from Li et al. [128]

A similar graph on the charge cycle for LFP has not been found for LMFP, but it is presumed that the graphs will exhibit a high degree of visual similarity [122, 30]. This renders LMFP a suitable alternative for the majority of applications previously addressed by LFP.

LMFP cathodes share many similarities with the manufacturing of LFP cathodes but are constantly being researched to reduce cost and improve performance [129]. This is needed because of certain disadvantages the introduction of Mn into the cathode imposes. LMFPs generally have a cycle life of around 2000-3000 cycles [126]. LMFPs also come with an increase in low-temperature performance and a relatively high capacity retention of around 75% at -20° [130]. The properties of LMFPs are rated as shown in Figure 2.25.

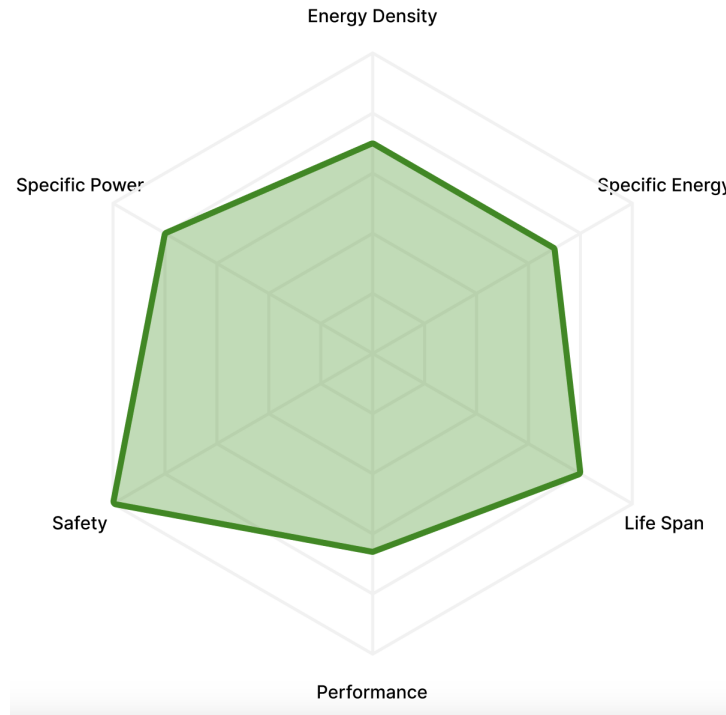


Figure 2.25: Performance Overview of LMFP Based On Data From Table 2.4

2.5.5 LNMO

LNMO (LiNiMnO_4) cathodes are a new material composition within battery technology. It is considered a prospective chemistry for high-power applications because of its potential high voltage delivery, reaching up to 5.0V during lab testing [131]. An illustration of the spinel structure is shown in Figure 2.26. Multiple battery manufacturers plan on commercializing these cathodes by the end of 2025, showing promise for mass manufacturing [132]. Since it is a fairly new technology, limited data regarding actual cell characteristics are available.

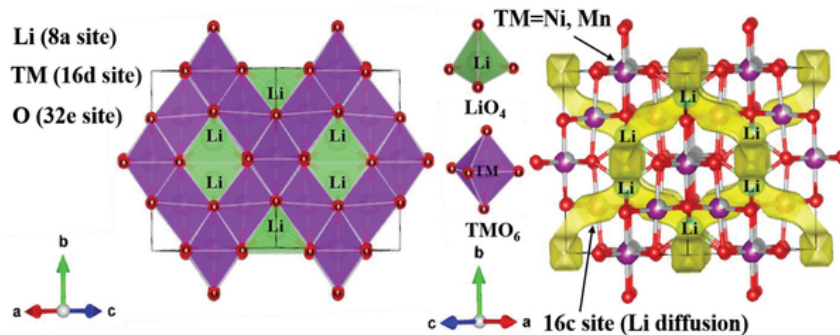


Figure 2.26: Illustration of the crystal structure of LNMO. Reprinted from He et al. [133]

However, there are some theoretical values available. According to *Ossila*, a cathode material

producer, and a study conducted by Cui et al., the cathode composition has a high theoretical energy density of $\approx 690 \text{ Whkg}^{-1}$ [134]. In addition, a study by Nisja found that the LNMO composition suffers from several degradation mechanisms, including carbonate electrolyte deterioration and surface degradation resulting from the high contents of Mn [135]. However, an SEI layer is not formed, which is explained further in [122]. The cathode material also demonstrates low resistance in low temperatures.

2.5.6 Summarising values

There have been rapid advancements within the cathode chemistries over the last decade. Ultimately, this has led to properties no longer being compatible with values dating back to 2015 or even 2017. The specific energy of LIBs has improved from a density of 140 Wh/kg to over 250 Wh/kg. In EV applications, this allows for a range of ca. 600 km on a single charge. For the various cathode chemistries, this implies that there is a broad range of values on specific energy. [124]

Table 2.4 is a summary of the characteristics of different cathode chemistries.

Table 2.4: Table of the properties of different cathode materials

| Cathode chemistry | LCO | NMC 1-1-1 | NMC 5-3-2 | NMC 6-2-2 | NMC 8-1-1 | LFP | LMFP | LNMO |
|---------------------------|---------------------------------------|---------------------------------------|------------------|------------------|------------------|-----------------------------------------|------------------|------------------------------------|
| Voltage [V] | 3.8–4.4 [3] | 3.8–4.0 | | 3.8-4.0 | 2.5-4.2 [136] | 3.2–3.5 [3] | 3.4-4.0 [45] | 3.0-5.0 [136] |
| Specific energy [Wh/kg] | 120–150 [137] | 140-193 [138] | 219-250 [138] | 255-290 [138] | 144-300 [138] | 90-200 [138] | 210-250 [120] | 690* [134], 150-165 [136] |
| Energy density [Wh/L] | 250–450 [137] | 230-567 [138] | ~650 [138] | ~700 [138] | 532-740 [138] | 362-457 [138] | 280-300 [136] | 250-280 [139] |
| Specific power [W/kg] | 600 [137] | 500– 3000 [137] | | | | 1400– 2400 [137] | | |
| Power density [W/L] | 1200– 3000 [137] | 6500 [137] | | | | 4500 [137] | | |
| Cycle life (ideal DoD) | 500- 1000 [136] | 1250- 1750 [138] | 1750 [138] | 1200* [138] | 1500 [136] | 2000- 5000 [136] [138] | 2000- 3000 | 250-500 [136] |
| C-rate [C] | 1 [136] | 1 [136] | | | | 1-3 [136] | | |
| Thermal runaway [°C] | 150°C (higher when empty) [116] | 210°C (higher when empty) [116] | | | | 270°C (safe at full charge) [116] | | |
| Operating temp range [°C] | -20 to +60 [137] | -20 to +55 [137] | | | | -20 to +60 [137] | | -20 to +60 [140] |

* Indicates theoretical values

2.6 Anode materials

The anode material plays a crucial role in determining the safety and cycle life of a LIB [141]. In this chapter, carbon and non-carbon based materials will be presented. Figure 2.27 is a chart that illustrates the different kinds. This section focuses on graphite (C_6), graphite doped with silicon (Gr-Si), and hard carbon (HC) for the carbon-based materials. Among non-carbon-based anodes, lithium titanium oxide (LTO) is explored.

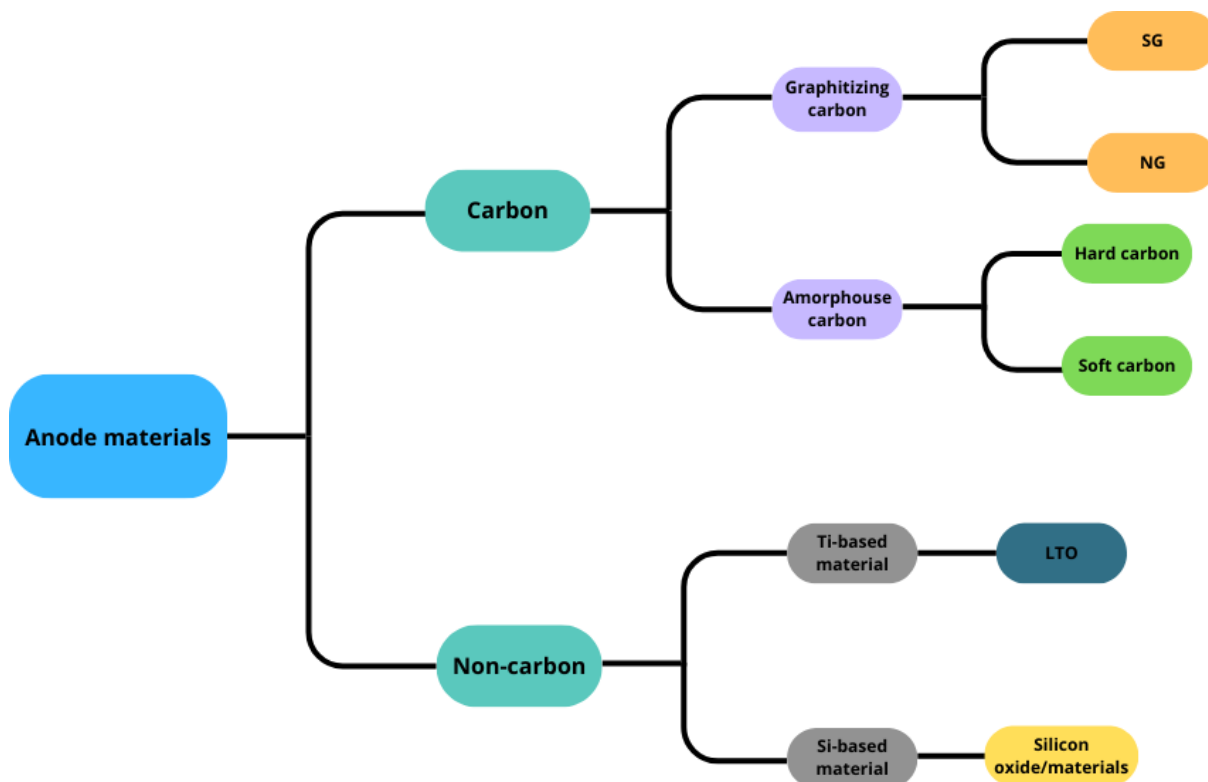


Figure 2.27: The chart displays an overview of anode characteristics. Reprinted from Xinghao Lu. [142]

Currently, carbon-based materials are seen as the most cost-effective and convenient anode materials. However, the safety of the anode materials can be limited in large-scale applications. Because of their low operating voltage (under 0 V vs Li^+/Li), the materials also have safety challenges regarding dendrite Li growth. This reduces the cycleability and safety of the anode [141]. The difference between graphite, soft carbon (SC), and HC is the level of crystallinity (structural order), as shown in Figure 2.28.

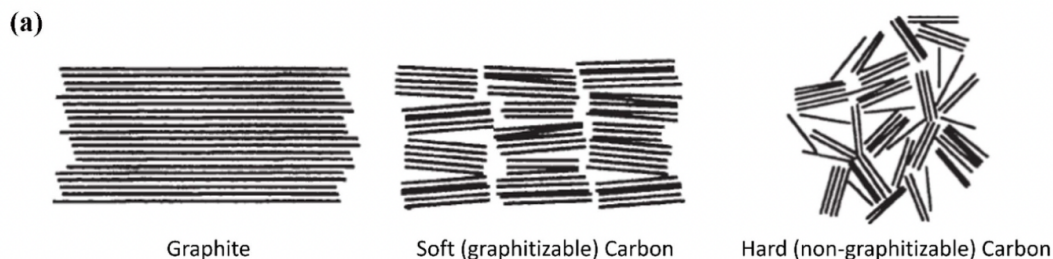


Figure 2.28: Illustration of carbon based anode materials different crystal structure during phase change used in LIBs, a) Graphite b) soft carbon c) HC. Reprinted from Crabtree et al. [143]

The properties of the relatively new anode material LTO seem to fill some of the gaps that carbon-based anode materials have not been able to fill. As a relatively new material, it's quite low down the TRL scale, but it's an exciting technology to keep an eye on. [144, 141, 145]

2.6.1 Graphite

The most frequently used anode material is graphite (C_6). It is cheap, has good electrical conductivity, and has a low reduction potential. It consists of multiple layers of graphene, which is six carbon atoms arranged in a hexagonal lattice, illustrated in Figure 2.29. The layered structure of C_6 makes it, as mentioned with the layered cathode material, easier to intercalate and deintercalate Li-ions in the 2D plane. The layered structure also reduces the capacity of the battery. Because of weak bonds between the layers, the material can only deintercalate 55% of the Li-ions to keep itself from breaking. Another aspect comes with the intercalation of Li-ions, which leads to mechanical wear in the battery and causes the battery's capacity to be reduced [53]. Eventually, the structure collapses and makes the battery uncyclable [3].

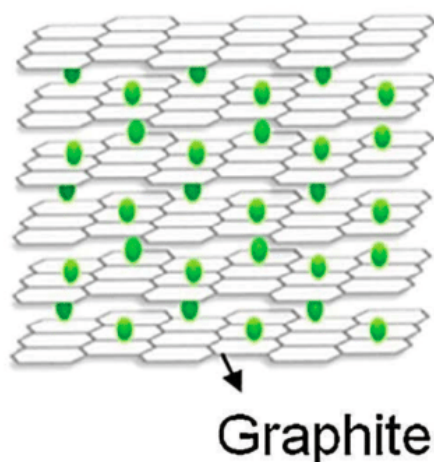


Figure 2.29: Illustration of the crystal structure of graphite. Reprinted from Katja Kretschmer. [146]

The structure also has a small volumetric change of 7% during the intercalations [124]. The two-dimensional mobility does however make the graphite able to expand and contract slightly. This means that there is some mechanical wear in the battery. More on this in 2.4.7.

Furthermore, the graphite can either be mined from the earth, categorized as natural graphite (NG), or obtained from petroleum coke (graphitized) and called synthetic or artificial graphite (SG). In terms of cost and carbon footprint, NG production is more economical and environmentally friendly. Yet, SG is preferred and the most common graphite type due to its longer life span, rapid charging and relatively more uniform performance in batteries. In addition, constructing an SG plant is less time-consuming than extracting NG through mining. [147]

2.6.2 Graphite doped with silicon

By doping the graphite with silicon, the silicon bonds between the layers in the crystal structure become stronger, thus leading to a strengthened anode material structure. The silicon can, in addition, absorb 10 times more Li-ions than graphite, which will increase the ionic conductivity of the anode material significantly [71]. The bonds between the Si and C also increase the ionic conductivity [148]. Overall, the ionic conductivity in the anode is increased with added Si in the graphite, which is crucial for achieving high performance and long battery life.

When the silicon is absorbed into the graphite, there is not much of a structural change, as shown in Figure 2.30. The silicon is formed in a hexagonal pattern and the layered structure is maintained, thus resulting in a preservation of stability and structural integrity. [148]

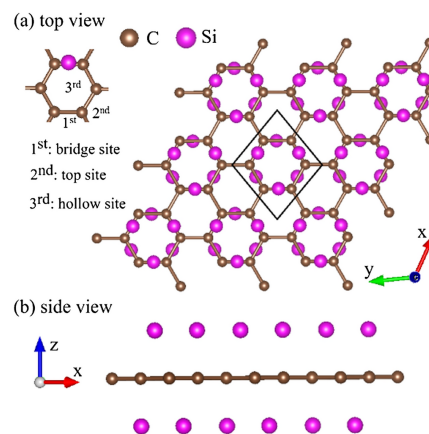


Figure 2.30: Illustration of the crystal structure of graphite doped with silicon. Reprinted from Nguyen et al. [148]

However, the addition of silicon in the graphite anode leads to accelerated degradation. From each cycle, the anode material swells by 400% as the Li ions intercalate [124], which eventually

leads to pulverization of silicon as shown in Figure 2.31. If the ratio of Si shows a volumetric change smaller than 60%, the energy density is still larger than that of graphite [149]. This shows that the ratio of silicon in the cathode is very important. If there is too much silicon, the battery casing can not handle the large volumetric change. The substantial enlargement of the battery also results in increased mechanical wear within the battery, which will affect the state of health of the battery. [150]

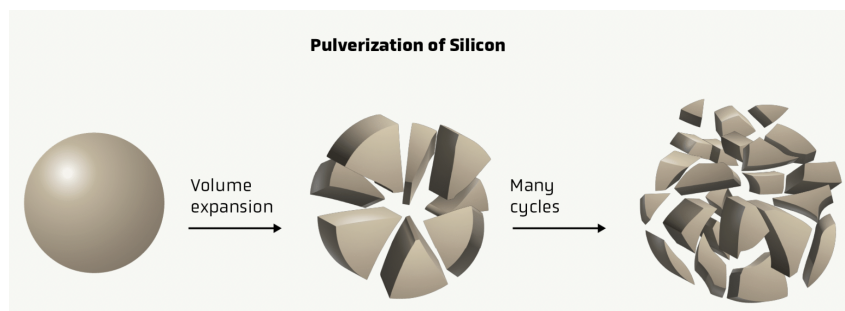


Figure 2.31: Illustration displays the pulverization of silicon when its volume expands during swelling. Reprinted from Choi and Aurbach. [150]

2.6.3 Hard carbon

Among the commercial alternatives to graphite, HCs are selected for their moderately superior ion conductivity. In this thesis, HC is looked into as this is the anode material Beyond utilizes [151]. HC is an anode material commonly used in sodium-ion (Na-ion) batteries and LIBs. It is composed of amorphous carbon and a three-dimensional cross-linking network. This is one of the factors that gives HC superior overall performance compared to graphite. [152]

HC is the least lamellar structure [142] of the three carbonaceous materials that does not transform into graphite at temperatures higher than 3000°C. In other words, HC is not graphitizable. The crystal structure is complicated and difficult to illustrate. Figure 2.32 shows the progression of making a detailed illustration of the HC structure throughout the years. The structure has a lot of non-planar, curved, bent, dented, twisted, and curled graphene layers [153].

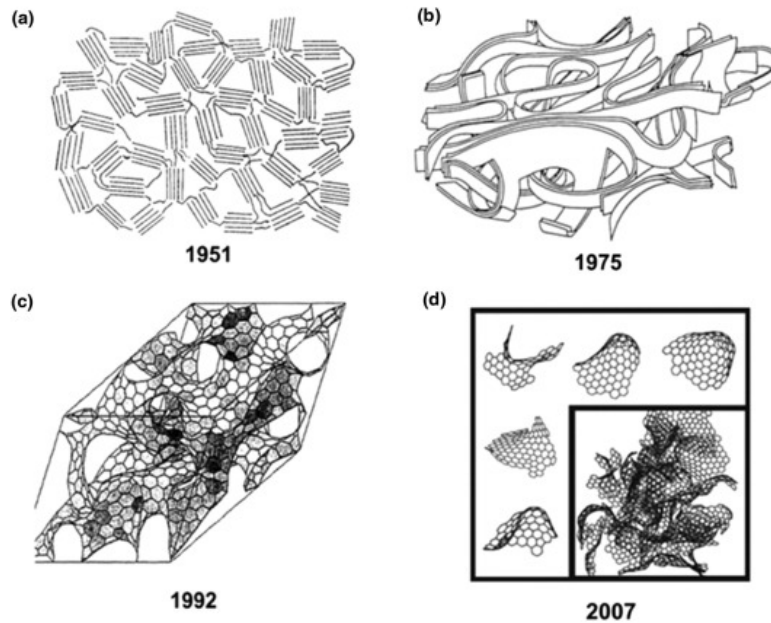


Figure 2.32: The atomic structure of HC in various years. Reprinted from Dou et al. [153]

The enhanced crystalline structure of HC enables it to accommodate a substantial quantity of Li-ions. This property facilitates the intercalation and deintercalation of ions, thereby enhancing the cycling performance and fast charging capabilities [152]. These characteristics give HC considerably different electrochemical properties than graphite, such as good cycling life and higher specific capacity, which is more suitable for high-power and hybrid vehicles. The complicated structure also gives undesirable properties, e.g., low efficiency, poor rate performance, low potential Li storage, and potential lag [142].

2.6.4 LTO

LTO anode is a new and promising anode material with a relatively high voltage. Under intercalation there is a minuscule phase change from spinel-LTO, shown in Figure 2.33a, to rock-salt-LTO, shown in Figure 2.33b. During the phase change, three Ti^{4+} ions (spinel-LTO) are reduced to Ti^{3+} (rock-salt-LTO) ions. During this redox reaction, Ti^{4+}/Ti^{3+} has a steady-state plateau at ~ 1.55 V vs. Li^+/Li where it accepts three inserted Li-ions [145]. The anode material has a large oxidation potential, which relates to a high cell voltage [141]. On the other hand, the spinel structure gives the material a low theoretical specific capacity [144].

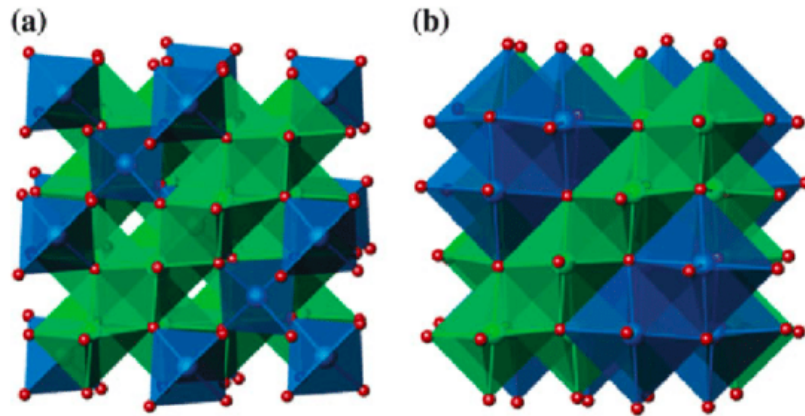


Figure 2.33: (a) Illustration of the spinel crystal structure of LTO (b) Illustration of rock-salt-LTO after intercalation of Li-ions and phase change. Reprinted from Katja Kretschmer. [154]

While LTO exhibits high thermodynamic stability, it can also operate at a high voltage and avoid dendrite formation. This correlates to the battery having high safety and cycle life [141, 145]. The spinel structure of LTO prevents the electrolyte from reducing on the electrode surface which enhances the stability of the battery [141]. For a considerable period, it was assumed that the absence of an SEI layer on the exterior of the LTO anode would be a permanent phenomenon. However, subsequent observations have demonstrated that this is not the case. [145]. As the reduction potential of LTO anodes is higher than the reduction potential of most electrolytes, the anode does not form a stable SEI layer. However, some stable layers may still appear in the mosaic structure. The stability of the different SEI layers differs with various operating conditions, such as temperature and charging rate. Therefore, the structure of the LTO SEI layers looks different from the regular SEI layer. Nevertheless, it remains important for the LTO anode's stability and safety and to protect it from reacting with the electrolyte and form gases [145].

There is almost no change in the volume of the solid-arranged spinel structure. The near-stationary anode is known as a “zero-strain” material [141, 145]. It therefore acts like a ceramic with open ion channels [122]. This means that LTO has a high specific power, high thermal capacity, and a high C-rate [145] of up to 10C [136].

The high C-rate and the outer layer of the material make the anode quite reactive. As mentioned earlier, this means that the material wants to react as much as possible. Therefore, there is a high risk of unwanted reactions occurring within the battery. This is a factor that reduces the security of LTO, but not to a large extent. Research shows that the outer layer can start to form

gases inside the battery, which decreases the stability of the battery. Despite this, the safety is still significantly better than the commercialized anodes. [145]

2.6.5 Summarising values

As it was not possible to find some of the values, a dot system has been used in Table 2.5. This system ranks the different values from one to four dots, the more dots the higher the value. these dots are only set up relative to each other and based on the authors' perception of the sources found. In order to be able to refer to some of the values and to get some perspective on the dots, the values that could be found have been retained.

Table 2.5: Table of the properties of different anode materials.

| Anode chemistry | C_6 | Gr-Si | HC | LTO |
|----------------------------------|---------------|------------------------|--------------------|-----------------------------------|
| Voltage [V] | • (0.1 [122]) | •• (>0.1 [122]) | • • • (0.75 [152]) | • • •• (2.4 [147]) |
| Specific energy [Wh/kg] | •• [147] | ••• [147] | ••• [142] | • (50-80 [147]) |
| Energy density [Wh/L] | • | • | ••• [152] | •••• (130-177 [147] [137]) |
| Specific power [Wh/kg] | | | | (750 [137]) |
| Cycle life (ideal DoD) | •• | • | ••• | • • •• (3000-7000 [147]) |
| C-rate [C] | | | | •••• (10 [136]) |
| Safety [overall] | • [45] | • [45] | •• [45] | • • •• (One of safest LiBs [116]) |
| Operating temperature range [°C] | | | | -40 to +55 [137] |
| Volume change [%] | •• (12 [155]) | • • • (12<X>400 [155]) | | • (1 [155]) |

2.6.6 Sodium-ion Batteries

Implementing Na instead of Li in the anode to make sodium-ion batteries (SIBs) has been explored, as the battery chemistries have demonstrated a high degree of similarity. Na is Earth's fourth most abundant element, making it substantially more available and cheaper than Li. Furthermore, Al current collectors can be used on both the anode and cathode as Na metal does not alloy with Al. A noteworthy point is that Na has a molar mass that is over three times that of Li and is a larger element, meaning that the specific energy and energy density of SIBs will typically be lower. [48, 156]

By weight percentage, about 7% of a typical LIB is made up of Li [157]. Because the anode element does not comprise too much of the total weight and size, shifting from Li to Na does not significantly impact the specific energy and energy density gravimetric and volumetric energy density [71, 156]. However, challenges remain in competing with LIB in terms of energy density while maintaining a sufficient cycle life [158].

2.7 Liquid-State Batteries

Liquid-state batteries are currently dominating the electrochemical market, particularly in areas such as EVs and mobile power devices [159]. Possessing a liquid electrolyte is what makes them a liquid-state battery. Li, aside from being a highly accessible and non-toxic resource, is incredibly light and electropositive. These fundamental traits enable LIBs to have greater energy storage capacity over other battery chemistries [109].

2.7.1 LIBs Compared to Other Batteries

Figure 2.34 displays both volumetric energy density and specific energy density. A typical LIB can provide a cell voltage of 3.6 V, three times as much as the Ni-Cd and Ni-MH batteries. For Ni-Cd to achieve the same cell voltage as LIBs, three Ni-Cd batteries must be connected in series [160]. As shown, Li-metal batteries (LMBs) have in theory greater energy densities than LIBs, however they continue to be labeled as unsafe [159]. More on this in section 2.8. Due to LIB being lightweight and having a high voltage, they have a greater energy density than other secondary batteries [160].

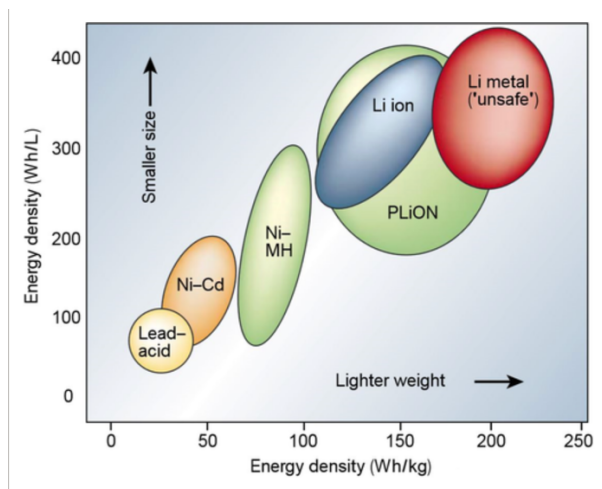


Figure 2.34: Illustration of energy densities in Wh/L and Wh/kg for different batteries. Reprinted from *Da Deng*. [159]

2.7.2 Liquid Electrolytes

LEs were the first commercially used electrolytes for batteries and are the most commonly used and widespread because of their maturity. These kinds of electrolytes, in the case of LIBs, are typically composed of a Li-salt dissolved in some type of solvent and additive [35]. The primary function of these electrolytes is to facilitate the movement of Li-ions between the cathode and anode during charge and discharge cycles. LEs are considered to have high flexibility due to the absence of solid components, and they exhibit high ionic conductivity. However, they are often lacking in mechanical strength and stability. [161, 162]

Most LEs are not electrochemically stable at both high and low voltages, which hinders the use of high-voltage cathodes and low-voltage anodes such as Li-metal, thereby limiting the energy density. [163]

Common solvents include different types of carbonates, such as ethylene and propylene. Ethylene carbonate-based electrolytes are the most popular of the two and have been proven to be a good option for low-voltage cathode materials, but they cannot facilitate the use of high-voltage cathodes because of relatively low anodic stability $\approx 4.3\text{V}$. This bottleneck restricting electrochemical performance has resulted in a shift towards new electrolyte compositions that cater to high-voltage cathodes. These electrolytes are often less expensive and more established than other types. [161]

Ionic liquids are extremely safe options and are considered to be “non-flammable” and can facilitate high-voltage cathodes with an electrochemical stability between 3V - 5V. Ionic liquids are

less established in the industry, meaning they are often expensive and difficult to manufacture electrolytes. [162, 164]

2.8 Solid State Lithium-ion Batteries

In recent years, there has been a growing interest in alternative battery technologies, among which SSBs stand out as one such technology. This type of battery was conceptualized earlier than the current conventional batteries, but LE batteries ended up being commercialized first. [165]. This section delves into what SSBs are, how they operate, and some of the different types of existing technologies.

2.8.1 Definitions and Basic Principles of SSBs

On a fundamental level, SSBs differ from conventional batteries in that the electrolyte is a solid state electrolyte (SSE), made up of a solid material rather than a liquid. The SSE generally acts as both a Li-ion conductor and separator membrane [166]. In addition, Li-metal is often utilized as the anode in favor of the commonly used carbon-based anodes. This has reportedly provided the batteries with higher energy densities, higher power densities, higher safety, and longer life cycles compared to LIBs [167]. Figure 2.35 depicts the solid components in an SSB

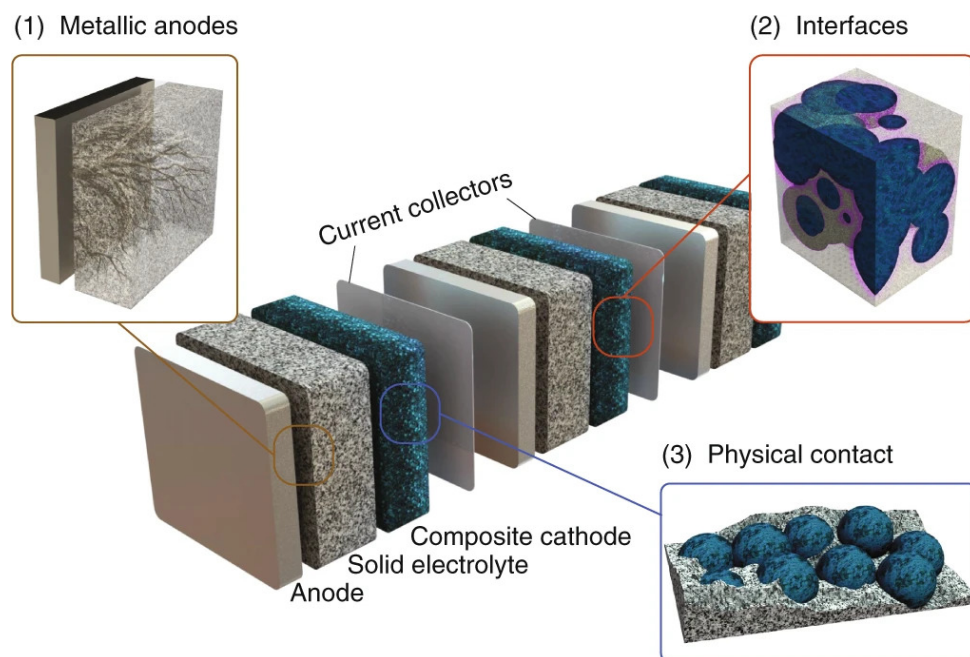


Figure 2.35: Schematic of an SSB cell. Reprinted from Famprakis et al. [168]

Based on their geometry, SSBs can be divided into three types:

- **Thin-film**

Thin-film types are usually made by placing layers of cathode, solid electrolyte, and anode one after another. Figure 2.36 illustrates this. The resulting structure usually has a thickness of less than 15 μm , but this can vary. These demonstrate good cycle stability for

thousands of cycles and SSEs with low ionic conductivity. However, due to limitations in the electrodes, the thickness needs to remain low, and therefore, the energy from thin-film SSBs is also limited. [167]



Figure 2.36: Thin-film SSB. Reprinted from Huang et al. [167]

- **Three-dimensional**

Three-dimensional has higher cell energy than thin-films, but their fabrication is more difficult as it is challenging to weave together the electrodes in the given patterns [167]. The way these patterns can differ from the thin-film is shown in Figure 2.37.

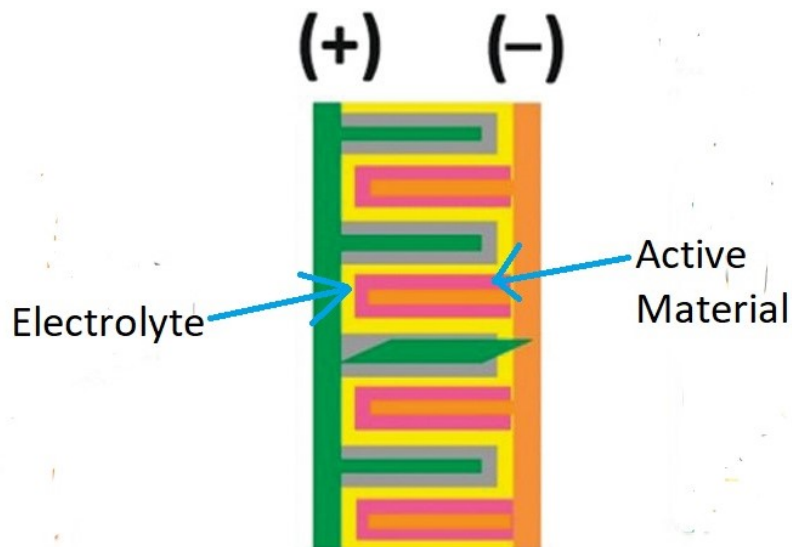


Figure 2.37: Three-dimensional SSB. Edited from Huang et al. [167]

- **Bulk-type**

Bulk-type geometries are electrode structures similar to conventional LIBs, where the electrodes are mixed with active materials, additives, and an SSE that is ionically conductive and electronically non-conductive. A visualization is shown in Figure 2.38. Since the thickness of the cell can be several hundred micrometers, the energy of the cell is high [167]. However, they have poor interfacial contact [169, 170]. Nevertheless, bulk-type SSBs are suitable for large energy storage devices compared to thin-films [171].

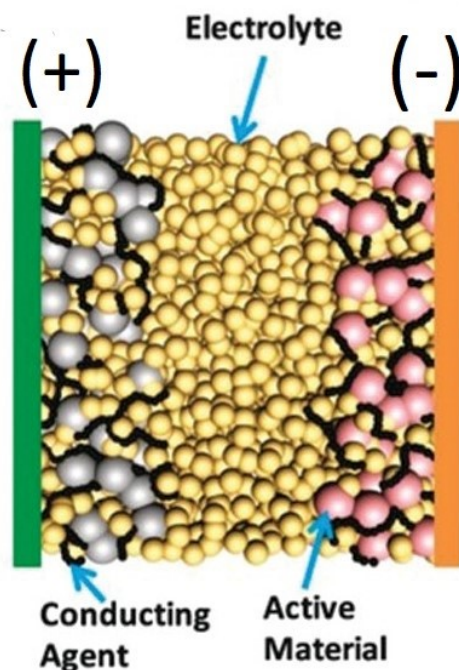


Figure 2.38: Bulk-type SSB. Edited from Huang et al. [167]

In contrast to LEs, it has been demonstrated that SSEs enable the utilization of high-voltage cathodes and low-voltage anodes. In several SSB chemistries, the use of a low-voltage Li-metal anode, in particular, is a key reason for the high energy density in an SSB. While replacing the LE with an SSE improves the safety of the battery, it also decreases the overall gravimetric density on an individual cell level. When combined with Li-metal, the individual cells show an increase in both the energy density and specific energy that can be compared to conventional LIBs [172]. Additionally, Li-metal has a high theoretical specific capacity, low density and the lowest reduction potential (-3.04 V vs. SHE) as shown in 2.5 [173, 174, 175, 176]. Table 2.6 shows the different properties of Li-metal. The dot is based on the same system as in the previous anode and cathode chemistry tables.

Table 2.6: Table of Li-metal properties

| Anode chemistry | Li-metal |
|-----------------|---------------|
| Voltage / V | 2.5-4.2 [147] |
| Specific energy | 400-450 [147] |
| Energy density | 800 [147] |
| Cycle life | • [147] |

Lastly, an SSB battery pack enables bipolar stacking where the layers are stacked in one package, thus reducing the amount of dead space and inactive parts that are involved in a series stack of conventional LIBs [167]. An illustration of this is shown in Figure 2.39.

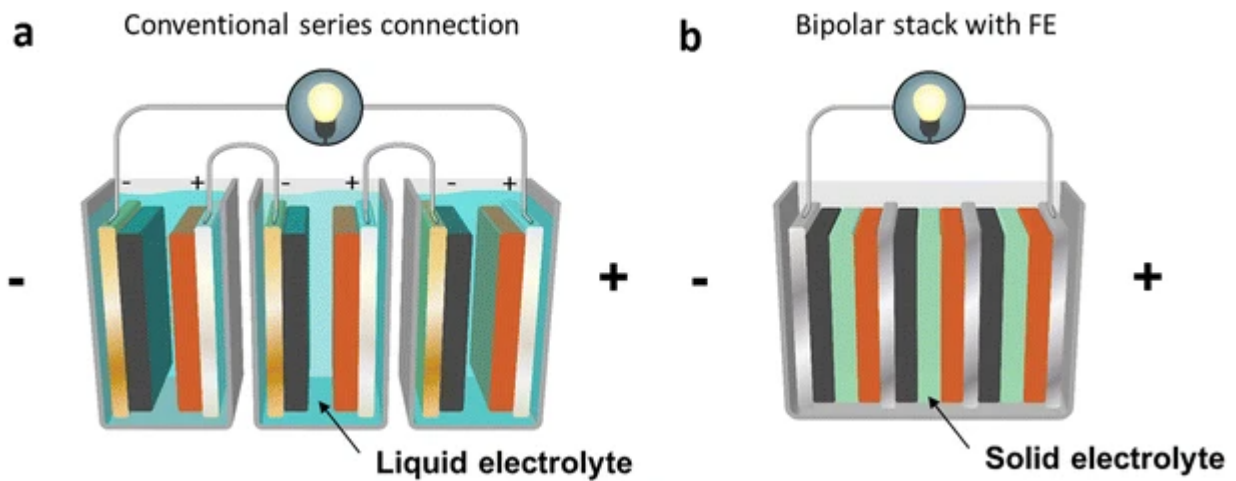


Figure 2.39: Comparison of the cell stacks in a conventional series connection and in an SSB stack. Reprinted from Placke et al. [177]

A prominent reason for an SSEs ability to facilitate Li-metal anodes is the reduction of Li dendrite formation rates. As mentioned in 2.4.7, dendrite formation is a major concern when dealing with Li-metal. During the beginning of commercialized LIBs, the use of Li-metal was deemed too dangerous as it caused several accidents due to dendrite formation appearing at faster rates in LEs than in SSEs. Therefore, an LE with a carbon-based anode became a safer alternative. However, in SSBs, Li-metal is more applicable. Dendrite formation remains a safety concern but to a significantly lesser degree. [93]

The solid materials in SSBs exhibit a higher thermal conductivity than the liquids in commercialized batteries. This can help remove temperature hotspots inside the battery and allow for better thermal stability, making SSBs more reliable than traditional LIBs under high-temperature conditions [167]. Moreover, the stiffness of the electrolyte often leads to poor physical contact

between the electrodes and the electrolyte [178]. Nevertheless, the kinetic performance of SSBs has been shown to give them a higher power density than conventional LIBs. The high ionic conductivity of some SSEs at low temperatures is one reason for the kinetic performance. This also means that SSBs have the potential to operate at very low temperatures where LIBs would decrease in performance, meaning that SSBs can have a wider operating temperature range. Another reason for the kinetic performance is that the Li-ion transference number in many SSBs is around the ideal, $t_{\text{Li}^+} = 1$ [91, 167, 179], which is significantly higher than the transference number in traditional LEs (less than $t_{\text{Li}^+} = 0.5$) as stated in 2.4.1. Because of this, there is both a higher amount of Li and no concentration overpotential involved in SSEs compared to LEs as depicted in the plots in Figure 2.40. Plot (a) shows one type of SSE with a higher ionic conductivity than an LE at low temperatures, and plot (b) shows that SSBs have higher Li-ion concentration and no concentration overpotential, as the concentration line is constant and above the LE line. Despite this, many SSEs display low ionic conductivity at room temperature [175].

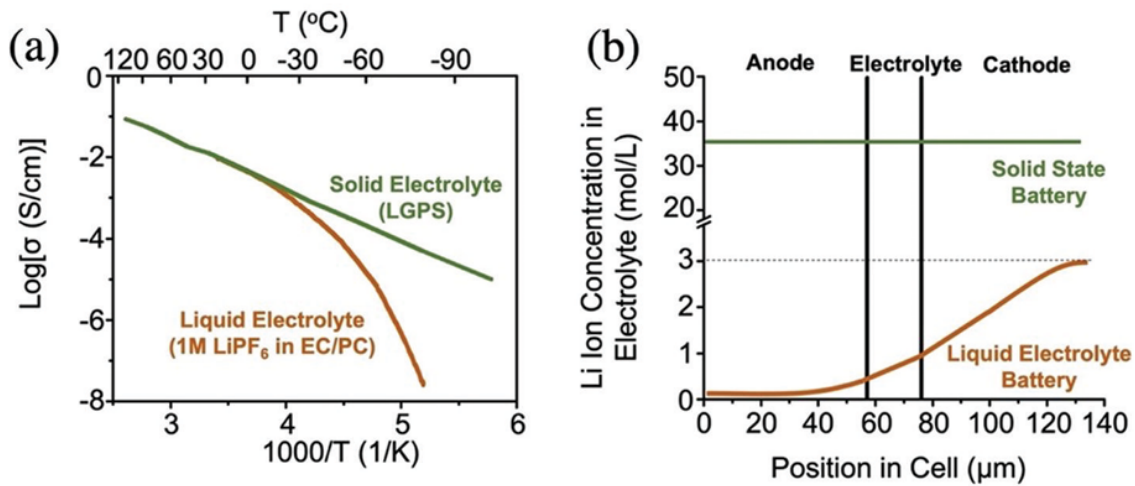


Figure 2.40: Comparing an SSE (a) with an LE (b). Reprinted from Huang et al. [167]

SSBs are not only categorized by their geometry. They are also separated into three types of SSE chemistries that are used. The first type of electrolyte is made of inorganic materials, usually ceramics, which are currently not produced as frequently. The second type is the polymer electrolytes, which form a coating. These are the only SSEs with large-scale production. The third type consists of a hybrid material of the previous two. [167]

2.8.2 Inorganic Solid-State Electrolytes

Inorganic solid electrolytes (ISEs) are a class of electrolytes that can address existing difficulties associated with traditional LEs, including but not limited to safety concerns such as flammability and poor stability. Among ISEs, sulfides and oxides stand out as the two most common categories,

each offering a wide variety of properties. Figure 2.41 illustrates an ISE in an SSB

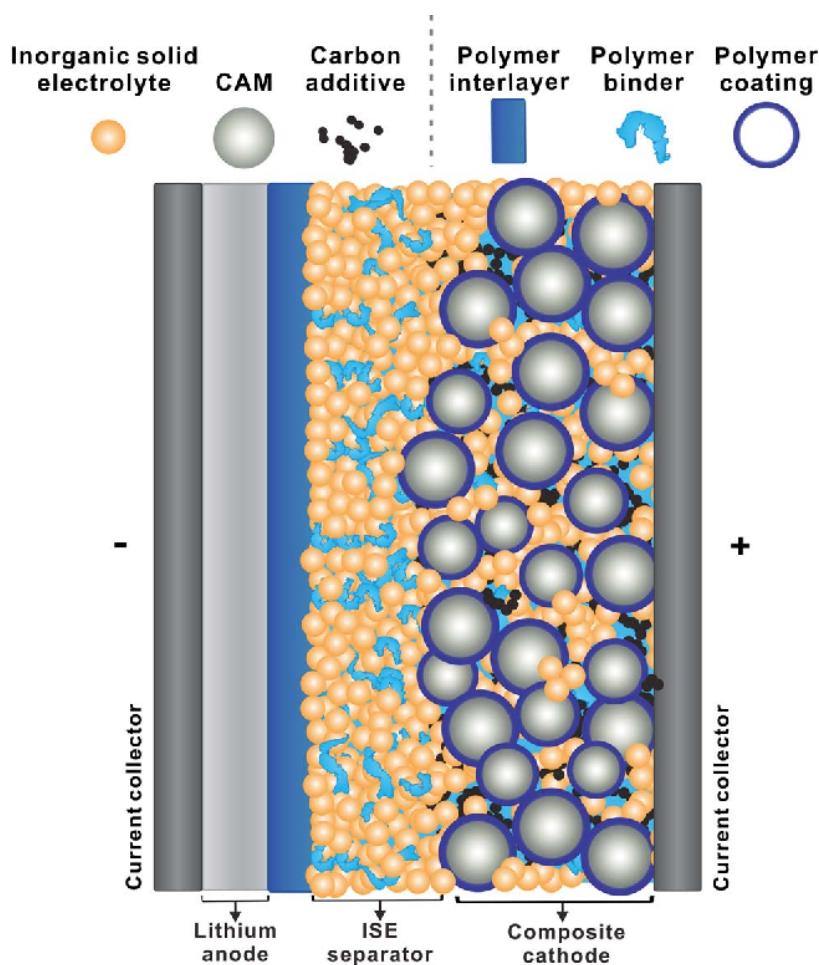


Figure 2.41: The components of an SSB with an ISE. Reprinted from Sen et al. [180]

Oxide solid-state electrolytes are often composed of oxide compounds, such as garnets and perovskites, each with their own crystal structure and ion transport mechanisms. [181]

Oxide electrolytes possess high electrochemical stability, making them resistant to most types of traditional degradation mechanisms. This stability increases long-term reliability, performance and safety, particularly in demanding applications where performance compromises are inapplicable. Oxides demonstrate good ionic conductivity across a wide range of temperatures, further stabilizing the battery. [181, 182]

Recently, sulfide electrolytes have emerged as a modern take on solid-state electrolytes. They originate from oxide electrolytes and are made by substituting O atoms with sulfide atoms within the electrolyte. As with oxide electrolytes, they offer an array of properties, making them applicable as an electrolyte of choice for solid-state batteries. [183]

There are a lot of similarities between oxide and sulfide electrolytes, such as their shared capacity

for ionic conductivity. However, sulfides are typically less brittle and have a wider electrochemical stability window than oxides, making them viable for multiple electrode materials such as Li- and Na-ions (Na^+). This results from sulfides having a relatively flexible composition, allowing for tuning of properties such as conductivity and stability. The adaptation enables the design of customized electrolyte formulations that are optimized for specific battery applications and requirements. ISEs also possess high mechanical strength and a very high Li-ion transference number at almost $t_{\text{Li}^+} = 1$. This translates to a reduction of Li-ions in the electrolyte and helps to prevent dendrite formation [184, 185]. Despite being safer than LIBs, there are distinct concerns involved, such as toxic H_2S being released when in contact with H_2O . This makes sulfides unstable in conventional environments [183].

ISEs are not exempt from having issues of their own, such as inflexibility, large interfacial resistance, and brittleness. In addition, sulfide electrolytes are often more expensive [186] to the point that they might not be viable for large-scale production or industrial use. Despite the high Li-ion transference number, dendrite growth can occur through the structure's interstitial voids [91] as explained in 2.4.7.

2.8.3 Solid Polymer Electrolytes

In the pursuit of safer and more efficient energy storage solutions, solid polymer electrolytes (SPEs) have emerged as an alternative alongside ISEs. SPEs typically consist of a polymer matrix infused with a conductive salt such as lithium perchlorate (LiClO_4) and lithium hexafluorophosphate (LiPF_6), and in some cases, additional additives, e.g. plasticizers to enhance performance [187]. Figure 2.42 is a schematic of an SSB with an SPE component used as the electrolyte.

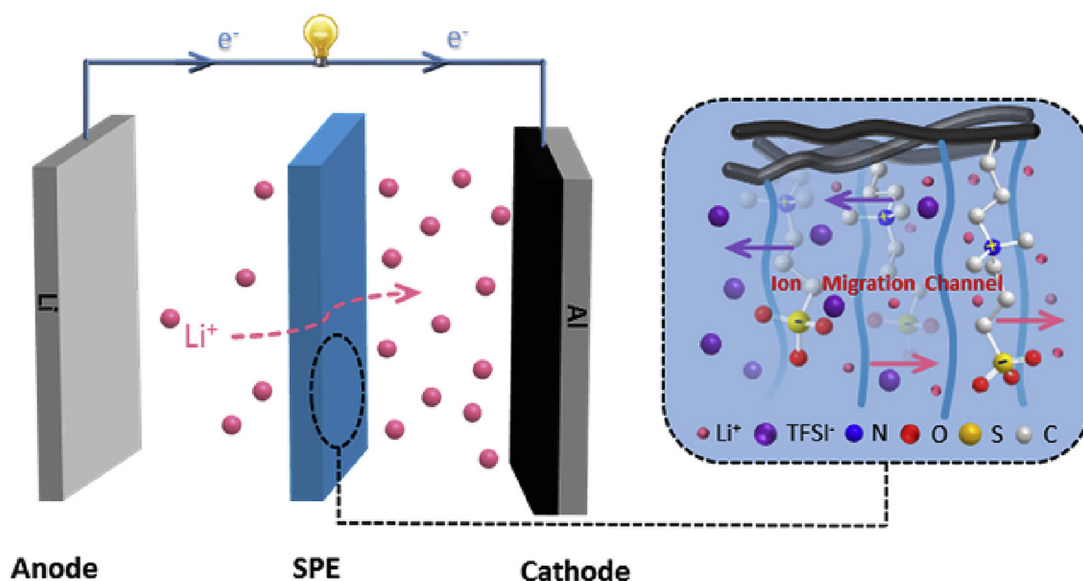


Figure 2.42: Illustration of an SSB with an SPE. Reprinted from Liu et al. [188]

Similar to ISEs, SPEs offer a higher safety factor by eliminating the flammable LEs and exerting a higher sense of stability. Furthermore, SPEs are more structurally flexible and processable than ISEs and can be used in various cell applications. Figure 2.43 shows a schematic comparing SPEs and ISEs. SPEs suffer from certain properties, such as the need for a BMS, and are prone to aging effects [189]. Additionally, SPEs exhibit a more limited thermal stability window, a narrower electrochemical stability window, and safety issues at high temperatures compared to ISEs [190, 191]. In LIBs and LMBs, the mobile cations and anions in batteries with an SPE cause concentration polarization, which compromises performance [192].



Figure 2.43: Comparison of ISEs and SPEs in LMBs. Reprinted from Song et al. [193]

2.8.4 Hybrid Solid-State Electrolytes

Hybrid SSEs, also known as composite SSEs, are a type of electrolyte technology whose aim is to combine ISEs and SPEs to achieve enhanced desired properties while minimizing their individual drawbacks. Characteristics of solid-state batteries (SSBs) include high energy and power density, longer life cycles, high tolerance to mechanical deformations and vibrations, high safety, and ease of fabrication. However, challenges include high cost, high interfacial resistance due to poor contact between solid-solid interfaces, low ionic conductivity caused by poor ion propagation, and decreased capacity due to volumetric changes in the SSB. As previously mentioned, the Li-ion transference number for ISEs is around 1, while it is less than 0.5 in SPEs. Therefore, by combining their properties, the transference number for hybrid electrolytes becomes higher than for SPEs and lower than for ISEs. [166]

Hybrid electrolytes can be classified into two different types depending on their base and filler components. The first one utilizes an SPE with an ISE filler, whilst the other uses an ISE with an SPE filler. Figure 2.44 illustrates a hybrid SSE. Since many studies focus on SPEs with an ISE filler [194], the focus in this thesis will be on SPEs with an ISE filler.

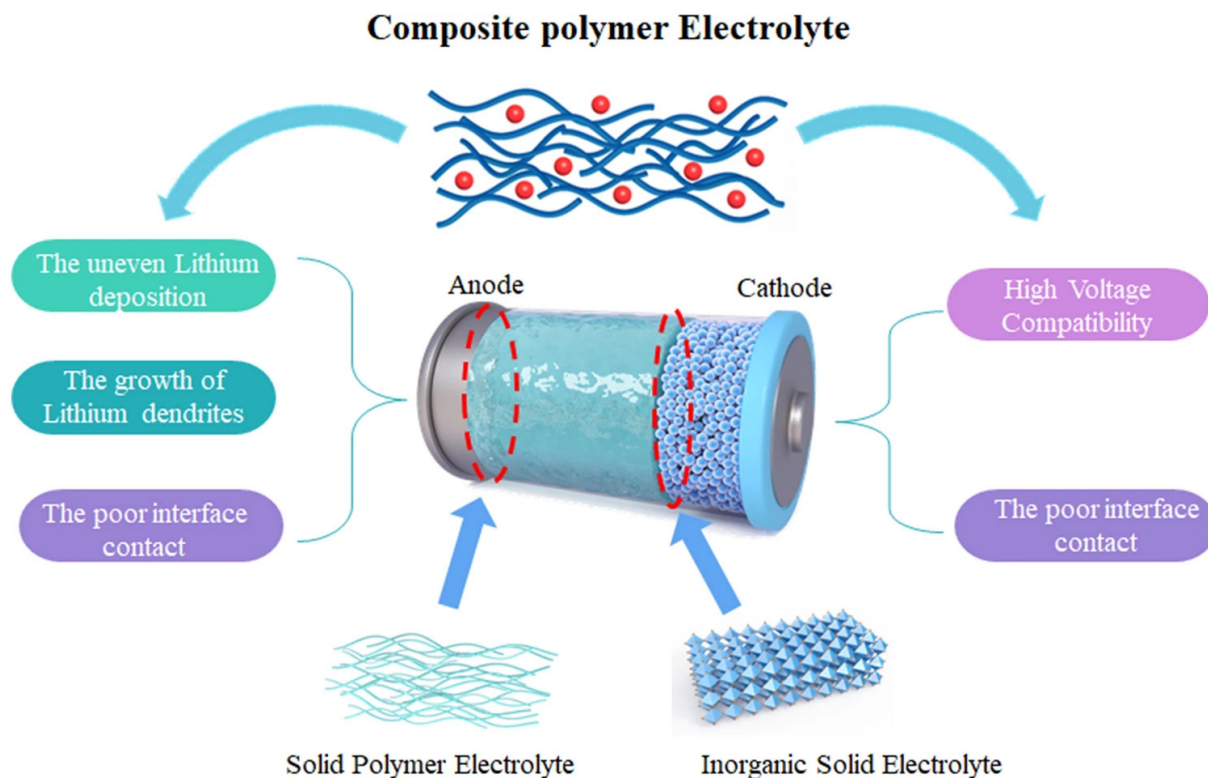


Figure 2.44: Illustration of a hybrid SSE in a battery. Reprinted from Yang et al. [185]

Further, SPEs with ISE fillers can be divided into passive and active ISE fillers. Both categories

generally show an improvement in performance, stability, strength, and the ability to restrain Li dendrites [185], but the ionic conductivity is low. Passive ISE fillers are typically ceramic and do not contain Li-ions. This means that they cannot significantly affect the ion conduction mechanism. Since these fillers are hard, their implementation helps improve the mechanical properties of a polymer matrix. While they do not improve the ion-conducting mechanism of SSEs, they increase the ionic conductivity and Li-ion transference number by preventing the crystallization of polymers with low glass transition temperatures (T_g) and enhancing mobility between the filler surface and polymer. In addition, the ionic conductivity is increased by the dissociation of Li-salts, thereby giving a rise to the concentration of mobile Li-ions [166].

Active ISE fillers contain Li-ions and can increase ionic conductivity because of their direct participation in Li-ion conduction. In addition, they provide high mechanical and thermal stability, as well as a wide electrochemical stability window. The Li-ion transport happens in a similar manner to the passive fillers but with new ion pathways. There are many different types of fillers that are used. For passive fillers, some of the types used are metal organic frameworks (MOFs), ferroelectric ceramics, zeolites, and clay materials. Some of the types used in active fillers include sulfide, sodium super ionic conductors (NASICONs) for Na types, and perovskites. Many active fillers are chemically unstable with Li-metal anodes and in natural environments, meaning that modifications are required. [166]

2.8.5 Manufacturing

Cathode

Manufacturing an SSB requires different steps than conventional LIBs. The most common methods for processing cathode materials are wet processing and dry processing. The active materials involved can be the same as in LIBs, such as NMC and LCO. LFP is often used in polymer electrolyte chemistries. [163]

Wet processing of cathode materials is slurry-based and therefore well established, such as in LIB processing as described in 2.3.9. In the case of ISEs, the SSE is also added to the slurry, which impacts the binder and the solvent that is used. Furthermore, there is no electrolyte filling step required in the manufacturing. If a sulfide ISE is used, it will react with polar solvents (i.e. NMP), meaning that non-polar organic solvents are needed as well [195]. Since the commonly used PVDF binder in LIB is not soluble in these non-polar organic solvents, other binder rubbers have been implemented instead, such as styrene-butadiene rubber (SBR) and silicon rubber (SR) [196]. Additionally, the sulfide manufacturing steps need to be done in a dry

or inert (chemically inactive) environment to avoid the generation of the aforementioned toxic H_2S gas, whereas conventional LIBs only need this for the anode manufacturing steps due to the reactive Li. [172]. Similar to in LIBs, the slurry is coated onto an Al current collector. The non-polar organic solvents used need to go through the solvent recovery and drying step along with NMP. After drying, the electrode is densified in order to achieve a good connection between the active materials and the ISE [163].

The calendaring step for ISEs varies depending on whether a sulfide or an oxide is used. With a ductile sulfide ISE, calendaring is similar to conventional LIB calendaring. With a brittle oxide ISE, a calendaring step followed by a sintering step, which means applying heat and/or pressure without melting the materials [197], is done to ensure low porosity. This needs to be done at lower temperatures so that the active material does not decompose. Furthermore, film drying the cathodes is expensive and energy-demanding. Wet processing is the most mature method used for ISEs, while an established dry processing method with no solvent is used for SPEs. In dry cathode processing, the cathode components (active material, SSE, binder, and conductive agent) are stored in an extruder, and the resulting mixture is coated on the Cu current collector [198]. It then goes through the calendaring step. For ISEs, some obstacles remain in accomplishing dry processing, partly because of their hardness and brittleness compared to polymers [163].

Anode

To incorporate Li-metal into the anode materials of SSBs, alternative methods to conventional processing are required. Some challenges arise from the properties of Li-metal, such as its high reactivity and adhesiveness. This makes it necessary for the anode manufacturing to happen in an inert environment such as a glove box. There are four main methods to process the SSB anode, and these are extrusion, melt-processing, vapor-based processing and anode-less. [163]

Extrusion is the most established process and works in a similar manner to the cathode dry extrusion process. Thin Li foil is produced in the extruder and then calendared to reduce thickness. The rollers are coated during the high-pressure calendaring step to prevent the adhesive Li-metal from sticking. Producing thin Li-metal foils of good quality is difficult and can be expensive. After calendaring the foil is coated on the current collector or separator. [163]

In melt-processing, Li-metal with a low melting point of $180\text{ }^\circ\text{C}$ [199], is melted before being set on an electrolyte or current collector. This is suitable for porous structures and has been able to produce thin foils. This method is not as mature as extrusion and requires additional measures in regard to the reactive liquefied Li [172].

Vapor-based processing is a third method that offers the advantage of producing thin, high-quality Li foil. Sputtering is an example of such a process in which Li-metal is deposited onto the current collectors by using ions to release Li particles from the metal [200]. The rate of production is restricted [172], and the method is expensive, which limits the possibility of bulk production [163].

Anode-less or anode-free approaches differ from the rest in that no Li-metal is involved during the production process. Instead, Li-ions stored in the cathode are coated on the current collector in the first charging cycle, thus forming the Li-metal anode [163]. An illustration of this is shown in 2.45.

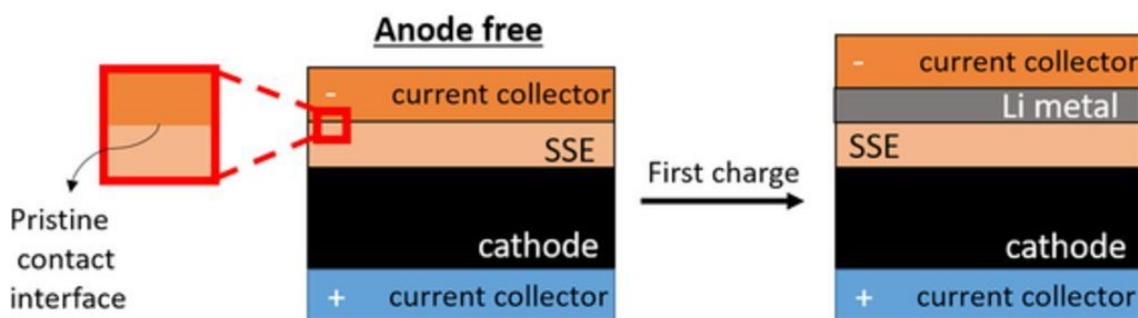


Figure 2.45: Illustration of anode-less SSB structure. Reprinted from Kerman et al. [201]

This approach can remove the need for producing expensive Li-metal foils as well as the anode processing in an inert environment [71], while simultaneously providing the battery with a higher energy density than LMBs [202]. However, challenges exist in the homogeneous coating of Li-ion, the current collector, and the SEI formation, leading to loss of Li, reduction in capacity, and Li plating. This can result in dendrites and an unstable SEI layer. To compensate for this, excess Li can be injected. Additionally, this method has not yet been established for large cells [163, 202].

For the different processes, challenges remain for attaining uniform layers and bulk production. Figure 2.46 shows the different processes.

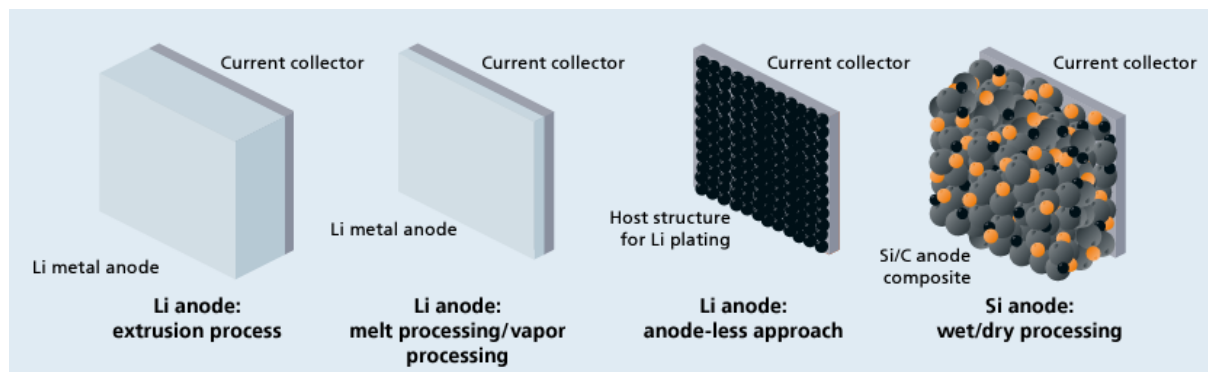


Figure 2.46: The different approaches to Li-metal anode processing. Reprinted from Schmaltz et al. [163]

Separator

The separator can also be implemented in the battery in various ways. Wet processing is a method that is especially viable for ISE separators. The separator can be set on the cathode directly or produced separately as a free-standing SSE before being applied on the electrodes [203]. Free-standing separators require greater thickness to maintain mechanical stability compared to directly coated separators. Thin ISE separators have been produced, but scale-up challenges remain. Regarding the calendaring step, SPEs can be used due to their high flexibility, and sulfide ISEs can be used because of their ductility. Oxide ISEs need an additional sintering process, which is energy-demanding, time-consuming, expensive, and leads to Li loss, thus resulting in less efficient production. Overall, wet processing is feasible to implement in SSEs as it is an established processing method in conventional LIBs [163].

The dry extrusion process is an established approach for SPE separators. However, more advancements are necessary for ISEs because of their hard and brittle nature. Additionally, a sintering step remains a requirement for oxide ISEs [163]. An alternative powder-based processing method exists for oxides to remove the sintering step and the solvent and avoid side reactions. This technique involves using an aerosol made up of a carrier gas and solid electrolyte powder to deposit the powder on the cathode. The deposition rates are low, and the technology is still too new to compete with the established wet and dry processing approaches for bulk SSE production [204].

Cell assembly and finishing

The last steps of SSB manufacturing are the cell assembly and finishing. This process is largely similar to that used in conventional LIBs. In the cell assembly, the electrodes are initially cut into stacks, e.g. by laser cutting. They are then stacked on top of each other to form a cell stack.

Subsequently, for sulfide ISEs, the stack is pressed together for improved interfacial contact between the layers. For oxide ISEs, a small amount of liquid or SPE should be involved in order to reduce interfacial resistance, while SPEs go through a heating process to reduce this resistance. The last processes are as described in 2.3.9. However, the housing can be formed into either a pouch cell through sealing or gluing or a prismatic cell through welding [203]. The process chains for cell assembly are shown in Figure 2.47

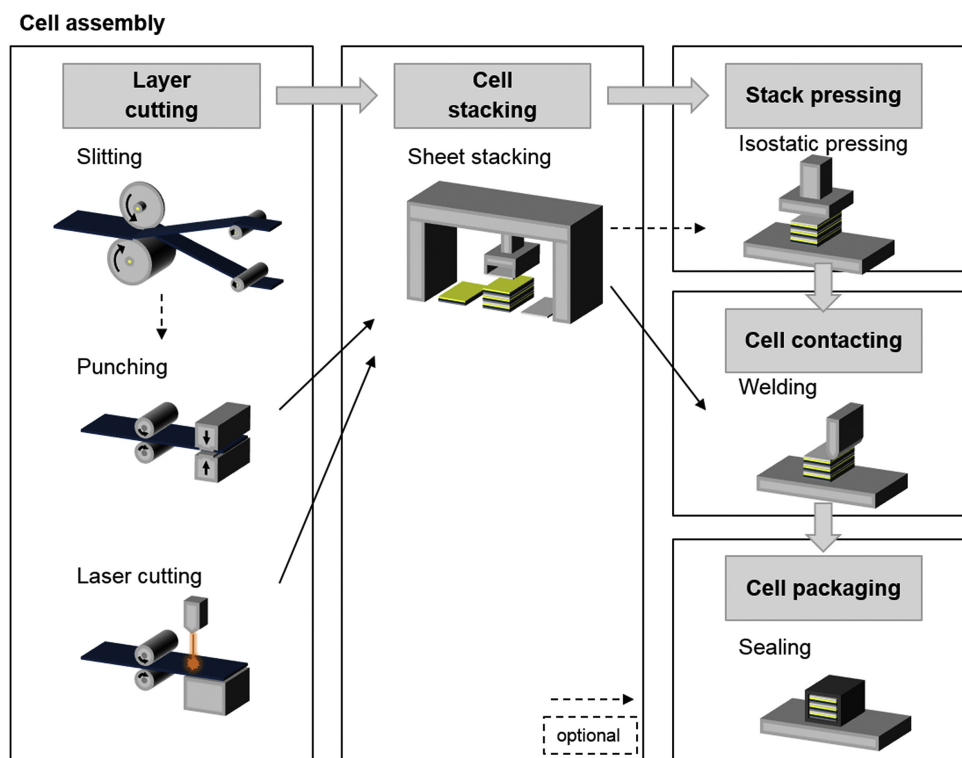


Figure 2.47: SSB cell assembly process. Reprinted from Schnell et al. [172]

Although it is possible for SSBs to be manufactured into other cell types, such as the common cylindrical cells in LIBs, winding the solid SSE makes this a difficult task, as cracks can form in the layers. This is particularly true for ISEs due to their hard and brittle properties. Pouch cells are therefore the most convenient cell format for SSBs. However, cell formats that require winding of the SSE could be a viable option for ductile SPEs [163]. For SSBs, the electrolyte injection and residual moisture removal steps in conventional LIBs can be omitted [172].

The cell finishing process is similar to 2.3.9. However, compared to conventional LIBs, the time and cost of the formation step are considerably lower. Furthermore, it is anticipated that SSBs will stabilize more rapidly than conventional LIBs and that the formation step will therefore be shorter or eliminated for SSBs. [163, 172, 205]

Besides the raw materials, the most expensive steps are expected to be the inert processing

environment required for sulfide processing and the high sintering temperature needed for oxide processing. However, some costs will be reduced by shortening or eliminating the formation and electrolyte-filling steps. [172]

Conventional LIBs deal with safety issues due to having an organic, volatile, and easily flammable material as an electrolyte. There are also limitations in the energy density. SSBs, on their end, face performance issues such as low ionic conductivity and poor interfacial contact [206]. This paper will therefore, additionally focus on semi-solid state Li-ion batteries as an alternative that has the potential to alleviate these issues found in LIBs and SSBs to improve the ionic conductivity, increase the electrochemical stability window as well as the overall safety.

2.9 Semi Solid State Lithium-ion Batteries

Semi-solid state lithium-ion batteries, or quasi-solid state batteries, represent an innovation within the field of energy storage, offering an alternative to conventional LEs and SSB technologies. SSLIBs are intended to address some of the limitations and challenges that exist when utilizing conventional batteries.

In essence, SSLIBs use a unique type of electrolyte in which the fluid in LEs is combined with the solid in SSEs. This results in an in-between, semi-solid electrolyte. Similarly to SSBs, utilizing Li-metal in the anode is one of the motivations for this technology. [173, 174]

2.9.1 Manufacturing

The manufacturing process of SSLIBs is largely similar to conventional LIB manufacturing [71, 207]. For example, Chang et al. reported the preparation of a stable pouch cell SSLIB with an MOF active filler, following the same steps as described in 2.3.9. The solvent recovery and calendaring step were omitted, and instead, a small pressing procedure was conducted. However, a PVDF binder agent was used, and the MOF film needed an evaporation step for the organic solvent. The resulting battery showed that it could sustain high temperatures and stress while maintaining electrochemical stability and safety. Furthermore, the ionic conductivity was higher than in an SSE and lower than in conventional LEs. At high operating temperatures, LEs can evaporate and decompose, causing cell failure and possible safety hazards [178]. A visual representation is shown in Figure 2.48.

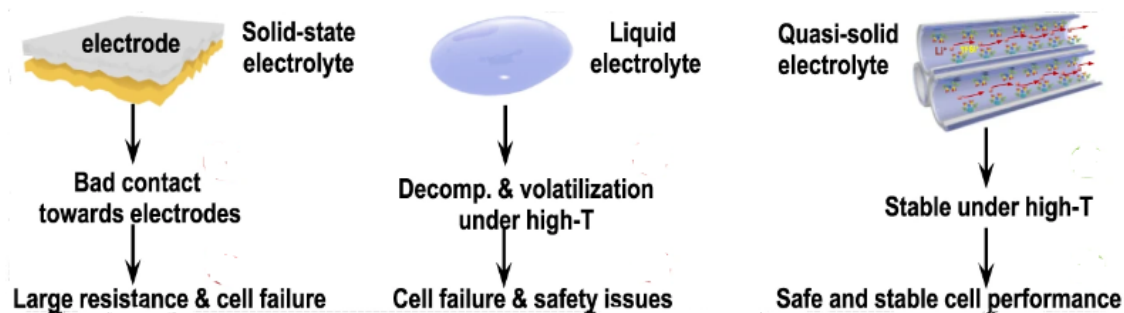


Figure 2.48: Comparing conventional LIB, SSB and SSLIB in operation. Edited from Chang et al. [178]

However, there is a non-traditional method of processing the electrodes that involves fewer steps, removing processes such as casting, drying, calendaring and binder agents from the LIB manufacturing process described in section 2.3.9. This takes away many of the inactive materials, thus reducing the cost in bulk production [208]. The process starts with slurry mixing carbon black and the active material in the electrolyte solvent, then filling these in the anode and cathode. By doing this, the electrodes become significantly thicker, as visualized in Figure 2.49. However, this structure has the downside of decreasing the total energy density [209].

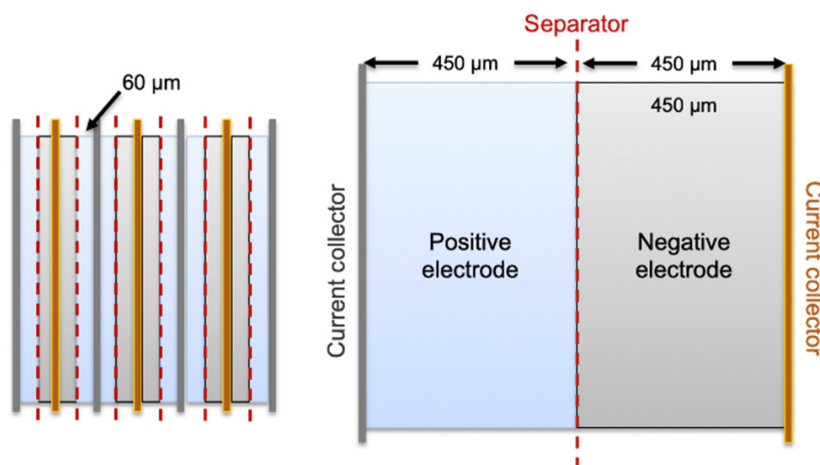


Figure 2.49: Conventional (left) and a type of SSLIB (right) cell structure. Reprinted from Bryntesen et al. [208]

An anode-less pouch cell semi-solid manufacturing process was presented by Liu et al. The process first involved the production of a free-standing cathode obtained through mixing and cold pressing. The electrolyte was then synthesized into a composite SPE. The synthesis method included both the casting and solvent recovery steps, but no calendaring was performed. Similarly to the semi-solid pouch cell manufacturing process, the PVDF binder agent was also included

here. The cell was then assembled by stacking Cu sheets, the free-standing cathodes, and the electrolyte. Finally, they were sealed and made to go through the formation process prior to undergoing further testing. [210]

2.9.2 Semi-Solid State Electrolytes

Semi-solid electrolytes bridge the gap between LEs and SSEs, integrating different parts from both to achieve an optimal electrolyte composition. With the growing demands for high-performance, safety, and long-lasting solutions, semi-solid electrolytes offer distinctive features, making them an option for resolving these demands. The following section will account for these properties, as well as exploring their role in advancing battery technologies.

Material Selection

Particularly for semi-solid electrolytes, material selection is pivotal to ensure an optimal compound composition. The different materials used within the electrolytes will influence the performance, stability, and longevity of the battery as a whole. The aforementioned ISEs, SPEs, and hybrid electrolytes are also used in SSLIB electrolytes along with polymer-gels, ceramic-polymer composites, and ionic liquids.

Gel Polymer Electrolytes

Gel polymer electrolytes (GPEs) are formed by combining SPEs and a liquid electrolyte. The combined electrolyte uses the liquid component for ion transport whilst the solid polymer matrix provides much-needed structural support and increase in safety, inhibiting the challenges associated with conventional LEs such as leakage, flammability, and poor interfacial stability [211]. Figure 2.50 visualizes a GPE in a LIB.

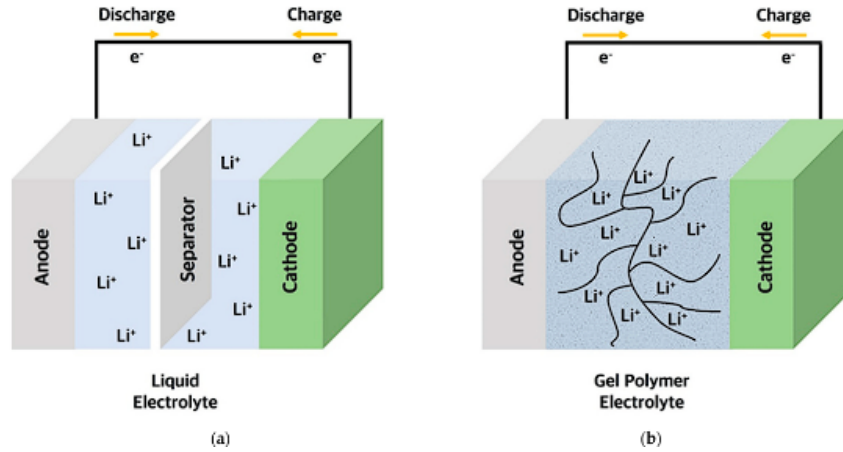


Figure 2.50: Schematic diagram of lithium batteries using (a) LE; and (b) gel polymer electrolyte. Reprinted from Chae et al. [211]

GPEs have mechanical flexibility, easy processing, good interfacial contact and are light-weight. They also contribute to forming a stabilized SEI layer, thus achieving long-term cycling stability. However, concerns regarding dendrite growth and ionic conductivity are present. In a polymer, the amorphous regions have shown to have the highest mobility of ions, and a low T_g supports the ion transfer in these regions. Using ILs as a precursor for poly(ionic liquids) and Li-salts has decreased the crystallinity, lowered the T_g , and increased the Li-ion transference number to improve the ionic conductivity. [212]

Gel Hybrid Electrolytes

Similar to SSBs, SPEs with an ISE filler can be utilized together in hybrid IL-based electrolytes to achieve more optimal electrolyte properties. These are called gel polymer-ceramic hybrid electrolytes (GHEs) [213]. Due to their brittleness, ISEs can deliver high ionic conductivity but have poor contact between the electrode and the electrolyte. SPEs have better interfacial contact owing to the soft and ductile polymers but are restricted by the low ionic conductivity and narrow electrochemical stability window. The benefits of combining them are mostly the same as mentioned in 2.8.4 [214]. Whether it is in ISEs, GPEs, or GHEs, using ILs has been shown to improve the electrochemical attributes in SSLIBs.

These kinds of electrolytes are fairly new and have therefore not reached a mature state. Because of this, limited research has been conducted in this area. However, experiments conducted by Foran et al. and Overhoff et al. found that the introduction of an ISE filler only contributed to an increase in mechanical strength. [215, 216]

As mentioned in 2.8.4, another possibility is using inverse compositions such as polymer in

ceramic. However, the feasibility of using it infused with liquid components is unclear. [217]

Ionic Liquids

One challenge ILs face, in general, is high viscosity at low temperatures. This means that the ionic conductivity is decreased in room temperature operation. Another challenge is the high cost, which limits widespread use and the ease of manufacture. Therefore, ILs are often combined with other SSEs, such as ISEs and SPEs to minimize these challenges. [212]

In general, for ILs used with ISEs, the ISE acts as the framework and provides the electrolyte with safety and stops the IL from leaking, while the liquid properties of ILs can lower interfacial resistances between the electrolyte and the electrodes, along with further hindering dendrite formation [218]. Using ILs as a coating in the ISE or electrode layers has also been attempted to reduce interfacial resistance, thus decreasing the overpotential. Overall, incorporating ILs in ISEs is yet to be practically applicable due to mechanical inflexibility and poor interfacial contact between the electrode and electrolyte. However, while many varieties of ILs have been synthesized, their diversity in ISEs is limited [212].

Single-Ion Conducting Electrolytes

Another type of electrolyte used both for SSBs and SSLIBs is single-ion conducting soft electrolytes (SICSEs) [91]. They are a class of SPE where the anion is covalently bonded to the polymer backbone or immobilized by anion acceptors, thus resulting in the cation being the single mobile ion. Some of these electrolytes have relatively high ionic conductivity and Li-ion transference number, low T_g and dendrite growth [176]. In addition, since only the cation is moving, the anion concentration overpotential is removed. This leads to a reduction in the overall concentration overpotential that is associated with traditional SPEs. However, large-scale application of SICSEs is limited by their low ionic conductivity at moderate temperatures and poor interfacial qualities. Additionally, due to the LE content in GPE, SICSEs in SSLIBs include an increase in safety issues and leakage, which is not present in SSBs [91, 192].

2.10 Economy

In a common LIB cell, materials can cover up to 75% of the cell cost as illustrated to the left in Figure 2.51. Of the materials in a LIB, the cathode takes up 50% of the cost, the anode covers 14.3% of the cost and the electrolyte accounts for 4.8 %. The bar chart in the middle of the display shows this. The distribution costs of materials in a cell reflect how the cathode chemistry consists of more materials than the anode. This pattern is indicated further in the bar chart to

the right, which breaks down the cell mass in percentages. It is further evident in Figure 2.52, displaying some of the various mass distributions within cathode materials, placing the cathode at a ratio of around 33% of the cell materials and anode with a mass covering up to 11% of the battery cell. [219]

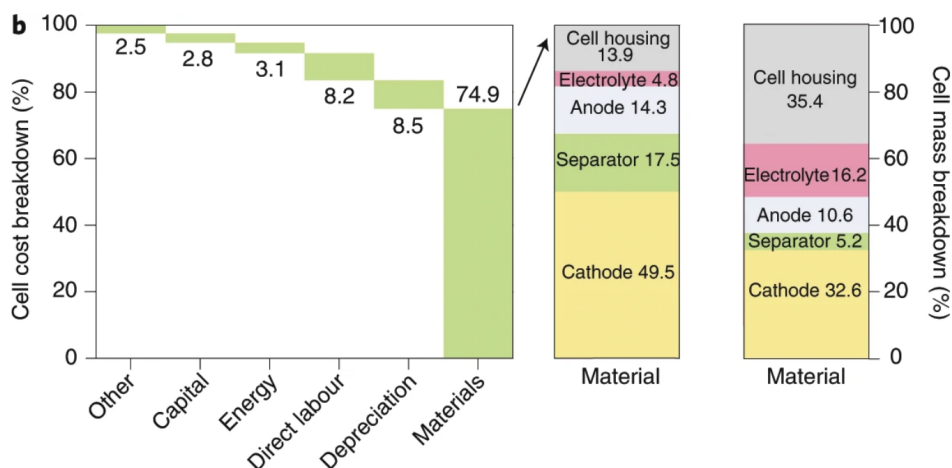


Figure 2.51: Overview of three bar charts showing the following: 1) breakdown of the cell cost, 2) the cost share of materials in a cell, 3) breakdown of the cell mass. Reprinted from Li et al. [219]

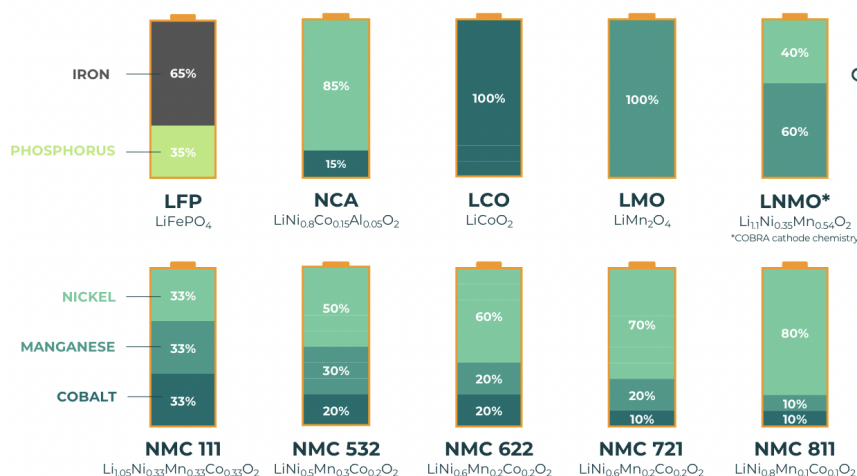


Figure 2.52: Overview of different cathode chemistries mass distribution of raw materials. Reprinted from COBRA. [139]

As stated, LIB technology plays a crucial role in advancing the electrical landscape, with manufacturing expenses having decreased by 85% in the last ten years. Since LIBs commercial commencement with LCO in 1991, there has been a significant reduction of 97% in the cost of LIBs. The price is given in terms of cost per kWh of energy capacity. As of 2020, the price was around 132 USD per kWh at pack level, meaning the assembled battery pack, and ca. 99 USD

per kWh at cell level, meaning individual battery cells within the pack. However, due to the COVID-19 pandemic and geopolitical tensions in Russia and Ukraine, the rate of decline in LIB prices has slowed down. The year 2022 was characterized by significant fluctuations in battery prices, which were largely unpredictable. Despite this, the cost of LIB packs has decreased by 14% since 2022, reaching 139 USD per pack, according to BloombergNEF. This reduction is attributed to cheaper raw materials, components, and an accelerated production capacity. [124, 220]

Not much data is available regarding the cost of an SSE, but Schmuch et al. estimates it to be about $50 \frac{USD}{kg}$. [221]

Comparing costs of essential materials

For active materials in anodes, the cost is solely dependent on the anode mix. According to Goldman Sachs, within the next year, the anode composition of active materials is projected to consist of around 70% SG, about 20% NG, and the remaining 10% goes to various shares of silicon, as shown in Figure 2.53. By implementing silicon, the energy density in the anode will be enhanced, resulting in a price reduction. However, as the proportion of SG rises, the share of NG is reduced. Therefore, the price increases as it is given that SG requires a greater amount of material per cell and is 20% more expensive than NG. Additionally, SG exhibits less capacity, meaning it requires a greater amount of material per cell. The rise of SG stems from its qualities, such as a greater life cycle than NG and reduced swelling. [125]

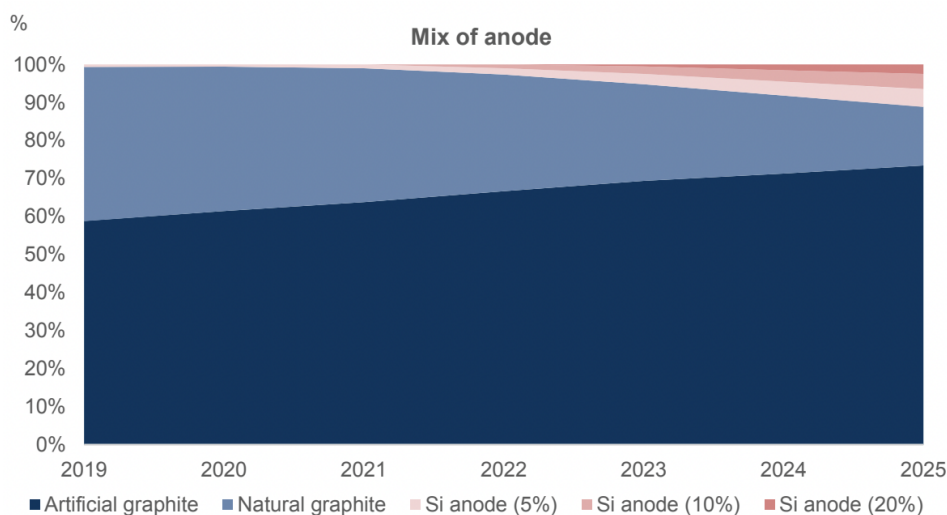


Figure 2.53: Graphic illustration of predicted anode mix advancements over a time period of 7 years. Reprinted from Bhandary et al. [125].

Table 2.7 displays the cost of anode active materials in USD/kg. Li-metal is the most expensive material by a good margin, lingering from 96-240 USD/kg. Graphite (both SG and NG) lies between 6-10.8 USD/kg. A mix of graphite and silicon has a value of 12 USD/kg, whereas a solid-dominated anode has a cost of 36 USD/kg. Titania and niobates cost 18 USD/kg. [222]

Table 2.7: The Table below shows cost per USD/kg of various anodes. Values obtained from Hetteshheimer et al. [222]

| | Graphite | Graphite-silicon composites | Silicon dominated | Li-metal | Titanates |
|--------|----------|-----------------------------|-------------------|----------|-----------|
| USD/kg | 6 - 10.8 | 12 | 36 | 96 - 240 | 18 |

As a result of the vast growth in the demand for batteries, the prices of raw materials have increased. The primary raw materials used in common cathode chemistries of a LIB are Li, Ni, Co, Mn, Al, and Cu. Figure 2.54 displays the variations of battery metal prices over a span of 6 years, showing Ni increasing by 500% since 2017, while Co increased to half the amount, staying at around 250%. Compared to 2021, both Li and Ni had a price surge at 300% [124]. As the Russia and Ukraine war unfolded at the start of 2022, the prices of the materials increased drastically, resulting in a hiccup in the price trend [125].

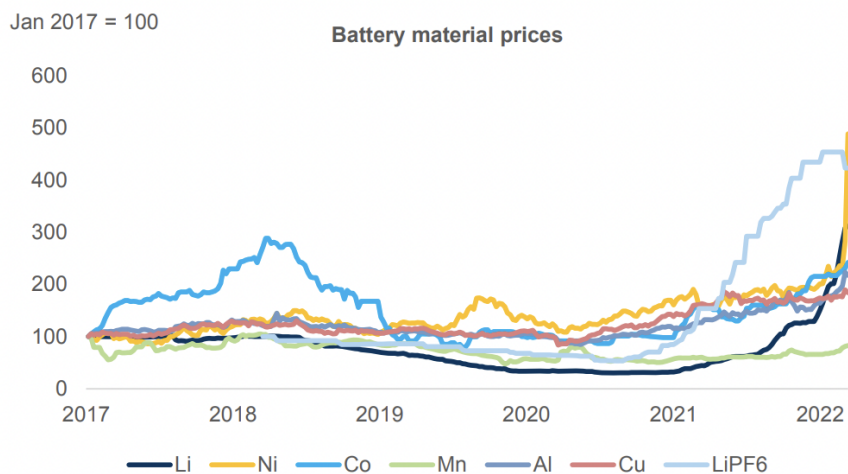


Figure 2.54: The graph illustrate the battery material prices for a 6 year period for different metals. Reprinted from Bhandari et al. [125]

Furthermore, estimations have been made for relatively high cost material prices for 2025 and 2030. Figure 2.55 displays the trajectories of material prices in USD/kg for Co, Ni, Mn, and Li over two decades, with historical data from 2010 to 2020 and projections for the decade from

2020 to 2030. In the wake of the pandemic, all materials increased in price from 2020 to 2025.

For Co, it is anticipated that it will reach its peak in 2025 with 80 USD/kg before it stabilizes in the following years at around 70 USD/kg, closing up to 2030. As a limited resource primarily retrieved from mining and additionally as a byproduct of Ni and Cu extraction, it is realistic to expect an increase in price. For Ni, it is estimated that the price will reach its peak at 25 USD/kg around 2023 before slowly declining towards 2030. Both Ni and Co have experienced a tightening in supply following the Russia-Ukraine situation. The gradual decrease in Ni supply reflects the aftermath as the price stays between 20-25 USD/kg. Yet, in contrast to Co, Ni reserves are sufficiently varied geographically and plentiful to facilitate the future manufacturing of cathode materials [221]. On the other hand, Mn is a raw material that is categorized as noncritical, meaning it comes at a low price [221]. The graph displays a small increase from 2-2.5 USD/kg to about 3 USD/kg in 2030. This makes Mn the cheapest of the four materials. Li has the highest incline going from around 25 USD/kg in 2020 to over 200 USD/kg between 2020 - 2025, before a rapid decline/stagnation in the following years, ending up at under 50 USD/kg by 2030 [124, 223].

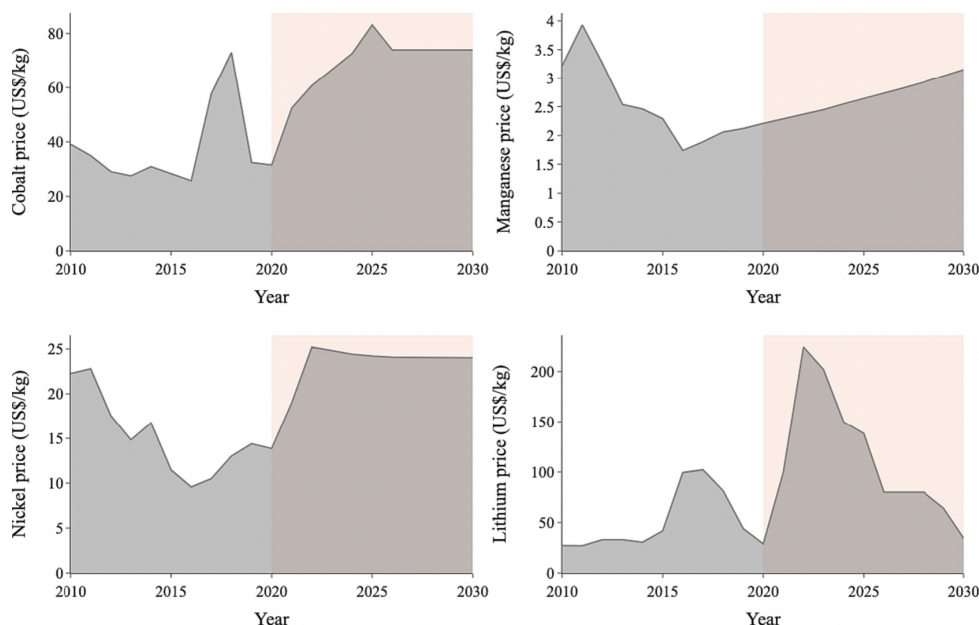


Figure 2.55: The graphs illustrate projected materials prices for cobalt, nickel, manganese and lithium in USD/kg from 2010-2030. Reprinted from Orangi et al. [124]

For raw materials such as iron and phosphate, both of which are non-toxic and non-critical, the supply chain and cost dynamics present no significant challenges. Iron is one of the most typical elements on earth and is therefore relatively low-cost compared to the materials listed above, leading LFP to be the most economical option for manufacturing 1kg of cathode material [45],

as shown in Figure 2.56.

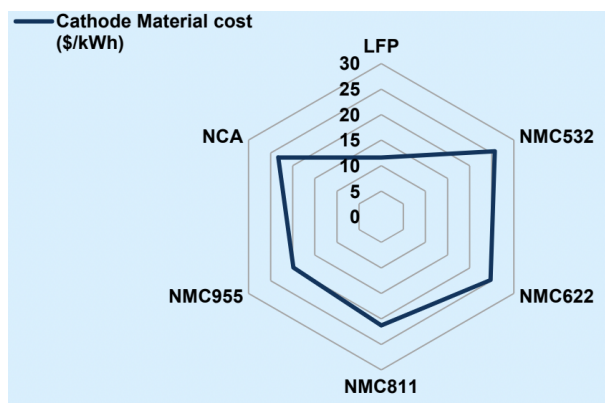


Figure 2.56: Compares different costs of cathode chemistries. Reprinted from Snowden et al. [224]

For the cathode chemistry, LMFP is considered to be considerably cheaper than LFP, with a cost difference of 13 USD/kWh between the two in 2022. In 2023, the gap became considerably smaller with a difference of 5 USD/kWh as shown in 2.57. [147]

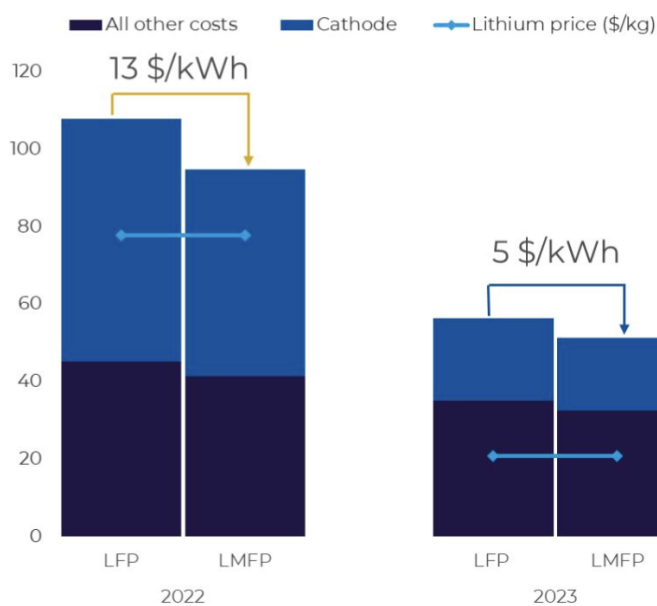


Figure 2.57: Compares LMFP and LFP costs over two years. Reprinted from Jinga et al. [147]

The price will also differ among various countries. China holds the lowest cost, while the remainder of Asia Pacific exhibits the highest [225]. China dominates the market across the entire battery supply chain, from extracting raw materials to cell assembly. With the exception of extracting raw materials, China covers the majority share of the battery value chain as shown in Figure 2.58. In terms of raw materials, Australia is the largest supplier with up to 50%, followed by Chile with almost 30%, while China stands for 19%. In the step of processing the materials,

China owns up to 92% of the market share, leaving the remaining 8% to Korea, Japan, and the EU. Regarding battery components and cell assembly, China covers 65%

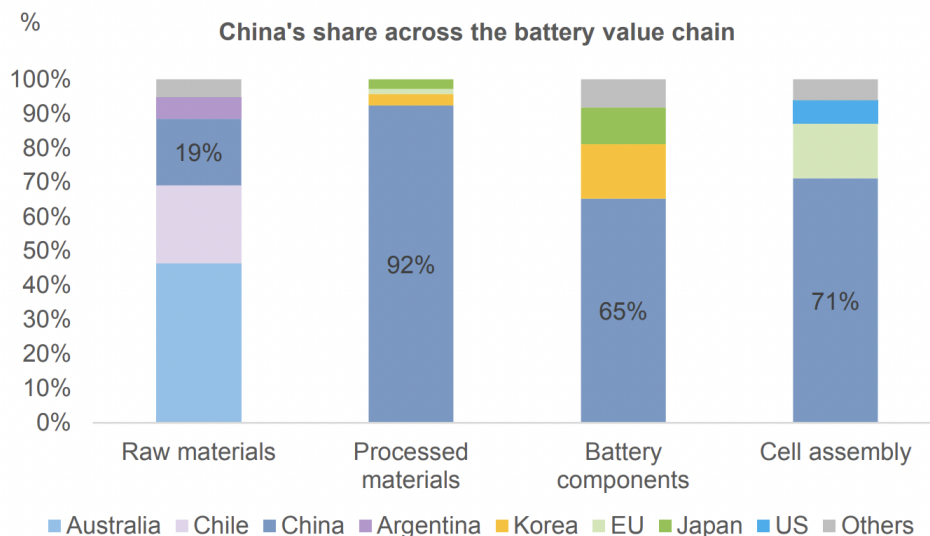


Figure 2.58: The bar chart illustrates the distribution of the battery supply chain across countries. Reprinted from Bhandari et al. [125]

2.10.1 Liquid State

Over the year 2022, it was LFPs that experienced the most significant increase by around 25% due to the rise in Li prices as shown in Figure 2.54. Additionally, since Fe and P are relatively cheap compared to Co or Ni, Li serves as a significant determinant in the final cost of LFP. NMC batteries had a price spike between 10-15%, as both Ni and Co also increased in cost. However, since the two materials are generally more expensive than Fe and P, NMC batteries are overall more expensive per unit of energy capacity compared to LFP batteries. [225]

The cost spikes of raw materials have resulted in elevated LIB prices. For battery packs in 2021, LFP was the most economical, being 10-20% cheaper, with a price between 110-120 USD/kWh as illustrated in 2.59. For the various NMC batteries, the price depended on the amount of Co and Ni. Since NMC 811 has the smallest share of the two raw materials, it is cheaper than NMC 622 and NMC 532, with its costs lingering from 130-140 USD/kWh.

Moreover, Goldman Sachs [125] predicts a cost decline in 2025 decline for all the battery packs, with LFP still being the cheapest of the commercialized LIBs, laying in a price gap between 90-100 USD/kWh. However, “new batteries” will be the most economical overall with a price estimation of 90 USD/kWh. This category can include batteries such as LMFP or LNMO.

Regarding NMC, it is predicted that the cost gap between NMC811 and 622 will increase, covering a price between 100-110 USD/kWh and over 110 USD/kWh respectively. The price will decrease further if recycling is part of the life cycle of the battery pack. More on recycling in 2.11.

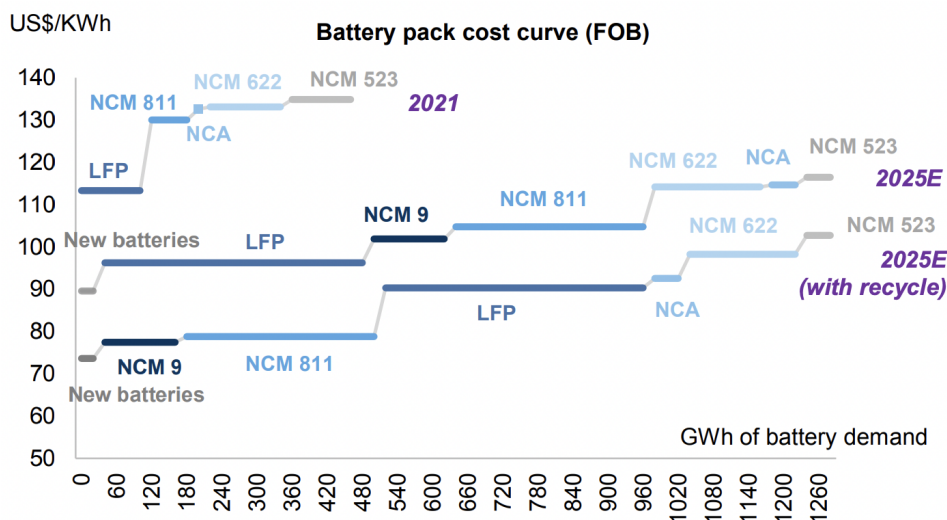


Figure 2.59: The graphs illustrate different costs in USD/kWh for cathode battery packs for different demands. One curve is from 2021, while the other two are projected graphs from 2025, both with and without recycling. Reprinted from Bhandari et al. [125]

Furthermore, in 2023, it was estimated that LFP batteries had a standard cost of 130 USD/kWh at the pack level and 95 USD/kWh at cell level. The cell price was 32% lower in cost than an NMC cell [220], showing a rise in price from 2021. This can be seen in Figure 2.58. However, due to the war between Ukraine and Russia that started in 2022, it is projected that the prices of batteries will increase [124].

2.11 Sustainability

In recent years, the supply chain of cathode materials has been affected by the pandemic and Russia's war with Ukraine. Given that Russia is one of the largest producers of Ni, the price of the material has risen considerably, and it is prone to price volatility [226]. However, of the cathode materials used in LIBs, Co is of particular concern. The price of Co, similar to Ni, is volatile and has increased over the years. It is anticipated that this trend will continue as more LIBs are produced. This is partly because Co is a scarce material that is subject to supply chain shortages [227]. Currently, the majority of Co is mined from the Democratic Republic of the Congo (DRC), accounting for approximately two-thirds of the global extraction [124]. In comparison, no other country produced more than 5% [228]. Moreover, there are geopolitical concerns in regards to the

ethical conditions of Co mining in the DRC, as well as challenges in international distribution. Additionally, Co is a toxic material for the environment, and overexposure is damaging to human health. Co is the material with the highest criticality in many LIB chemistries, as well as having a high environmental impact. This has led to a focus on transitioning to Co-free batteries [227, 229, 230].

In LFP cells that do not contain Co, the material with the highest criticality is graphite. China and Mozambique mine about 70% of the global graphite [228]. Around 50% and 22% of Li reserves are located in Chile and China respectively, while Australia accounts for 80% of the extraction [231]. This has given Li and graphite high impacts in criticality. When replacing the graphite anode with metallurgical grade Si, the criticality and the aggregated elemental impacts decrease [230].

In descending order, Co, Ni, Al and Cu are the largest contributors to the climate change impact in NMC batteries. Ni is the largest contributor in NMC811, where Ni occupies more of the cathode material compared to NMC622 and NMC111. Li and natural graphite show minimal environmental impact despite their high criticality. Titanium (Ti) used in the anode of LTO causes high emissions and contributes to the environmental impact. Transitioning from graphite to LTO in the anode does not benefit the criticality of environmental impact [230]. This is illustrated in Figure 2.60. Note that the bubble size is proportional to the total elemental mass per unit cell capacity and that the dotted lines show the median criticality and environmental impacts across all the cells.

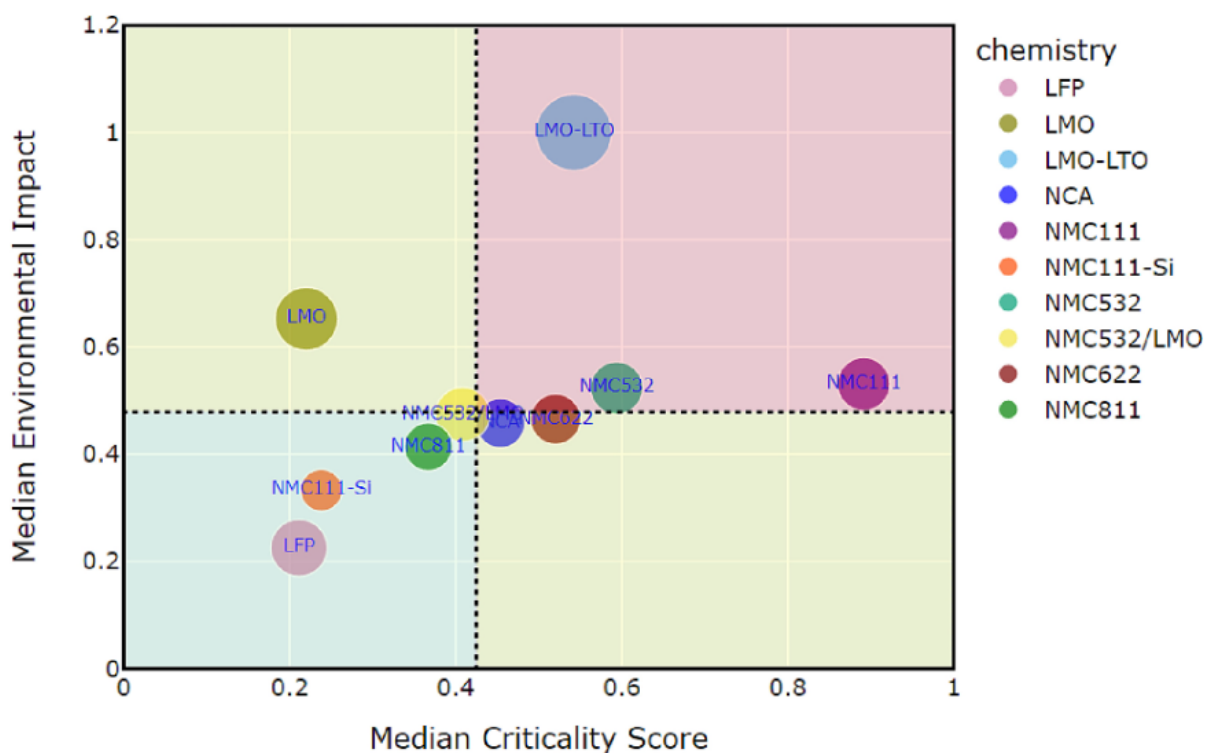


Figure 2.60: Criticality and environmental impact quadrant matrix. Reprinted Manjong et al. [230]

Recycling

The recycling of LIBs is a relatively new concept, and the industry is not as well established as the growing LIB manufacturing industry. Furthermore, the intricate cell chemistry of LIBs and the lack of standardization in design compared to other chemistries, such as lead-acid batteries, makes the recycling process more difficult. This is because LIBs are designed for safety and longevity, but the consequence is that recycling becomes less efficient and incapable of being automated. The current technologies are primarily focused on the recovery of the cathode materials and Li since these are the most valuable from a recycling perspective [232, 233, 234, 235, 236]. The recycling technology of LIBs is divided into three main categories: direct recycling, pyrometallurgical, and hydrometallurgical [236].

- **Direct recycling**

Direct recycling is a solvent extraction process that utilizes supercritical carbon dioxide (CO_2) to extract the cathode and anode materials. First, the cells are treated with the CO_2 , which extracts the electrolyte. Subsequently, the electrolyte is recovered and can be reused in future manufacturing. Afterward, the cells are dismantled and crushed, and the components are separated. Lastly, the cathode materials are collected and reused [237]. Direct recycling is not as mature as the other recycling methods and therefore has not been

applied on a large scale [236].

- **Pyrometallurgical recycling**

Pyrometallurgical recycling is a process whereby reusable metals are melted at high temperatures and separated according to their melting or boiling point. It is known for being simple and more profitable at large scales. However, the method requires high temperatures and presents significant challenges in terms of the yield of pure metals. This often results in the need of a hydrometallurgical treatment. Due to the design of LIBs, pyrometallurgical recycling is sometimes the only option. [233, 238]

- **Hydrometallurgical recycling**

Hydrometallurgical recycling is considered the main option, using chemical processes to recycle. This method has a lower environmental impact, consumes less energy, and has a higher recovery efficiency, especially in the case of Li. Ordinarily, hydrometallurgical recycling is preceded by either a mechanical or pyrometallurgical pretreatment [239]. The resulting recovery rates under optimal conditions are 98.7% for Ni, 97.1% for Mn, 98.2% for Co, and 81.0% for Li. Moreover, steel, polypropylene, Al, and Cu are other cell components that can also be recovered in this process [240]. NMC is more suitable for hydrometallurgical recycling, as multiple metals need to be separated, while pyrometallurgical methods are simpler for LFP [235]. However, LFP recycling can also be carried out using hydrometallurgical methods [241].

Due to the low recycling potentials of Li, a risk regarding primary material use is involved in LIBs [230]. A comparison of the different recycling methods with their attributes is illustrated in Figure 2.61.

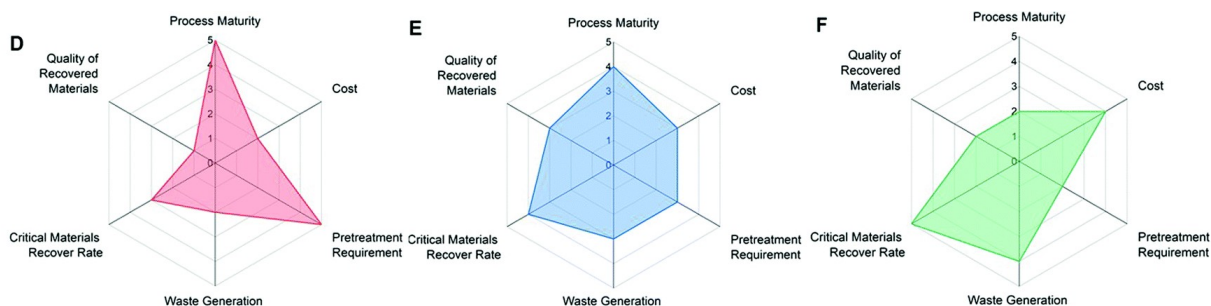


Figure 2.61: Characteristics of the different recycling methods. *D* = Pyrometallurgy, *E* = Hydrometallurgy, *F* = Direct Recycling. Reprinted from Mao et al. [236]

3 Methods

Throughout the course of this thesis, the sources that were used have been checked in detail, and the authors or organizations were examined for credibility. Moreover, multiple sources were reviewed in order to ascertain the consistency of the information. Additional care was taken when researching various values that are recent and consistent. However, this was not carried out in the cases where the available information was severely limited. In those situations, the limited sources were thoroughly checked to ensure reliability.

At the start of the thesis, the first priority was to gather documentation on the topic of SSBs and SSLIBs. This was subsequently condensed in order to gain a general understanding of the subject. The structure of the thesis was then formed with the advice of the internal and external supervisors taken into account. Afterwards, the theory section was developed. Each of the four authors was assigned a portion of the theory.

Various techniques were used to collect the relevant theory for the project. Websites such as Google Scholar, ScienceDirect and MDPI were used to find reliable research journals and papers. When finding more specific information, the sources used within these papers were delved into. Moreover, to effectively find information, keywords were utilized in the searches. In different sections of the general theory and LIBs this included keywords such as "properties", "crystal structure", "cathode chemistry", "cost" "recycling" and "battery report". In SSBs and SSLIBs, some common keywords used were "polymer", "ceramic", "dendrites", "electrolyte", "LMB", "gel", "hybrid/composite" and "anode-free". Additionally, the "Ctrl+F" function was used as a tool to rapidly navigate the sources.

Once the necessary theory had been established, the discussion was written based on the collective findings. Lastly, the remainder of the thesis was written in the order of the introduction, methods and conclusion. The role distribution gave a general framework, but all of the authors worked on the different sections. Furthermore, one author was assigned to periodically maintain the structure and consistency of the text. During the last phases of writing, all of the authors went through the thesis collaboratively in order to further ensure cohesiveness.

4 Discussion

In this section, a discussion will take place in order to concisely evaluate these findings and will be the basis of the conclusion and recommendation for *Beyond*. It will start by evaluating the advantages and disadvantages present in different cathode and anode chemistries and choosing which ones to focus on during further discussion. After this, an evaluation between the different electrolyte states will take place, narrowing in on specific points such as costs and attributes. Lastly, a consideration of which chemistries and electrolytes are viable for different use cases will be conducted.

4.1 Comparison of the cathode materials

Over the course of the thesis, numerous cathode chemistries have been identified as potential candidates for further research by *Beyond*. These include LCO, NMC ratios (111, 532, 622, 811 and 955), LFP, LMFP and LNMO. In order to make a concise assessment of these potential compositions, an analysis of cell voltage, specific energy, energy density, specific power, cycle life and degradation, thermal stability, economy and TRL is required. The data used is shown in Table 2.4.

4.1.1 Cell voltage

The operating voltage of different batteries is an important factors when selecting an appropriate battery for a given application.

The highest voltage of LIBs currently produced, comes from LNMO with a voltage of ceiling 5.0 V and LCO with a voltage ceiling of 4.4V. These are closely followed by the different NMC-material distributions reaching a maximum of 4.0V. LIBs that exclude the use of cobalt and nickel, in contrast to those that do, generally see a lower operating voltage, with LMFP reaching 3.7 V and LFPs ranging from 3.2 V to 3.5 V.

These numbers show that LNMO, LCO and NMC are the cathode materials which are best suitable for high power applications. The cathode materials best suited for lower power applications is however LFP and LMFP.

4.1.2 Specific energy

In applications where the minimisation of battery weight is essential to minimise the impact on system performance and efficiency, the specific energy density (Wh/kg) is crucial. This is

particularly important in automotive applications, where the battery's weight directly affects the vehicle's performance.

According to Table 2.4 the LFP cathode chemistry have/has the lowest specific energy. Both the lower cell voltage and the weight of Fe, along with its larger olivine structure, contribute to a reduced specific energy at 90-180 Wh/kg. By implementing Mn, the ratio of iron is reduced in LMFP which elevates the cell voltage, resulting in a 20-40% higher energy density at roughly 210-240 Wh/kg compared to LFP. While the LCO cathode chemistry has a specific energy ranging from 150-200 Wh/kg. This is a result of LCO being cobalt rich as demonstrated in Figure 2.52, Co offers high energy density, due to its high voltage. NMC cathode compositions differ in specific energy between a range from 140-300 Wh/kg. Similar to LCO, NMC cathodes contain cobalt, known to be energy dense. Additionally, since they include nickel, NMC cathode chemistries achieve an even higher specific energy range. This stems from both cobalt and nickel having great voltage and their complementary advantage. However since nickel is slightly lighter than cobalt, NMC cathodes with a higher nickel ratio will have greater specific energy. Therefore NMC811 will have the greatest specific energy with a potential reaching up to 300 Wh/kg. Since NMC 622, 532 and 111, are not as nickel rich chemistries, they will have values at 255-290 Wh/kg, 219-250 Wh/kg and 140-193 Wh/kg respectively. On the other hand, LNMO is projected to exhibit a specific energy from 150-165 Wh/kg, which is comparatively limited. Yet, it is higher than that of LFP. In addition, it is important to note that it has extremely high theoretical specific energy at 690 Wh/kg which shows great promise for the future.

This leads to NMC ratios with 811 at the top, to be the most suitable for mobile applications where weight is essential such as passenger EVs. While for LCO, LMNO and LFP should be compatible in transport applications where weight is not as pivotal.

4.1.3 Energy density

Energy density (Wh/L) is of significant importance within applications where spatial limitations are a design factor, such as in fields for mobility and electronics.

Cathodes containing Co, such as LCO and NMC, exhibit notable superiority in terms of heightened energy density. The presence of Co, with its great reversal potential, implies that LCO has one of the highest energy densities at 560 Wh/L as it primarily consists of this material along with Li, as shown in Figure 2.52. In contrast to LCO/Unlike, NMC incorporates nickel and manganese, indicating that its energy density is not solely reliant on Co. Ni also contributes to increased cell voltage, enabling NMC compositions to achieve even higher energy densities with a higher

ratio of nickel. While Mn has substantially lower reversal potential, which implies NMC ratios with greater Mn will have lower energy density. Similarly, to specific energy, NMC811 ends up with the highest energy density at 700 Wh/L. While, NMC 622 has a slightly lower value of density at 650 Wh/L. NMC111 ends up being surpassed by LCO with a value of 230-567 Wh/L. The cathode chemistry LFP, with iron and phosphate, occupies a larger volume relative to other chemistries. Consequently, reducing the amount of stored energy/overall energy storage capacity, resulting in a diminished energy density at 362-457 Wh/L. However, for LMFP, with Mn, the cell voltage falls, resulting in a lower energy density than LFP, staying at 280-300 Wh/L. LMNO is estimated to have the lowest energy density of 250-280 Wh/L. Nonetheless, it has the potential to increase even further as it moves towards commercialization.

In summary, NMC811 exhibits the highest energy density, followed by NMC622, LCO, and then NMC111. This implies that these batteries are well-suited for applications requiring smaller batteries and saving space, such as in electric vehicles (EVs). Further, LFP is trailed by LMFP and LNMO, making them more relevant for areas where volume is not as vital, such as energy storage. In other words/ that is to say/ This indicates that for EV applications, both the energy per mass and volume are pivotal. Particularly within lighter transportation, such as passenger cars and even aircraft, the size and weight of the battery are crucial factors determining the optimal performance of mobile devices. Therefore, NMC cathodes become the optimal choice in terms of specific energy and energy density within this area.

4.1.4 Thermal stability

Safety is a critical consideration within battery design. In order to have a high thermal stability, a battery must be capable of operation at ambient temperatures.

When the battery is operating at a temperature that is under its temperature range, this will decrease the reactivity, which lowers the capacity. This also slows down the growth of SEI, which is positive because it stabilizes the formation. On the other hand, does the formation utilize more Li-ions, which again reduces the capacity of the battery. The slow reactivity also increases the formation of lithium plating and dendrites. From the properties shown in Table 2.4, all the cathode materials have the same minimum operating temperature. This makes all the cathode materials equally sensitive to degradation from low temperatures.

Several factors inside the battery can increase the temperature and the internal energy. As the temperature rises, the volume of the internal battery can increase, causing mechanical wear. Irreversible heat is created exponentially with a high C-rate. If the battery operates at a temperature

that is higher than the operation temperature, the reactivity of the materials increases. Among other things, this leads to an increase in ionic conductivity, which causes irreversible reactions such as the SEI layer to grow faster. This, in turn, leads to the storage of exothermic energy. The increased exothermic energy in the SEI layer is released at excessively high temperatures. The increased temperature will also begin to decompose, destabilizing the outer organic SEI layer and potentially triggering thermal runaway. In addition, the increased ionic conductivity makes the structures more susceptible to fracture, resulting in loss of active material and an overall shorter cycle life. The listed C-rates in Table 2.4 are very limited, but this is an important factor to consider. The maximum operating temperature for the cathode materials shown in Table 2.4 is quite similar. The only material that stands out is NMC111, which has a bit smaller operating range than the other cathode materials. This makes NMC111 a bit more sensitive to higher temperatures.

The increase in thermal energy can also activate several non-spontaneous chemical reactions in the battery. If the chemical composition of the battery is reactive, the likelihood of unwanted chemical reactions taking place is increased. The most reactive materials is the ones with the largest reduction potential and oxidation numbers, from Figure 2.4. The cathode materials, including Ni and Co, are therefore the most reactive ones. This makes NMC, LCO, and LNMO the most prone to degradation and low cycle life, while LFP and LMFP have a more stable and long life cycle, as shown in Table 2.4.

The thermal runaway shows the maximum temperature the battery can handle before These numbers can give an indication of which environment the battery. The values in Table 2.4 shows that LCO is the most sensitive to heat with a thermal runaway at 150 °C, then NMC111 with thermal runaway at 210 °C and LFP with thermal runaway at 270 °C. Although these temperatures may seem high, they are important to illustrate because it can get warm in an operating room, e.g. with machinery.

4.1.5 Cycle life and Degradation

Degradation is the key technological aspect for a long cycle life. The rate of battery degradation affects the battery's cycle life. If the battery degrades rapidly, the battery's cycle life is shortened. Conversely, if the battery degrades slowly, the battery's cycle life is extended.

From the numbers in Table 2.4 and Figure 2.23 it is shown that the cathode materials with the longest cycle life are LFP and LMFP with a cycle life of 2000-300, then comes NMC with a cycle life of 1000-2000. LCO has the lowest cycle life of only 500-1000.

The factors that contribute to the shortened life cycle of batteries are degradation and the three main causes of battery degradation, which are operational, environmental and time. The operational aspect of battery management concerns the manner in which the battery is treated and maintained during use. This factor is not specific to a particular cathode material but is influenced by the user. However, the time and environmental impact of different cathode materials can vary.

While time is an inevitable factor in all batteries, the different cathode materials have varying abilities to maintain a long life cycle. For instance, the layered structure is not particularly stable. The weak bonds between the layers make the cathode material more likely to crack. This can also be observed in the significant volumetric change in the layered structure for LCO and NMC. The volumetric changes are of significance with regard to the cycle life of the battery, as they give rise to mechanical stress and particle cracking, which in turn can lead to loss of active material and subsequent degradation and uncyclability. In contrast, LFP and LMFP with an olivine crystal structure exhibit a small but significant volumetric change. This structure is more stable than the layered structure, which makes it less prone to cracking and degradation. Consequently, LFP and LMFP have a higher life cycle than LCO and NMC. The spinel structure, in contrast, exhibits almost no volumetric change under the transport of Li-ions. This indicates that the cathode materials, such as LNMO have a longer life cycle for the battery.

The environmental factor is concerned with the application of the battery and the environment in which it is used, and factors such as temperature. While the temperature stability of the different cathode materials was discussed in the subsection over 4.1.4, the importance of the temperature can be looked at in combination with the cycle life. The thermal stability analysis is based on four factors: reactivity, C-rate, operating temperature range and thermal runaway. The results of these analyses show that LFP and LMFP are the most thermally stable cathode materials, while LCO, NMC and LNMO are the least thermally stable. This correlates well with the cycle life where LFP and LMFP is significantly better than NMC, LCO and LNMO with the lowest cycle life. This shows that thermal stability is a significant factor in battery cycle life.

4.1.6 Cost

The material expenses significantly impact the total economic viability. Cathode materials should both be able to have tolerable overall performance properties, as well as be cost-effective for large scale manufacturing. As stated in 2.10, all cathode materials have experienced an increase in costs over the last two years, partially due to the pandemic and the Ukraine-Russia war. Yet, the

increase in raw material costs may also be a result of the current demand for battery cathodes due to the global need for a green transition, hence an increase in the need for LIB, as can be seen in the figure.1.1. Rather than relying solely on fluctuations in the availability or direct cost of raw materials. Li and Ni has drastically kept on rising after high spikes since 2020, primarily as a result of the surge in demand for Li-ion batteries with high nickel content as NMC. If the increases continue, there could be a risk of a shift for producers to utilize more abundant materials such as LFP, LMFP, or LMNO

The LCO cathode chemistry is estimated to be mid-low cost-effective compared to LFP and NMC. Even though NMC too consists of cobalt, LCO is the cathode with the highest cobalt usage, as shown in Figure 2.52. While LFP has a relatively significant cost advantage compared to the different NMC cathodes, as shown in Figure 2.56. Since LFP is a nontoxic and free for Co and Ni, it is not affected by the price implications that follow. In addition to iron and phosphate being abundant and considerably more affordable raw materials, the cathode chemistry had an estimated price at 5-10 USD/kWh according to Figure 2.56. Regarding LMFP, the inclusion of manganese results in a reduction of the iron ratio, leading to decreased costs. Figure 2.57 displays the discrepancy at 5 USD/kWh in 2023 between LFP and LMFP, giving them a price estimation at around 55-60 USD/kWh and 50-55 USD/kWh. Considering the diverse NMC chemistries, it appears NMC 622 exhibits the highest cost at 20 USD/kWh, which aligns with the chemistry having the greatest portion of Co and Ni content. NMC811 appears to be the best choice in terms of price as it is slightly more affordable due to its lower Co ratio.

An LNMO cathode chemistry has the potential to be low cost as it is cobalt free, as well as it consists of more environmental materials as the low-cost material Mn as illustrated in Figure 2.56 and 2.55. As well as Mn covers up to 60% of the cathode chemistry shown in Figure 2.52. Leaving the remaining 40% to Ni, which is rather affordable compared to Co and Li but has experienced a high incline in cost. However, it is important to note that, as a relatively new chemical composition, cost evaluations on the same scale as the other ternary cathodes have not yet been made.

Cost is a highly relevant subject within all utilization applications. The lower the cost, the more desirable the cathode chemistry becomes for different areas. This indicates that LFP and LMFP are the cathode chemistries with the lowest cost. They are most likely followed by LMNO and LCO, which have reasonable costs. NMC is the most expensive composition, with NMC 822 being significantly more affordable than NMC 622.

4.1.7 Overall performance

In conclusion, LCO exhibits a relatively high specific energy of 120-150 Wh/kg and high energy density of 250-450 Wh/L, which is a result from the high cell at 3.8-4.4 V attributed by presence of Co. Therefore, it is considered one of the better chemistries to use in applications of limited space such as portable electronics. However, it suffers from a short life span at 500-1000 due it it is easily degradable. As well as it features poor specific power and safety, implicating the low thermal runaway temperature. Furthermore, the environmental impacts of mining cobalt, and the unethical geopolitical issues, contributes to the high cost of LCO compared to other cathodes.

NMC, with a regulated mass ratio of nickel, manganese, and cobalt, all offer higher cell voltage, specific energy, and energy density. With NMC cathode 811 resending the highest values as it consist of a larger share of Ni which correlates well with Co, resulting in the highest values within both fields energy content. In regard of safety, NMC offers better thermal stability than LCO as it has better properties for thermal runaway. However NMC 822 exhibit poorer stability than NMC 622 as nickel-rich cathodes contributes to lower thermal stability and overall cathodes with no or less nickel and cobalt perform better at safety. In addition, NMC was concluded to be the most expensive cathode chemistry due to high Co prices as well as increaed nickel prices. Since Co is more expensive than Ni, culminating in ratios with higher Co content to have the largest cost with NMC 622, while NMC 811 is cheaper. The NMC cathode that is best suited for high voltage mobile applications where a battery's size and weigh is important.

On the other hand, LFP cathodes are perceived as remarkably safe due to their good thermal stability. It relies exclusively on environmentally friendly and abundant materials, being cobalt-free, thus resulting in its low cost. Other advantages of LFP as great specific power and longer life cycles comes from the olivine crystal structure, which is more than most NMC chemistries. The lower level of reactivity also extends the cycle life of LFP compared to the other cathode materials. As established, LFP has lower cell voltage compared to cathodes with Ni and Co and lacks significant performance in specific energy or energy density, staying between 90-200 Wh/kg and 362-437, respectively. Primarily, because its materials occupy more volume, resulting in other cathode options like NMC and LCO to outperform LFP. These key indicators hold particular importance within residential and stationary storage applications, as metrics such as energy density are being less emphasized due to weight being less critical. In addition to this, mobile applications are not dependent on traveling longer distances. The rate of charge for LFP also makes the cathode well suite for

However, a measure to achieve higher specific energy and energy densities was to incorporate manganese in the cathode chemistry, creating LMFP. This cathode chemistry exhibits the same features as LFP but with enhanced properties in regard to energy densities reaching values of 210-240 Wh/kg and 280-300Wh/L. Meaning the cathode chemistry is both nontoxic and of safe materials for the environment compared to other heavy metal compounds in cathodes. As well as it is lower in cost than LFP and still has a superior cycle life as the added manganese lowers the reactivity of the material. LMFP still remains to be broadly commercialized as it is relatively new within the LIB market. With enhanced values for energy content, LMFP can be a suitable option for vehicles aiming to travel far as it is not affected by the battery size or weight. SATE RATE OF CHARGE AS LFP

Lastly, LNMO, a battery not yet commercialized, shows high promise in the future with good theoretical aspects. Therefore, the current values presented have a high potential of increasing in the next couple of years. Its cell voltage has shown promise of reaching 5V but also lingers down to 3V. Giving a relatively big gap in the cell voltage. While the specific energy is given from 150-165 Wh/kg, however, the theoretical is at almost 700 Wh/kg, anticipating an increase in years to come. In terms of energy density, it has relatively high values for being cobalt-free at around 250-280 Wh/L. As it does not include any toxic heavy metals and is rather low-cost compared to NMC and LCO, LNMO is considered eco-friendly. Currently, LNMOs exhibit the shortest life cycle at 250-500. Again, this is most likely due to the cathode being less researched. LMNO can be fit for both stationary and mobile applications, as it is still quite new and still has a potential for longer life cycles and energy content. In terms of TRL, LNMO has mainly been experimented with in lab environments, giving it a TRL of 4, whereas LCO, NMC, and LFP are very well established with a TRL of 9. LMFP has complete systems with many companies aiming to use them in the coming years, resulting in the chemistry being assigned a TRL of 8.

4.2 Comparison of the anode materials

The capacity and performance of the battery depend significantly on the intrinsic properties of the electrodes. Concurrently with the cathodes being presented and discussed comparing vital characteristics of each composition, the anodes will be assessed for *Beyonder*. The potential anode materials include Gr, Gr-Si, LTO, HC and Li-metal.

4.2.1 Cell voltage

In order for the battery to have a high voltage, it is important that the anode has as large a difference in cell voltage from the cathode as possible. Since the only thing discussed in this

section is the voltage of the anode material, it is assumed that the Beyonder is looking for batteries with a high voltage. So this is what will be taken into account.

As Table 2.5 shows, Gr has a remarkably low and neutral voltage. This may be one of the reasons why it fits so well with several cathode materials. The value of the voltage for Si-doped Gr is not clear, but it is known that Si does increase the voltage significantly, which makes the ratio of Si important. The voltage of Gr-Si is therefore put as everything over Gr. HC does have a relatively high voltage and is hence suitable for relatively high voltage applications, while LTO has the highest voltage, meaning it is the best when it comes to high voltage applications.

4.2.2 Specific energy

Anode materials with greater specific energy (Wh/kg) are able to accommodate a higher number of Li-ions, thereby enhancing the total energy storage capability of LIBs. Si can be used to replace all or some of the Gr in the anode in order to make it lighter, thus increasing the specific energy. On its own, Gr does not exhibit great specific energy. The same applies for LTO with lower energy density at 50-80 Wh/kg, which is even lower than Gr. As for HC, it has better overall performance compared to the commercialized Gr, implying greater specific energy as well. Another anode material is the innovative Li-metal, which can yield an impressively greater specific energy at 400-450 Wh/kg.

In terms of TRL, the lack of specific energy is a disadvantage within EV vehicles, making Gr and LTO not the best choice when relying solely on this characteristic. Gr-Si or Li-metal are the preferred anode materials in mobile applications where weight is essential.

4.2.3 Energy density

Energy density for Gr is low as a result of its limited capacity and layered structure since the weak bonds between the layers only allow 55% of Li-ions to deintercalate. Furthermore, the same applies for Gr-doped Si, but the bonds between these layers are strengthened, so the limited percentage of the allowed deintercalated Li-ions is increased. This leads to a higher energy capacity. However, the Si expands during cycling which increases the volume of the anode material. Overall, this results in a lower energy density. The crystal structure of LTO is more complex compared to other anode materials. Therefore, its structure takes up more space, resulting in a lower energy density. Moreover, the structure of HC is highly complex and is still unknown. Because of this, it is hard to give a value of energy density, but it is assumed that it is higher than Gr since it has an overall better performance. Meanwhile, Li-metal exhibits the

greatest energy density.

4.2.4 Cycle life and degradation

It is just as important that the anode has a high cycle life as the cathode for the battery as a whole to have a high cycle life. In order to get this, the anode has to have as little degradation as possible. Since the Gr has weak bonds between its layered structure, the material will not take as much strain as the other materials. Si-doped Gr does, on the other hand, have stronger bonds between the layers and can therefore withstand more stress than Gr. The crystal structure of HC is very complicated, but literature refers to the structure as “enhanced”. HC is therefore considered, as seen in Table 2.5, to have a more stable structure than Gr and Gr doped with Si. Finally, we have LTO, which has a superb cycle life of 3000-7000.

The volumetric changes of the anode materials is also an important factor for the degradation of the materials. If the anode has too big of a change, this will lead to mechanical wear and stress in the SEI layer, which results in even more increased growth. Faster growing SEI leads to a decrease in the cycle life. From the values in Table 2.5, Gr has a volume change of 12%. Since the volume increase of Gr-Si will vary with the ratio of Si, the percentage in the table is set to between 12% and 400%. This is the largest volumetric increase of the anodes because LTO only increases with 1%. Gr doped with Si is more likely to degrade faster than the other anode materials and will therefore have a lower cycle life, followed closely by Gr. LTO is in the best position, with by far the least volume change, which means that in theory, it will have an even longer life than the other anode alternatives.

4.2.5 Cost

The intrinsic qualities of the anode largely depend on the anode mix, which is heavily influenced by the cost of the anode materials used. Gr is comparatively the most cost-effective choice among the various anode materials with a price of 6-11 USD/kg as shown in Table 2.7. With NG being 20% lower in cost than SG, NG is the most economical material to mix with. Gr-Si costs 12 USD/kg, whereas a Si-dominated anode costs around 36 USD/kg. This results in an anode mix with less Si being more affordable than an anode with a dominant material use of Si. LTO cost is set to be over 18 USD/kg, due to this being the price of titanium, staying in between the price gap of Gr-Si and Si dominated. This makes SG and NG the most affordable materials to use in the anode, followed by Gr-Si, LTO, and then any Si-dominated anode material.

4.2.6 Overall performance

It is important to state, when considering the TRLs for anodes, that they are not as vital as for cathode materials. This is evident in the widespread commercialization of Gr within all sorts of applications as it does not exceed in all of the discussed characteristics.

To conclude, Gr with a cell voltage of 0.1 V is dominating the anode market for LIBs. Compared to other anode materials, it has become the traditional material of choice given its low cost, long commercialization within the LIBs field, stability, and relatively good cycle life. Despite its higher specific energy compared to LTO, it does not surpass materials like Gr-Si and Li-metal. As stated, when Gr is mixed with an amount of Si, it provides a higher specific energy. However, a drawback of Si is that it causes swelling during charging and discharging, which expands the volume and affects the energy density. In addition, the swelling also contributes to the degradation of the cell, reducing the cycling performance. For TRL, Gr and HC are already well established with a TRL of 9. Gr-Si is still in development but has had several advancements, so it is estimated that it has a TRL of 7. The optimal application of Gr-Si is in areas where weight is a primary consideration but not volume or cycle life.

LTO anodes exhibit the lowest potential of specific energy compared to the other anode materials. In contrast, it is assumed that it offers the longest cycle life performance and relatively good safety. LTO is particularly well-suited for mobile applications where larger and heavier batteries are acceptable, as well as for energy storage applications where cycle life is of the utmost importance. Since LTO anodes are fairly new, they have not been demonstrated in an operational environment. This means that their estimated TRL is 6.

HC has gained commercial attention because of its excellent overall performance, which has the potential to even outperform Gr anodes in the future. HC exhibits relatively good cycling performance, specific energy, and energy density and has a cell voltage of 0.75 V. It is applicable in both mobile applications where weight and volume are relevant and in energy storage devices.

Li-metal has one of the highest performances in both specific energy and energy density, however they are prone to various challenges. Li-metal is appropriate for all mobile applications as it has very high-performance rates but not energy storage systems as its cycle life is relatively low. Similarly to LTO, Li-metal has not been demonstrated yet so the estimated TRL is 6.

4.2.7 Sodium-ion Batteries

SIBs present a promising alternative for the battery industry in the future. Utilizing Na can alleviate the criticality issues that Li is predisposed to because of the increasingly high demand of LIBs. Since the performance of SIBs is lacking compared to LIBs, it is currently not practical for as many situations. Nevertheless, the abundance of Na, the low costs involved, and the chemistry similarity to Li give potential for cheap and sustainable batteries in the upcoming years.

While the different anode and cathode chemistries are vital for a battery, the selection of a suitable electrolyte for the different compositions is crucial for optimal compatibility.

4.3 Electrolytes

As previously stated, there are three main types of electrolytes: liquid, solid, and semi-solid electrolytes. To evaluate each of these concisely, they will be compared using different metrics. The metrics used will be ionic conductivity, general safety, mechanical strength, maturity, costs, and Li-metal compatibility.

4.3.1 Ionic Conductivity

In terms of ionic conductivity, the LEs score the highest, with both carbonate-based electrolytes and ILs exhibiting extremely high ionic conductivity compared to the electrolytes that incorporate solid elements. For both solids and semi-solids, a common theme is that the lower the distributions of polymers, the higher the ionic conductivity. For semi-solid electrolytes, this means that GHEs outperform GPEs, but both still exhibit lower ionic conductivities than LEs. Lastly, SSEs perform the lowest, by nature of consisting entirely of solid materials. ISEs perform better than hybrid SSEs, while SPEs are the least conductive.

4.3.2 Safety

In aspects of safety, the common denominator is that the more solid elements are incorporated, the safer the electrolytes. This means that SSEs rank the highest, followed by semi-solid electrolytes and LEs. For SSEs, electrolytes partially consisting of inorganics perform better, leading to hybrid-SSEs and ISEs exhibiting the highest safety followed by SPEs. It is important to note that the use of sulfide SSEs can develop toxic gases when in contact with water, which could potentially limit the usage of these considerably in applications where water is involved. Semi-solid electrolytes follow the same trends, with GHEs outperforming GPEs. Finally, LEs shows

the least amount of safety. ILs are however, considerably safer than carbonates, with carbonates being the only ones to deteriorate because of higher cell voltages.

4.3.3 Mechanical Strength

As mechanical strength means to maintain structural integrity, this metric will largely follow the same trends for the different electrolytes as in the previous section about safety. SSEs generally perform the best, closely followed by semi-solid electrolytes. LEs do not exhibit any mechanical strength in the context of maintaining structural integrity. For SSEs, ISEs are the most beneficial, with both hybrid-SSEs and SPEs following. In terms of semi-solid electrolytes, GHEs and GPEs perform similarly. Lastly, both LEs exhibit a relatively low strength due to their liquidus nature compared to electrolytes that incorporate solid elements.

4.3.4 Costs

When it comes to costs related to manufacturing the different kinds of electrolytes, one has to look at the level of maturity, establishment and manufacturing difficulties. LEs being the first commercialized electrolytes, it is highly established in the industry, leading to optimized manufacturing and lower costs. Although this is true for carbonates, ILs are considered to have a difficult manufacturing process and have a substantially higher cost in comparison. Although there are limited sources regarding the costs of manufacturing SSE and semi-solid electrolytes, they are considered to be higher than that of LEs. However, LEs are a saturated technology, whereas SSEs and semi-solid electrolytes still have room for improvement, such as in the manufacturing processes. More on this in section 4.4.

4.3.5 Li-metal compatibility

Li-metal compatibility is an interesting topic with the recent emergence of SSEs. LEs can not facilitate the use of Li-metal anodes because of the dendrite formations that occur. SSEs and semi-solid electrolytes, however, have higher mechanical strength, thereby maintaining their structural integrity and resisting protrusions. Semi-solid electrolytes do contain a small amount of LE, lowering their inhibition, but are not found to have as prominent dendrite formation issues as LEs. Generally, the incorporation of active fillers in hybrid electrolytes results in instability with Li-metal anodes, whereas passive fillers do not experience these issues.

4.3.6 Summary

There are certain trends noticeable when considering the given metrics. Generally, an increase in solid elements increases both safety and mechanical strength. Furthermore, the incorporation of certain inorganics bolster these attributes. In contrast, an increase in solids translates to higher manufacturing costs. This can be attributed to the establishment and maturity of the technologies. The final noticeable pattern is that a higher amount of polymers leads to a decrease in ionic conductivity.

Given the results of the metrics, SSEs are more optimal for uses that require high safety, whereas LEs are better for high power applications. Semi-solid electrolytes gain the properties of both LEs and SSEs, but not to the extent of either one.

4.4 Manufacturing

A few characteristics are present in the unconventional SSLIB manufacturing method compared to conventional batteries and SSBs, which makes them beneficial. Among these are the elimination of several processes required in liquid and solid electrolytes, such as the drying and solvent recovery processes. One advantage is the omission of NMP use since NMP is a toxic solvent. As can be seen in Table 2.2, the drying and solvent recovery processes require a considerable amount of energy, taking up almost half of the total energy consumption. In addition, the duration of the process is around 60% of the total cell manufacturing duration. With the non-traditional SSLIB production method, the most demanding process in battery manufacturing can be eliminated, thereby massively increasing efficiency and reducing energy use. However, this does not result in a correspondingly large impact in solvent recovery cost, since 2.1 shows that it accounts for less than 5% of the total yearly cost. When recommending a battery for *Beyond*, despite the immense potential of this unconventional manufacturing method, it is not accounted for due to the limited scope of data used in this thesis.

The reduction in cost from the omission of drying and calendaring is greater than that from solvent recovery. In particular, drying represents one of the most expensive processes, accounting for a portion of 15% of the total cost. However, the removal of these steps does not significantly affect the total energy consumption or time reduction. A disadvantage in SSLIB manufacturing is that both the solid and the liquid have to be manufactured before being combined. This adds to the cost and time consumed for producing them separately for either a conventional LIB or an SSB. Nevertheless, the overall attributes indicate that transitioning to this unconventional SSLIB manufacturing method is greatly beneficial for reducing cost, time and energy consumption, thus creating an opportunity for more efficient and sustainable bulk production of LIBs in the future.

For processing the cathode and separator in SSBs, using a wet processing method facilitates a highly practical transition from conventional batteries since it is already the most mature method. This is particularly the case for ISEs which have an established wet processing method for both the cathode and the separator. The use of oxide ISEs is hindered by their brittle properties. Requiring a calendaring and sintering step for the cathode, as well as an additional challenging sintering step for the separator renders them less viable. Sulfide ISEs, in turn, can not be used with polar solvents and a PVDF binder, meaning that slight manufacturing changes are needed. Despite this, sulfide ISEs have shown to be more promising in wet processing. Moreover, forming bulk-type SSBs further supports the transition as the electrode structure resembles LIB electrodes. With SSLIBs, the calendaring step and binder are omitted, leading to

fewer considerations in this process.

While dry processing is different from the existing LIB processing approach, making the transition to SSBs more challenging, there are other benefits to it that make it valuable. One aspect is that it is an established method for SPEs, and LFP cathodes are commonly used with SPEs. In addition, pouch cell packing is the most convenient for SSBs. This results in a natural transition for *Beyond*. Another aspect is that no solvent is used in dry processing, thus leaving out the most arduous task in typical processing. Dry extrusion is also applicable and established for SPE separators. Lastly, SPEs have the advantage of being significantly cheaper than ISEs.

Therefore, one promising manufacturing alternative for *Beyond* within SSBs and SSLIBs would be to use dry processing of an SPE with an ISE filler for bulk-type pouch cells. This would allow for an achievable transition from LIBs while simultaneously capitalizing on the advantageous properties of Hybrid SSBs and maintaining an affordable cost.

Anode-less manufacturing is an attractive technology within LMBs in SSBs and SSLIBs due to the need of anode processing in an inert environment. This eliminates the time consumed and the cost involved for this step and for the production of Li-metal foils. Additionally, their high energy density makes them highly appealing. The biggest drawback is the loss of Li during battery cycling, therefore requiring excess Li to balance it. This is not ideal, as the market price of the metal is volatile and increasing. This results in an unstable production and supply chain, thereby raising the risk to the businesses involved. Furthermore, the sources of Li are limited, so the added dependence on it would not be sustainable in the long term. While anode-less batteries are not viable at present, their benefits could make them immensely valuable in the future.

Although Na is not a primary focus of this report, there is some potential for its use as an anode over Li in certain instances. One side is that Na is considerably more abundant than Li and can be extracted from a broader range of global locations. Another is that Na is significantly less expensive than Li. However, the larger size and less electronegative nature of Na slightly limits the energy and power density, rendering it less successful in several commercial applications. Nevertheless, applying Na in batteries where the optimal performance that Li provides is not necessary could help mitigate the increased use and cost of Li. This is particularly the case for Na in stationary energy storage devices compared to mobile ones such as EVs. Moreover, the flexibility of options may be more sustainable in the long term.

4.5 Sustainability

The use of Li-metal in SSBs and SSLIBs eliminates the conventional Gr anodes in LIBs and therefore the criticality of the materials decrease. The upside is that we become less dependent on other countries for the materials and there is a smaller risk involved in the supply chain.

Shifting away from using Co in the cathode material would alleviate some of the issues, such as the dependency on the material, toxicity, material shortages, and the high and volatile price. More recently, other cathode materials have also been affected by external factors. The global conflicts, in particular the one between Russia and Ukraine, as well as the pandemic, have drastically influenced the price and availability of Ni and other battery materials. In light of this, LFP batteries have shown to be capable of withstanding unforeseen external and uncontrolled environmental and economical risks. *Beyonder* is already a producer of LFP batteries, which as shown in Figure 2.60 has a low median environmental impact and criticality score in large part because the chemistry uses no Co or Ni. The shift to SSB or SSLIB technologies would therefore, further strengthen the company's position as a manufacturer of sustainable batteries while possibly maintaining sufficient performance and safety.

Recycling

There is a significant potential for recycling of LIBs in the future. The largest challenge to be overcome for all battery types is to achieve a more standardized design. This would make the recycling process easier and more efficient. It could also make automation of the recycling process feasible. Despite the reduced environmental impact and criticality of LFP cathode chemistries compared to the other discussed cathode chemistries, pyrometallurgical treatment remains the most suitable option when approaching the end-of-life recycling stage. Nevertheless, it can be anticipated that developments in hydrometallurgical approaches will render them more suitable for LFP batteries.

Pyrometallurgical recycling has the drawback of needing high temperatures, thus expending more energy. Furthermore, this treatment yields fewer pure metals than other methods. Nevertheless, with increased developments in direct recycling and more standardized pack designs, these issues could be mitigated. With the possible advent of SSBs and SSLIBs, a standardized design for simple recycling is also an important aspect to consider.

4.6 Recommendation

When choosing the optimal combinations of cathode, anode, solid electrolyte and semi-solid electrolyte chemistries, it is crucial to evaluate their applicability for *Beyonder*. This implies that the batteries will be considered from an environmental, economic and safety aspect, as well as from the standpoint of their ability to deliver high power for large-scale use. This is because, as mentioned prior, European battery manufacturers have not reached the same level of maturity as China in regards to small-scale batteries. With this in mind, the technologies are recommended from a stationary energy storage perspective and from a transportation perspective based on what has been discussed in the preceding sections.

It can be assumed that the majority of the data found and used in this thesis is reliable, with several peer-reviewed articles being examined for consistency. However, there are a few exceptions. An example is the estimated cost of manufacturing an SSB. Moreover, changes in technology throughout the years have an influence on the data, giving rise to a degree of fluctuation. This is especially the case for SSBs and SSLIBs, which are relatively new technologies. With this in mind, the thesis has attempted to stay as current as possible in regard to its sources.

4.6.1 Energy storage

For energy storage, a battery's long cycle life, safety and cost are a desirable attributes. While specific energy and energy densities are not as highly prioritized as they are in the transportation sector. Therefore, an attractive battery would be a prismatic solid-state, LFP battery with an SPE and a Li-metal anode. The LFP cathode is a low-cost, high-sustainable option that is safe and can have a high number of cycle lives. The low cost stems from its use of abundant materials Fe and P. The sustainability aspect of LFP comes from the fact that both of these abundant materials are non toxic and has low carbon footprint. Yet, it is harder to recycle since it uses pyrometallurgical recycling, which has a higher environmental impact than other recycling methods. In this context, it is crucial that the battery is capable of absorbing and storing a large amount of energy. However, the fact that the battery for energy storage is stationary means that it is not dependent on weight. Consequently, energy density is not a significant factor in the case of energy storage. The relatively low energy density of LFP does not significantly impact its capacity for energy storage. Further, LFP has a high power density which is beneficial but not crucial within this application. The current input is relatively stable, and the discharge has no specific requirements. However, if an additional production of electricity arises, for instance, from a wind or solar farm, it is advantageous that the LFP has a high power density, thus the

ability to absorb energy in a shorter time interval. The high cycle life of LFP and LMFP batteries is an important characteristic for investors in energy storage. A battery with a long cycle life will thereby derive greater value. This makes LMFP also a suitable cathode candidate within the storage stationary applications. Additionally, LMFP has a slightly lower cost than LFP. Even though it has enhanced electrochemical properties, LMFP is a relatively new technology compared to the widespread commercialized LFP. With *Beyonders* prospect of LIB technology in 5-10 years, LFP with a TRL at 10 would be the best choice as this is a familiar cathode for the company. Since they have a production chain for LFP, meaning the transition is smoother than for other candidates making / than that of LMFP.

The SPE, while exhibiting relatively poor performance, represents a highly cheap alternative with a simple and established production chain. Furthermore, the solid nature of the electrolyte provides safety and stability. The prismatic design enables good structural stacking, which is ideal for energy storage. From a long-term perspective, hybrid SSEs could be viable for energy storage for higher thermal stability and a wider electrochemical stability window compared to LIBs. In particular, an SPE with an ISE passive filler provides increased safety, stability, and mechanical properties. The drawback of low ionic conductivity is counteracted by the standpoint that it is not as massively needed. The largest barrier to overcome is the increase in cost and the added manufacturing step, however improvements in these areas can be anticipated.

It is advantageous for the ideal battery composition to have an anode material with similar characteristics to the cathode. This can enhance the battery's vital properties for energy storage applications. However, it is also solely dependent on the type of electrolyte. The use of SPE excludes the choice of Li-metal. An anode with similar properties to LFP is HC, with a superior overall performance compared to Gr. It exhibits a relative good overall safety with a long life cycle performance, in addition a high cell voltage. This is also the anode material utilized by *Beyonder*, making it a preferred candidate in terms of time-saving benefits, as well as cost and safety advantages. However, in a long-term prospect for *Beyonder*, LTO would be a good investment. This is due to its excellent performance in crucial areas for energy storage applications, such as high safety, long cycle life, and relatively low cost, compared well with the cathodes of choice.

4.6.2 Transportation

In terms of transportation, it is advantageous to consider the various modes of transport differently. This is because, for passenger and commercial vehicles, lighter weight is an important factor (e.g., in aircraft, ferries, and passenger cars), whereas in other vehicles, it is less crucial

(e.g., in trucks). For heavy weights, the specific energy and energy density are less vital than the power density, whereas the opposite is the case for light weights.

When it comes to heavy transportation properties such as high specific power, safety, cost and long life cycle are vital to account for to create the ideal battery. A conventional LFP battery with a HC anode and prismatic design remains a very appealing alternative for *Beyonder*. Due to their high specific power, LFP and LMFP are well suited to heavy-duty ground transport. As previously stated, LFP and LMFP are heavier than other cathode materials, but in heavy transport, the weight of the battery becomes a smaller proportion of the total weight of the vehicle. The high power density is an important factor for heavy transport, as it enables the battery to start up and accelerate to speed. In contrast, the energy density of LFP and LMFP is relatively low, which is a disadvantage for vehicles that require long-distance travel or that lack the option of charging along the route. Furthermore, the low environmental impact of LFP batteries enables this battery to be highly sustainable. As established, both cathode options are cost-effective. It is up to *Beyonder* to decide what TRL they want to invest in for the future.

Transitioning would be a challenging ordeal with limited rewards in the coming years. This is because both SSBs and SSLIBs are currently too underdeveloped to match the power density requirement due to their issues of lower ionic conductivity and higher interfacial resistances between the electrode and the electrolyte. Moreover, the relative immaturity, higher costs, and more demanding manufacturing processes associated with these batteries often render them less practical than LIBs for heavy-weight transportation. Nevertheless, while many of the SSBs and SSLIBs benefits are not applicable here, GHEs stand out as a promising avenue for further exploration in the far future, as these have the potential to provide the batteries with the necessary ionic conductivity while maintaining sufficient interfacial contact. Currently, high costs and difficult manufacturing are a concern. However, the increased safety, enhanced electrochemical, and high Li-ion transference make GHEs notable for long-term potential advancement.

Anode materials suitable within the prospect of a TRL at 9-10 for *Beyonder* are Gr, Gr-Si, or HC. Regardless of size and weight, cycle life is an important metric within this transport sector. This makes Gr-Si least suitable, in addition to its higher cost than Gr and high safety concerns. It is assumed Gr is cheaper than HC, unless this is the most favourable factor within this area HC will be the best alternative within this prospect. For a TRL on 5-6, LTO would be the best to apply as an anode material due to its overall better performance than HC, with the exception of specific energy. Since this is less of a concern for these vehicles, LTO makes a good candidate with its relatively low-cost, high safety, and long cycle life.

One viable battery chemistry for light weight purposes in the coming future is a pouch semi-solid NMC/LMFP battery with a GPE and Li-metal anode. In vehicles where weight is a significant factor, NMC811 is a more suitable cathode material. Given the importance of weight in certain forms of transportation, NMC is the most commonly used material despite its challenges. Among other considerations, the cathode material is expensive, less stable, and has a shorter cycle life than other cathode materials. Conversely, NMC exhibits a relatively high energy density, which, when combined with a reduced weight, results in a considerably longer range, for instance, for passenger vehicles, than other cathode materials would. Currently, range represents a significant obstacle in the EV market, thus influencing the prioritization of this technology and its subsequent development. If *Beyonder* wants to look at a longer prospect within this field, LNMO with a TRL at around 3 could be a suitable option. Despite LNMOs' present values, it is anticipated that these will increase due to the sky-high theoretical specific energy and high cell voltage. As discussed, within the next decade, it is anticipated that this battery will, with the exception of cell voltage, enhance its performance rates by a lot. Therefore, it can be a very suitable application for passenger and commercial EVs since it is anticipated to weigh less and be cheaper and safer compared with NMC811.

With a GPE, the battery gains the advantage of higher ionic conductivity than SPEs and higher safety than LEs while also remaining relatively easy to manufacture and cost-effective. Additionally, the pouch cell format is ideal in this case due to its lighter weight, thereby further facilitating a seamless transition for *Beyonder* in the manufacturing process. Initially, the use of ionic liquids seems to be the best liquid component for semi-solid electrolytes. However, carbonate-based electrolytes can be a viable alternative for cost reduction in the case of LMFPs and NMCs. In the future, hybrid SSEs is promising for the same reasons as in the field of energy storage applications. Utilizing an active filler could be more appropriate here when it comes to vehicles that require an increase in ionic conductivity. In spite of the safety risks involved with the Li-metal anode instability, it can be expected that safety improvements are due for this type.

Further, the anode material, similar to the cathode candidate is expected to be of higher specific energy and energy density. Gr with Si ends up being the most suitable application compared with Gr as it has a higher specific energy range. However, HC, in addition to having longer energy density, also exhibits a better cycle life and safety than that of Gr with Si. In addition, this anode is already used by *Beyonder*. For a longer prospect, HC would most likely still be the preferred option, as LTO has a very low specific energy. A property that is highly prioritized over the value of safety, cycle life, and cost, as pointed out with the NMC811 cathode candidate.

5 Conclusion

The purpose of this thesis was to investigate the existing electrode technologies and the feasibility of semi-solid state electrolytes. Based on the values found in literature reviews and studies, the aim was to assess which compositions would be suitable for the energy storage and transport market sectors, depending on the TRL of the compositions.

When considering energy storage applications, the most important characteristics to consider are safety, costs, reliability and cycle life. For energy storage systems in 5-10 years, this analysis will, due to the short time span, recommend using components with a high TRL level. This will include using LFP or LMFP as cathode material within stationary storage applications since great cycle life performance, low cost and high safety are key metrics. In addition, it is not reliant on the size nor the weight of the cathode in these applications which suits LFP and LMFP well due to their low specific energy and energy density. This works well in combination with HC since it has good overall performance. In addition to SPE electrolyte, which fulfills these requirements, without compromising much regarding performance characteristics.

Furthermore, for automotive applications, there are two different types to consider: vehicles for which weight is an important factor, and vehicles for which weight is less important. The first one is heavy transport, where power density of the cell is vital rather than the specific energy and energy density. In addition properties such as safety, costs, sustainability and cycle life are important. It was concluded that for these properties, a prismatic cell with either an LFP or LMFP cathode in combination with an HC anode, utilizing an IL electrolyte, is the optimal configuration in the coming years.

In terms of lighter automotive applications, the battery chemistry is dependent on features such as specific energy, energy density, cost and safety. It was reasoned that for upcoming years, a pouch cell NMC battery with a graphite anode and GPE electrolyte is ideal. Looking ahead, hybrid SSEs were deemed to be exceedingly promising.

Overall, SSLIBs are currently too immature and underdeveloped to be recommended in the near future other than for light transport. From a long-term perspective, they have vast room for improvement, giving them the possibility to compete with current commercialized batteries.

5.1 Further Research

If *Beyond* aims to look at long term prospects on relevant battery chemistries in 10-20 years, various technologies can be considered due to their promising potential within these application fields.

LNMO, with a TRL of 4 has a lot of potential due to its high voltage and specific energy. Additionally, Sodium-ion batteries are promising largely because of the abundance of sodium. It is also relevant to mention that ILs have untapped potential for use in SSLIBs, as many of the synthesized types of ILs have not been attempted in SSLIB production yet. This should therefore be taken into account when considering promising SSLIB batteries in the long-term.

References

- [1] Statista. ‘High Demand for Lithium-Ion Batteries’. In: (2020). URL: <https://www.statista.com/chart/23808/lithium-ion-battery-demand/> (visited on 18/05/2024).
- [2] Battery University. ‘BU-101: When Was the Battery Invented?’ In: (2022). URL: <https://batteryuniversity.com/article/bu-101-when-was-the-battery-invented> (visited on 18/05/2024).
- [3] Odne Stokke Burheim. *Engineering Energy Storage*. Elsevier Science, 2017.
- [4] Moran Michael J. et al. *Principles of Engineering Thermodynamics*. John Wiley & Sons Inc, July 2018.
- [5] The editors of Encyclopaedia Britannica. ‘internal energy’. In: (2024). URL: <https://www.britannica.com/science/internal-energy> (visited on 11/04/2024).
- [6] Lars Egil Helseth. *termodynamikk*. 2024. URL: <https://snl.no/termodynamikk> (visited on 22/03/2024).
- [7] oiu. ‘Entropi’. In: (2011). URL: <https://www.mn.uio.no/ibv/tjenester/kunnskap/plantefys/leksikon/e/entropi.html> (visited on 11/04/2024).
- [8] Khan Academy. *Gibbs free energy and spontaneity*. URL: <https://www.khanacademy.org/science/chemistry/thermodynamics-chemistry/gibbs-free-energy/a/gibbs-free-energy-and-spontaneity> (visited on 04/04/2024).
- [9] Khan Academy LLC. *What is power?* URL: <https://www.khanacademy.org/science/physics/work-and-energy/work-and-energy-tutorial/a/what-is-power> (visited on 19/03/2024).
- [10] uio. *Kjemisk likevekt*. 2019. URL: <https://www.mn.uio.no/ibv/tjenester/kunnskap/plantefys/leksikon/k/kjemisk-likevekt.html> (visited on 31/03/2024).
- [11] Unni Eikeseth. ‘redoksreaksjon’. In: (2022). URL: <https://snl.no/redoksreaksjon> (visited on 18/04/2024).
- [12] UIO. ‘Redoksreaksjoner’. In: (2011). URL: <https://www.mn.uio.no/ibv/tjenester/kunnskap/plantefys/leksikon/r/redoksreaksjoner.html> (visited on 18/04/2024).
- [13] Halvor Aarnes. ‘redokspotensial’. In: (2023). URL: <https://snl.no/redokspotensial> (visited on 18/04/2024).
- [14] Einar Skarstad Egeland. ‘oksidasjonstill’. In: (2024). URL: <https://snl.no/oksidasjonstill> (visited on 18/04/2024).
- [15] uio. ‘Kjemisk potensial’. In: (2011). URL: <https://www.mn.uio.no/ibv/tjenester/kunnskap/plantefys/leksikon/k/kjemiskpo.html> (visited on 11/04/2024).

- [16] Robert J. Ouellette and J. David Rawn. '1 - Structure of Organic Compounds'. In: (2015). Ed. by Robert J. Ouellette and J. David Rawn, pp. 1–32. DOI: <https://doi.org/10.1016/B978-0-12-802444-7.00001-X>. URL: <https://www.sciencedirect.com/science/article/pii/B978012802444700001X> (visited on 26/04/2024).
- [17] W. Wang et al. 'Chapter 1 - Electrochemical cells for medium- and large-scale energy storage: fundamentals'. In: *Advances in Batteries for Medium and Large-Scale Energy Storage*. Ed. by Chris Menictas, Maria Skyllas-Kazacos and Tuti Mariana Lim. Woodhead Publishing Series in Energy. Woodhead Publishing, 2015, pp. 3–28. ISBN: 978-1-78242-013-2. DOI: <https://doi.org/10.1016/B978-1-78242-013-2.00001-7>. URL: <https://www.sciencedirect.com/science/article/pii/B9781782420132000017> (visited on 23/02/2024).
- [18] The editors of Ensyclopedia Britannica. 'electromotive force'. In: (). URL: <https://www.britannica.com/science/electromotive-force> (visited on 05/04/2024).
- [19] GeeksforGeeks. 'Battery Capacity'. In: (2023). URL: <https://www.geeksforgeeks.org/battery-capacity/> (visited on 30/04/2024).
- [20] Bašić Hrvoje, Bobanac Vedran and Pandžić Hrvoje. 'Determination of Lithium-Ion Battery Capacity for Practical Applications'. In: (2023). URL: <https://www.mdpi.com/2313-0105/9/9/459#> (visited on 13/05/2024).
- [21] Ronald Dell and David Anthony James Rand. *Understanding batteries*. Royal society of chemistry, 2001. URL: https://books.google.no/books?hl=no&lr=&id=-VJg6gLmy2UC&oi=fnd&pg=PR15&dq=batteries&ots=s09YpUogN6&sig=0NxcRLgIHTdInTOBHHGHkThwmbc&redir_esc=y#v=onepage&q=batteries&f=false.
- [22] Gregory L Plett. *Battery Management Systems, Volume 1: Battery Modeling*. Artech House USA, 2015. ISBN: 9781630810238.
- [23] The editors of Ensyclopedia Britannica. 'electrode'. In: (). URL: <https://www.britannica.com/science/electrode> (visited on 05/04/2024).
- [24] Bjørn Pedersen. 'periodesystemet'. In: (2023). URL: <https://snl.no/periodesystemet> (visited on 05/04/2024).
- [25] NTNU. *Om Periodesystemet*. URL: <https://www.ntnu.no/periodiske-system/om-are> t.
- [26] Geir Martin Haarberg. *standard elektrodepotensial*. URL: https://snl.no/standard_elektrodepotensial (visited on 07/05/2024).
- [27] Abdirisak A Isse and Armando Gennaro. 'Absolute potential of the standard hydrogen electrode and the problem of interconversion of potentials in different solvents'. In: *The*

- Journal of Physical Chemistry B* 114.23 (2010), pp. 7894–7899. URL: <https://pubs.acs.org/doi/full/10.1021/jp100402x> (visited on 08/05/2024).
- [28] Geir Martin Haarberg. *spenningsrekken*. URL: <https://snl.no/spenningsrekken> (visited on 03/05/2024).
- [29] Shilpi Nagpal. ‘Electrochemical Series’. In: (July 2023). URL: <https://classnotes.org.in/class12/chemistry12/electro-chemistry/electrochemical-series/> (visited on 23/04/2024).
- [30] Jacob Joseph Lamb. *Personal communication*. Apr. 2024.
- [31] UiO. *Elektrokjemi*. Universitetet i Oslo. 2023. URL: <https://www.mn.uio.no/ibv/tjenster/kunnskap/plantefys/leksikon/e/elektrokjemi.html> (visited on 22/05/2024).
- [32] Battery University. *BU-307: How does Electrolyte Work?* Battery University. 2021. URL: <https://batteryuniversity.com/article/bu-307-how-does-electrolyte-work> (visited on 21/05/2024).
- [33] Dongjiang Li et al. ‘Modeling the SEI-Formation on Graphite Electrodes in LiFePO₄ Batteries’. In: *Journal of The Electrochemical Society* 162.6 (Feb. 2015), A858. DOI: 10.1149/2.0161506jes. URL: <https://dx.doi.org/10.1149/2.0161506jes>.
- [34] E. Peled, D. Golodnitsky and G. Ardel. ‘Advanced model for solid electrolyte interphase [SEI] electrodes in liquid and polymer electrolytes’. In: *Journal of The Electrochemical Society - J ELECTROCHEM SOC* 144 (Aug. 1997). DOI: 10.1149/1.1837858.
- [35] The Limiting Factor. *How a Lithium Ion Battery Actually Works // Photorealistic // 16 Month Project*. Youtube. 2021. URL: <https://www.youtube.com/watch?v=4-1psMHSpKs>.
- [36] Yitao He et al. ‘Thermodynamic Understanding of Formation and Evolution of Solid Electrolyte Interface in Li-ion Batteries’. In: *Batteries & Supercaps* n/a.n/a (), e202400059. DOI: <https://doi.org/10.1002/batt.202400059>. eprint: <https://chemistry-europe.onlinelibrary.wiley.com/doi/pdf/10.1002/batt.202400059>. URL: <https://chemistry-europe.onlinelibrary.wiley.com/doi/abs/10.1002/batt.202400059>.
- [37] A. Wang, S. Kadam and H. Li. ‘Review on modeling of the anode solid electrolyte interphase (SEI) for lithium-ion batteries’. In: *npj Comput Mater* (2018). DOI: <https://doi.org/10.1038/s41524-018-0064-0>. URL: <https://www.nature.com/articles/s41524-018-0064-0> (visited on 12/04/2024).
- [38] K. Kanamura et al. ‘Morphology and chemical compositions of surface films of lithium deposited on a Ni substrate in nonaqueous electrolytes’. In: *Journal of Electroanalytical Chemistry* 394.1 (1995), pp. 49–62. ISSN: 1572-6657. DOI: <https://doi.org/10.1016/0>

- 022-0728(95)03972-J. URL: <https://www.sciencedirect.com/science/article/pii/S002207289503972J>.
- [39] D Aurbach et al. ‘On the correlation between surface chemistry and performance of graphite negative electrodes for Li ion batteries’. In: *Electrochimica Acta* 45.1 (1999), pp. 67–86. ISSN: 0013-4686. DOI: [https://doi.org/10.1016/S0013-4686\(99\)00194-2](https://doi.org/10.1016/S0013-4686(99)00194-2). URL: <https://www.sciencedirect.com/science/article/pii/S0013468699001942>.
- [40] Doron Aurbach et al. ‘A short review of failure mechanisms of lithium metal and lithiated graphite anodes in liquid electrolyte solutions’. In: *Solid State Ionics* 148.3 (2002). Proceedings of the Symposium on Materials for Advanced Batteries and Fuel Cells. Organised in conjunction with the International Conference on Materials for Advanced Technologies (ICMAT 2001), pp. 405–416. ISSN: 0167-2738. DOI: [https://doi.org/10.1016/S0167-2738\(02\)00080-2](https://doi.org/10.1016/S0167-2738(02)00080-2). URL: <https://www.sciencedirect.com/science/article/pii/S0167273802000802>.
- [41] Doron Aurbach. ‘Review of selected electrode–solution interactions which determine the performance of Li and Li ion batteries’. In: *Journal of Power Sources* 89.2 (2000), pp. 206–218. ISSN: 0378-7753. DOI: [https://doi.org/10.1016/S0378-7753\(00\)00431-6](https://doi.org/10.1016/S0378-7753(00)00431-6). URL: <https://www.sciencedirect.com/science/article/pii/S0378775300004316>.
- [42] Peng Lu and Stephen J. Harris. ‘Lithium transport within the solid electrolyte interphase’. In: *Electrochemistry Communications* 13.10 (2011), pp. 1035–1037. ISSN: 1388-2481. DOI: <https://doi.org/10.1016/j.elecom.2011.06.026>. URL: <https://www.sciencedirect.com/science/article/pii/S1388248111002657>.
- [43] Thomas Waldmann et al. ‘Temperature dependent ageing mechanisms in Lithium-ion batteries – A Post-Mortem study’. In: *Journal of Power Sources* 262 (2014), pp. 129–135. ISSN: 0378-7753. DOI: <https://doi.org/10.1016/j.jpowsour.2014.03.112>. URL: <https://www.sciencedirect.com/science/article/pii/S0378775314004352> (visited on 12/04/2024).
- [44] E. Peled and S. Menkin. ‘Review-SEI: Past, Present and Future’. In: *Journal of The Electrochemical Society* (2017). URL: <https://iopscience.iop.org/article/10.1149/2.1441707jes> (visited on 12/04/2024).
- [45] Stephan Leuthner. ‘Lithium-ion battery overview’. In: *Lithium-Ion Batteries: Basics and Applications*. Ed. by Reiner Korthauer. Berlin, Heidelberg: Springer Berlin Heidelberg, 2018, pp. 13–19. ISBN: 978-3-662-53071-9. DOI: [10.1007/978-3-662-53071-9_2](https://doi.org/10.1007/978-3-662-53071-9_2). URL: https://doi.org/10.1007/978-3-662-53071-9_2.

- [46] Fangfang Liu and Xiuyun Chuan. ‘Recent developments in natural mineral-based separators for lithium-ion batteries’. In: *RSC Advances* (2021). DOI: 10.1039/d1ra02845f. URL: <https://pubs.rsc.org/en/content/articlepdf/2021/ra/d1ra02845f> (visited on 13/05/2024).
- [47] Pengcheng Zhu et al. ‘A review of current collectors for lithium-ion batteries’. In: *Journal of Power Sources* 485 (2021), p. 229321. ISSN: 0378-7753. DOI: <https://doi.org/10.1016/j.jpowsour.2020.229321>. URL: <https://www.sciencedirect.com/science/article/pii/S0378775320316098> (visited on 18/05/2024).
- [48] Naoaki Yabuuchi et al. ‘Research development on sodium-ion batteries’. In: *Chemical reviews* 114.23 (2014), pp. 11636–11682. DOI: <https://doi.org/10.1021/cr500192f>. URL: <https://pubs.acs.org/doi/full/10.1021/cr500192f> (visited on 29/04/2024).
- [49] Epec Engineered Technologies. ‘BATTERY ENCLOSURE DESIGN’. In: (). URL: <https://www.epectec.com/batteries/battery-enclosure-design.html> (visited on 15/05/2024).
- [50] Marshall Brain, Charles W Bryant and Clint Pumphrey. ‘How batteries work’. In: *Battery Arrangement and Power—HowStuffWorks*, <http://electronics.howstuffworks.com/everyday-tech/battery6.htm/printable>, accessed Dec 14 (2015). URL: <https://skol.ca/wp-content/uploads/2012/09/battery.pdf> (visited on 15/05/2024).
- [51] EV FireSafe. ‘03.1 What is a lithium-ion battery?’ In: (2021). URL: <https://www.evfiresafe.com/what-is-lithium-ion-battery> (visited on 15/05/2024).
- [52] IOP Institute of Physics. ‘What is really flowing and does it flow? (Expansion – tell me more)’. In: (). URL: <https://spark.iop.org/what-really-flowing-and-does-it-flow-expansion-tell-me-more> (visited on 09/04/2024).
- [53] Anand Bhatt, Ray Withers FAA and Guoxiu Wang. *Lithium-ion batteries*. Australian Academy of Science. 2016. URL: <https://www.science.org.au/curious/technology-future/lithium-ion-batteries>.
- [54] David Beck et al. ‘Inhomogeneities and Cell-to-Cell Variations in Lithium-Ion Batteries, a Review’. In: *Energies* 14 (June 2021), p. 3276. DOI: 10.3390/en14113276. URL: <https://www.mdpi.com/1996-1073/14/11/3276> (visited on 14/05/2024).
- [55] United States Environmental Protection Agency. ‘EPA Finds NMP and 1-BP Present Unreasonable Risks to Human Health’. In: (2022). URL: <https://www.epa.gov/chemicals-under-tsca/epa-finds-nmp-and-1-bp-present-unreasonable-risks-human-health> (visited on 21/05/2024).

- [56] Stéphane Melançon. ‘Pouch Cell Assembly: New Methods to Improve Manufacturing’. In: (2022). URL: <https://www.laserax.com/blog/pouch-cell-assembly> (visited on 14/05/2024).
- [57] Targay. *PROCESS OF MANUFACTURING POUCH CELL*. URL: <https://www.targray.com/li-ion-battery/equipment/pouch-cell-manufacturing> (visited on 14/05/2024).
- [58] Zhiqun Daniel Deng et al. ‘Good Practices for Rechargeable Lithium Metal Batteries’. In: *Journal of The Electrochemical Society* (2019). DOI: 10.1149/2.0691916jes. URL: <https://iopscience.iop.org/article/10.1149/2.0691916jes> (visited on 14/05/2024).
- [59] Yangtao Liu et al. ‘Current and Future Lithium-Ion Battery Manufacturing’. In: *IScience* (2021). URL: [https://www.cell.com/iscience/pdf/S2589-0042\(21\)00300-X.pdf?fbclid=IwAR0Mk6i1y34s-C0uaEXwGL1D9_XyMtsU4ataaVLM0iVK-wXinbfaA9XtcdQ](https://www.cell.com/iscience/pdf/S2589-0042(21)00300-X.pdf?fbclid=IwAR0Mk6i1y34s-C0uaEXwGL1D9_XyMtsU4ataaVLM0iVK-wXinbfaA9XtcdQ) (visited on 22/04/2024).
- [60] Chris Yuan et al. ‘Manufacturing energy analysis of lithium ion battery pack for electric vehicles’. In: *CIRP Annals* 66.1 (2017), pp. 53–56. ISSN: 0007-8506. DOI: <https://doi.org/10.1016/j.cirp.2017.04.109>. URL: <https://www.sciencedirect.com/science/article/pii/S0007850617301099>.
- [61] John Owen. ‘21 - Ionic Conductivity’. In: *Comprehensive Polymer Science and Supplements*. Ed. by Geoffrey Allen and John C. Bevington. Amsterdam: Pergamon, 1989, pp. 669–686. ISBN: 978-0-08-096701-1. DOI: <https://doi.org/10.1016/B978-0-08-096701-1.00058-6>. URL: <https://www.sciencedirect.com/science/article/pii/B9780080967011000586> (visited on 09/05/2024).
- [62] Praveen Balaji T and Soumyadip Choudhury. ‘7 - Separators for lithium–sulfur batteries’. In: *Lithium-Sulfur Batteries*. Ed. by Ram K. Gupta et al. Elsevier, 2022, pp. 121–156. ISBN: 978-0-323-91934-0. DOI: <https://doi.org/10.1016/B978-0-323-91934-0.00021-1>. URL: <https://www.sciencedirect.com/science/article/pii/B9780323919340000211> (visited on 09/05/2024).
- [63] John Owen. ‘21 - Ionic Conductivity’. In: (1989). Ed. by Geoffrey Allen and John C. Bevington, pp. 669–686. DOI: <https://doi.org/10.1016/B978-0-08-096701-1.00058-6>. URL: <https://www.sciencedirect.com/science/article/pii/B9780080967011000586> (visited on 21/03/2024).
- [64] J. Barthel et al. ‘Electrolyte Solutions, Transport Properties’. In: (2003). Ed. by Robert A. Meyers, pp. 243–259. DOI: <https://doi.org/10.1016/B0-12-227410-5/00209-X>.

- URL: <https://www.sciencedirect.com/science/article/pii/B012227410500209X> (visited on 21/03/2024).
- [65] L. Ye and Z. Feng. '14 - Polymer electrolytes as solid solvents and their applications'. In: Woodhead Publishing Series in Electronic and Optical Materials (2010). Ed. by César Sequeira and Diogo Santos, pp. 550–582. DOI: <https://doi.org/10.1533/9781845699772.2.550>. URL: <https://www.sciencedirect.com/science/article/pii/B9781845697723500145> (visited on 21/03/2024).
- [66] Battery University. 'BU-402: What Is C-rate?' In: (2021). URL: <https://batteryuniversity.com/article/bu-402-what-is-c-rate> (visited on 05/04/2024).
- [67] Laura Bravo Diaz et al. 'Measuring Irreversible Heat Generation in Lithium-Ion Batteries: An Experimental Methodology'. In: *Journal of The Electrochemical Society* 169.3 (Mar. 2022), p. 030523. DOI: 10.1149/1945-7111/ac5ada. URL: <https://dx.doi.org/10.1149/1945-7111/ac5ada>.
- [68] Biologic. *Battery states: State of charge (SoC), State of Health (SoH)*. 2023. URL: <https://www.biologic.net/topics/battery-states-state-of-charge-soc-state-of-health-soh/> (visited on 16/03/2024).
- [69] Battery University. *Battery Definitions and What They Mean*. 2021. URL: <https://batteryuniversity.com/article/bu-105-battery-definitions-and-what-they-mean> (visited on 16/03/2024).
- [70] Federal Batteries. 'What is Depth of Discharge and why is it so important?' In: (2020). URL: <https://federalbatteries.com.au/news/what-depth-discharge-and-why-it-so-important> (visited on 09/05/2024).
- [71] Frode Håskjold Fagerli. *Personal communication*. Apr. 2024.
- [72] Carlos Rufino Jr and Eleonora Riva et al. Sanseverinoc. 'A Comprehensive Review of EV Lithium-Ion Battery Degradation'. In: *ResearchGate* (2023). URL: https://www.researchgate.net/publication/375830373_A_Comprehensive_Review_of_EV_Lithium-Ion_Battery_Degradation (visited on 23/04/2024).
- [73] Exro. 'Battery Degradation At a Glance'. In: *Exro Insights* (2023). URL: <https://www.exro.com/industry-insights/battery-degradation-explained> (visited on 23/04/2024).
- [74] Guoqing Lou, Yongzhi Zhang and Aihua Tang. 'Capacity Degradation and Aging Mechanisms Evolution of Lithium-Ion Batteries Under Different Operating Conditions'. In: *MDPI* (2023). URL: <https://www.mdpi.com/1996-1073/16/10/4232> (visited on 23/04/2024).

- [75] Jingyi Chen, Billy Wu and Max Naylor-Marlow. ‘Battery pack degradation - Understanding aging in parallel-connected lithium-ion batteries under thermal gradients’. In: *ResearchGate* (2023). URL: https://www.researchgate.net/publication/377208267_Battery_pack_degradation_-_Understanding_aging_in_parallel-connected_lithium-ion_batteries_under_thermal_gradients (visited on 23/04/2024).
- [76] Seong Jin An et al. ‘The state of understanding of the lithium-ion-battery graphite solid electrolyte interphase (SEI) and its relationship to formation cycling’. In: *Carbon* 105 (2016), pp. 52–76. ISSN: 0008-6223. DOI: <https://doi.org/10.1016/j.carbon.2016.04.008>. URL: <https://www.sciencedirect.com/science/article/pii/S0008622316302676>.
- [77] Maureen Tang, Sida Lu and John Newman. ‘Experimental and Theoretical Investigation of Solid-Electrolyte-Interphase Formation Mechanisms on Glassy Carbon’. In: *Journal of The Electrochemical Society* 159.11 (Aug. 2012), A1775. DOI: 10.1149/2.025211jes. URL: <https://dx.doi.org/10.1149/2.025211jes>.
- [78] John Christensen and John Newman. ‘A Mathematical Model for the Lithium-Ion Negative Electrode Solid Electrolyte Interphase’. In: *Journal of The Electrochemical Society* 151.11 (Oct. 2004), A1977. DOI: 10.1149/1.1804812. URL: <https://dx.doi.org/10.1149/1.1804812>.
- [79] E. Peled. ‘The Electrochemical Behavior of Alkali and Alkaline Earth Metals in Non-aqueous Battery Systems—The Solid Electrolyte Interphase Model’. In: *Journal of The Electrochemical Society* 126.12 (Dec. 1979), p. 2047. DOI: 10.1149/1.2128859. URL: <https://dx.doi.org/10.1149/1.2128859>.
- [80] E. Peled, D. Golodnitsky and G. Ardel. ‘Advanced Model for Solid Electrolyte Interphase Electrodes in Liquid and Polymer Electrolytes’. In: *Journal of The Electrochemical Society* 144.8 (Aug. 1997), p. L208. DOI: 10.1149/1.1837858. URL: <https://dx.doi.org/10.1149/1.1837858>.
- [81] John Christensen and John Newman. ‘Cyclable Lithium and Capacity Loss in Li-Ion Cells’. In: *Journal of The Electrochemical Society* 152.4 (Mar. 2005), A818. DOI: 10.1149/1.1870752. URL: <https://dx.doi.org/10.1149/1.1870752>.
- [82] Ali Awarke, Stefan Pischinger and Jürgen Ogrzewalla. ‘Pseudo 3D Modeling and Analysis of the SEI Growth Distribution in Large Format Li-Ion Polymer Pouch Cells’. In: *Journal of The Electrochemical Society* 160.1 (Nov. 2012), A172. DOI: 10.1149/2.022302jes. URL: <https://dx.doi.org/10.1149/2.022302jes>.

- [83] Matthew B. Pinson and Martin Z. Bazant. ‘Theory of SEI Formation in Rechargeable Batteries: Capacity Fade, Accelerated Aging and Lifetime Prediction’. In: *Journal of The Electrochemical Society* 160.2 (Dec. 2012), A243. DOI: 10.1149/2.044302jes. URL: <http://dx.doi.org/10.1149/2.044302jes>.
- [84] Yuanyuan Xie, Jianyang Li and Chris Yuan. ‘Multiphysics modeling of lithium ion battery capacity fading process with solid-electrolyte interphase growth by elementary reaction kinetics’. In: *Journal of Power Sources* 248 (2014), pp. 172–179. ISSN: 0378-7753. DOI: <https://doi.org/10.1016/j.jpowsour.2013.09.059>. URL: <https://www.sciencedirect.com/science/article/pii/S0378775313015553>.
- [85] Xianke Lin et al. ‘A Comprehensive Capacity Fade Model and Analysis for Li-Ion Batteries’. In: *Journal of The Electrochemical Society* 160.10 (Aug. 2013), A1701. DOI: 10.1149/2.040310jes. URL: <https://dx.doi.org/10.1149/2.040310jes>.
- [86] Harry J. Ploehn, Premanand Ramadass and Ralph E. White. ‘Solvent Diffusion Model for Aging of Lithium-Ion Battery Cells’. In: *Journal of The Electrochemical Society* 151.3 (Feb. 2004), A456. DOI: 10.1149/1.1644601. URL: <https://dx.doi.org/10.1149/1.1644601>.
- [87] The Editors of Encyclopaedia Britannica. *tunneling*. 2024. URL: <https://www.britannica.com/science/tunneling> (visited on 22/04/2024).
- [88] Tetsuya Osaka et al. ‘Proposal of novel equivalent circuit for electrochemical impedance analysis of commercially available lithium ion battery’. In: *Journal of Power Sources* 205 (2012), pp. 483–486. ISSN: 0378-7753. DOI: <https://doi.org/10.1016/j.jpowsour.2012.01.070>. URL: <https://www.sciencedirect.com/science/article/pii/S0378775312001693>.
- [89] Xianke Lin et al. ‘Lithium Plating Mechanism, Detection, and Mitigation in Lithium-Ion Batteries’. In: *Progress in Energy and Combustion Science* 87 (2021), p. 100953. ISSN: 0360-1285. DOI: <https://doi.org/10.1016/j.pecs.2021.100953>. URL: <https://www.sciencedirect.com/science/article/pii/S0360128521000514>.
- [90] D.U. Sauer. ‘SECONDARY BATTERIES – LEAD– ACID SYSTEMS | Lifetime Determining Processes’. In: *Encyclopedia of Electrochemical Power Sources*. Ed. by Jürgen Garche. Amsterdam: Elsevier, 2009, pp. 805–815. ISBN: 978-0-444-52745-5. DOI: <https://doi.org/10.1016/B978-044452745-5.00137-4>. URL: <https://www.sciencedirect.com/science/article/pii/B9780444527455001374> (visited on 20/05/2024).
- [91] Kyeong-Seok Oh et al. ‘Single-Ion Conducting Soft Electrolytes for Semi-Solid Lithium Metal Batteries Enabling Cell Fabrication and Operation under Ambient Conditions’. In:

- Advanced Energy Materials* 11.38 (2021), p. 2101813. DOI: <https://doi.org/10.1002/aenm.202101813>. eprint: <https://onlinelibrary.wiley.com/doi/pdf/10.1002/aenm.202101813>. URL: <https://onlinelibrary.wiley.com/doi/abs/10.1002/aenm.202101813> (visited on 20/03/2024).
- [92] David G. Rethwisch and William D. Callister Jr. *Materials Science and Engineering: An Introduction, 10th Edition*. John Wiley & Sons Inc, Jan. 2020. ISBN: 9781119453918. (Visited on 20/05/2024).
- [93] Florian Flatscher. ‘Lithium dendrites in solid-state batteries - Where they come from and how to mitigate them’. In: (2023). URL: <https://hdl.handle.net/11250/3108658> (visited on 20/03/2024).
- [94] Seungpyo Kang, Minseon Kim and Kyoungmin Min. ‘Discovery of Superionic Solid-State Electrolyte for Li-Ion Batteries via Machine Learning’. In: *The Journal of Physical Chemistry C* 127.39 (2023), pp. 19335–19343. DOI: 10.1021/acs.jpcc.3c02908. eprint: <https://doi.org/10.1021/acs.jpcc.3c02908>. URL: <https://doi.org/10.1021/acs.jpcc.3c02908> (visited on 10/05/2024).
- [95] Ganguli Babu and Pulickel M. Ajayan. ‘Good riddance, dendrites’. In: *Nature Energy* 4 (2019), pp. 631–632. DOI: <https://doi.org/10.1038/s41560-019-0423-1>. URL: <https://www.nature.com/articles/s41560-019-0423-1> (visited on 13/05/2024).
- [96] Battery University. *Will Secondary Batteries replace Primaries?* Battery University. 1st Oct. 2010. URL: <https://batteryuniversity.com/article/will-secondary-batteries-replace-primaries> (visited on 18/03/2024).
- [97] OLEM US EPA. *Lithium-Ion Battery Recycling*. 17th June 2023. URL: <https://www.epa.gov/hw/lithium-ion-battery-recycling> (visited on 18/03/2024).
- [98] Stéphane Melançon. ‘Prismatic vs Cylindrical Cells’. In: *Laserax Information Archive* 12 (2022). URL: <https://www.laserax.com/blog/prismatic-vs-cylindrical-cells> (visited on 26/04/2024).
- [99] Battery University. ‘BU-301a: Types of Battery Cells’. In: (2019). URL: <https://batteryuniversity.com/article/bu-301a-types-of-battery-cells#:~:text=Introduced%20in%20the%20early%201990s,by%20using%20the%20layered%20approach>. (visited on 29/04/2024).
- [100] Qaisar Abbas et al. ‘Current State and Future Prospects for Electrochemical Energy Storage and Conversion Systems’. In: *MDPI* (2020). DOI: 10.3390/en13215847. URL: <https://www.mdpi.com/1996-1073/13/21/5847> (visited on 09/05/2024).

- [101] River James. ‘For EV Battery Packs, Does The Shape Matter?’ In: (2023). URL: <http://www.recurrentauto.com/research/battery-packs-does-the-shape-matter> (visited on 29/04/2024).
- [102] Scantech. ‘What Are Pouch Cells?’ In: *Scantech Informtion Archive* 12 (2023). URL: <https://scantech.com/information/industry-energy-information/batteries/what-are-pouch-cells/> (visited on 25/04/2024).
- [103] Epec Engineering Technologies. ‘PRISMATIC & POUCH BATTERY PACKS’. In: *Epec Blog* 12 (). URL: <https://www.epectec.com/batteries/prismatic-pouch-packs.html> (visited on 25/04/2024).
- [104] European Commission et al. *Technology readiness level – Guidance principles for renewable energy technologies – Final report*. Publications Office, 2017. DOI: doi/10.2777/577767. URL: <https://op.europa.eu/en/publication-detail/-/publication/d5d8e9c8-e6d3-11e7-9749-01aa75ed71a1> (visited on 11/05/2024).
- [105] European Commission. ‘Horizon 2020 Work Programme 2014-2015 General Annexes’. In: (2014). URL: https://ec.europa.eu/research/participants/data/ref/h2020/wp/2014_2015/annexes/h2020-wp1415-annex-ga_en.pdf.
- [106] Allan J. Jacobson and Linda F. Nazar. ‘Intercalation Chemistry’. In: *Encyclopedia of Inorganic and Bioinorganic Chemistry*. John Wiley & Sons, Ltd, 2011. ISBN: 9781119951438. DOI: <https://doi.org/10.1002/9781119951438.eibc0093>. eprint: <https://onlinelibrary.wiley.com/doi/pdf/10.1002/9781119951438.eibc0093>. URL: <https://onlinelibrary.wiley.com/doi/abs/10.1002/9781119951438.eibc0093>.
- [107] Naoki Nitta et al. ‘Li-ion battery materials: present and future’. In: *Materials Today* 18 (5 2024), pp. 252–264. ISSN: 369-7021. DOI: <https://doi.org/10.1016/j.mattod.2014.10.040>. URL: <https://www.sciencedirect.com/science/article/pii/S1369702114004118?via%3Dihub>.
- [108] Christina Kostandi and Clayton Wadsworth. *The types of Lithium-ion Batteriers*. 2023. URL: <https://elements.visualcapitalist.com/the-six-major-types-of-lithium-ion-batteries/> (visited on 15/04/2024).
- [109] Ghassan Zubi et al. ‘The lithium-ion battery: State of the art and future perspectives’. In: Volume89 (2018). Ed. by A. Foley, pp. 292–308. DOI: <https://doi.org/10.1016/j.rser.2018.03.002>. URL: <https://www.sciencedirect.com/science/article/pii/S1364032118300728> (visited on 20/02/2024).
- [110] Chen Liao. ‘Fundamentals of rechargeable lithium ion and beyond lithium ion batteries’. In: *Batteries, Materials principles and characterization methods*. Ed. by Chen Liao. IOP

- Publishing, 2021, pp. 1–24. ISBN: 978-0-7503-2682-7. DOI: <https://doi.org/10.1088/978-0-7503-2682-7>. URL: <https://iopscience.iop.org/book/edit/978-0-7503-2682-7/chapter/bk978-0-7503-2682-7ch1.pdf> (visited on 15/02/2024).
- [111] Peter Kurzweil. *Electrochemical Energy Storage for Renewable Sources and Grid Balancing*. Electrochemistry Laboratory, University of Applied Sciences, Amberg, Germany: Elsevier B.V., 2015. Chap. 16: Lithium Battery Energy Storage: State of the Art Including LithiumAir and LithiumSulfur Systems.
- [112] *layer lattice*. DOI: 10.1093/oi/authority.20110803100055381. URL: <https://www.oxfordreference.com/view/10.1093/oi/authority.20110803100055381>.
- [113] Steven Tyler Boles. *Personal communication*. Apr. 2024.
- [114] Yang Shao-Horn et al. ‘Atomic resolution of lithium ions in LiCoO₂’. In: *Nature materials* 2 (Aug. 2003), pp. 464–7. DOI: 10.1038/nmat922.
- [115] The University of Liverpool. *Lithium Cobalt Oxide – LiCoO₂ – Conduction animation*. URL: https://www.chemtube3d.com/lib_lco-2/ (visited on 01/05/2024).
- [116] Battery University. *BU-205: Types of Lithium-ion*. Battery University. 8th Dec. 2023. URL: <https://batteryuniversity.com/article/bu-205-types-of-lithium-ion> (visited on 20/03/2024).
- [117] Rong Xu et al. ‘Mechanical and Structural Degradation of LiNi_xMn_yCo_zO₂ Cathode in Li-Ion Batteries: An Experimental Study’. In: *Journal of The Electrochemical Society* 164.13 (Nov. 2017), A3333. DOI: 10.1149/2.1751713jes. URL: <https://dx.doi.org/10.1149/2.1751713jes>.
- [118] Juan C. Garcia et al. ‘Surface Structure, Morphology, and Stability of Li(Ni_{1/3}Mn_{1/3}Co_{1/3})O₂ Cathode Material’. In: *The Journal of Physical Chemistry C* 121.15 (2017), pp. 8290–8299. DOI: 10.1021/acs.jpcc.7b00896. eprint: <https://doi.org/10.1021/acs.jpcc.7b00896>. URL: <https://doi.org/10.1021/acs.jpcc.7b00896>.
- [119] H.H. Sun, UH. Kim and JH. et al. Park. ‘Transition metal-doped Ni-rich layered cathode materials for durable Li-ion batteries’. In: *Nat Commun* 12.6552 (2021).
- [120] John-Joseph Marie and Stephen Gifford. *Developments in Lithium-Ion Battery Cathodes*. The Faraday Institution. URL: https://www.faraday.ac.uk/wp-content/uploads/2023/09/Faraday_Insights_18_FINAL.pdf.
- [121] Jiangtao Hu et al. ‘Structure and performance of the LiFePO₄ cathode material: from the bulk to the surface’. In: *Nanoscale* 12 (28 2020), pp. 15036–15044. DOI: 10.1039/D0NR03776A. URL: <http://dx.doi.org/10.1039/D0NR03776A>.
- [122] Odne Stokke Burheim. *Personal communication*. Apr. 2024.

- [123] Astrid Fagertun Gunnarshaug, Odne Stokke Burheim and Signe Kjelstrup. ‘Reversible heat effects of lithium metal- and porous lithium iron phosphate electrodes’. In: *Electrochimica Acta* 462 (2023), p. 142739. ISSN: 0013-4686. DOI: <https://doi.org/10.1016/j.electacta.2023.142739>. URL: <https://www.sciencedirect.com/science/article/pii/S0013468623009179>.
- [124] Sina Orangi et al. ‘Historical and prospective lithium-ion battery cost trajectories from a bottom-up production modeling perspective’. In: *Journal of Energy Storage* 76 (2024). ISSN: 109800. DOI: <https://doi.org/10.1016/j.est.2023.109800>. URL: <https://www.sciencedirect.com/science/article/pii/S2352152X23031985#bb0095>.
- [125] N. Bhandari et al. *Batteries: The Greenflation Challenge*. 2022. URL: <https://www.goldmansachs.com/intelligence/pages/gs-research/batteries-the-greenflation-challenge/report.pdf> (visited on 19/04/2024).
- [126] Jian Zhao. ‘LITHIUM MANGANESE IRON PHOSPHATE (LMFP) BATTERIES RECEIVING RENEWED ATTENTION IN CHINA’. In: (2023). URL: https://www.mitsui.com/mgssi/en/report/detail/_icsFiles/afieldfile/2023/09/19/2308t_zhao_e.pdf (visited on 30/04/2024).
- [127] Scooter Doll. ‘Gotion unveils LMFP EV battery it says can deliver 1,000 km per single charge for a lower price’. In: (2023). URL: <https://electrek.co/2023/06/06/gotion-unveils-lmfp-ev-battery-it-says-can-deliver-1000-km-per-single-charge-for-a-lower-price/> (visited on 30/04/2024).
- [128] Shaoqing Li et al. ‘Structural and electrochemical properties of $\text{LiMn}_{0.6}\text{Fe}_{0.4}\text{PO}_4$ as a cathode material for flexible lithium-ion batteries and self-charging power pack’. In: *Nano Energy* 52 (2018), pp. 510–516. ISSN: 2211-2855. DOI: <https://doi.org/10.1016/j.nanoen.2018.08.007>. URL: <https://www.sciencedirect.com/science/article/pii/S221128551830569X>.
- [129] Srihari Molgund. ‘How LMFP Batteries Can Power India’s Electric Vehicle Market’. In: (2024). URL: https://www.ey.com/en_in/automotive-transportation/how-lmfp-batteries-can-power-india-s-electric-vehicle-market (visited on 30/04/2024).
- [130] Elsa Liu. ‘What is Lithium manganese iron phosphate battery (LMFP Battery)?’ In: (2024). URL: <https://www.lifepo4-battery.com/News/what-is-lmfp-battery.html> (visited on 01/05/2024).
- [131] Harry Geary et al. ‘Developing a High-Performance, Cobalt-Free, 3V Battery Cell Based on High-Voltage Spinel (LNMO) Cathode and Mixed Niobium Oxide (XNO) Anode’. In:

- (2022). URL: <https://www.topsoe.com/hubfs/DOWNLOADS/DOWNLOADS%20-%20White%20papers/Whitepaper%20LNMO-XN0%203V%20System.pdf> (visited on 02/05/2024).
- [132] Morrow. 'Our Latest Battery Technologies'. In: (2023). URL: <https://www.morrowbatteries.com/products> (visited on 02/05/2024).
- [133] Jiarong He et al. 'Surface Structure Evolution and its Impact on the Electrochemical Performances of Aqueous-Processed High-Voltage Spinel LiNi_{0.5}Mn_{1.5}O₄ Cathodes in Lithium-Ion Batteries'. In: *Advanced Functional Materials* 32.46 (2022), p. 2207937. DOI: <https://doi.org/10.1002/adfm.202207937>. eprint: <https://onlinelibrary.wiley.com/doi/pdf/10.1002/adfm.202207937>. URL: <https://onlinelibrary.wiley.com/doi/abs/10.1002/adfm.202207937>.
- [134] Yongpeng Cui et al. 'N-doped engineering of a high-voltage LiNi_{0.5}Mn_{1.5}O₄ cathode with superior cycling capability for wide temperature lithium-ion batteries'. In: (2022). DOI: <https://doi.org/10.1039/D2CP00835A>. URL: <https://pubs.rsc.org/en/content/articlelanding/2022/cp/d2cp00835a> (visited on 09/05/2024).
- [135] Arnstein Nisje. 'LNMO as a cathode material in Li-ion batteries: Reasons for capacity fade and measures taken to prevent it'. In: (2023). URL: <https://ntnuopen.ntnu.no/ntnu-xmlui/handle/11250/3071932> (visited on 09/05/2024).
- [136] A. Demaray et al. *Battery Talk: Battery Application Break Down 1/01/2024 (Version 2.0)*. 2023. URL: <https://docs.google.com/spreadsheets/d/1BmUIc7glVppOUBByrKPAhSImwjPMJMecZis9XyAKiG8/edit#gid=0> (visited on 25/04/2024).
- [137] John Warner. 'Chapter 7 - Lithium-Ion and Other Cell Chemistries'. In: *The Handbook of Lithium-Ion Battery Pack Design*. Ed. by John Warner. Amsterdam: Elsevier, 2015, pp. 65–89. ISBN: 978-0-12-801456-1. DOI: <https://doi.org/10.1016/B978-0-12-801456-1.00007-5>. URL: <https://www.sciencedirect.com/science/article/pii/B9780128014561000075>.
- [138] Samuel Hasselwander, Markus Meyer and Ines Österle. 'Techno-Economic Analysis of Different Battery Cell Chemistries for the Passenger Vehicle Market'. In: *Batteries* 9.7 (2023). ISSN: 2313-0105. DOI: 10.3390/batteries9070379. URL: <https://www.mdpi.com/2313-0105/9/7/379> (visited on 20/05/2024).
- [139] Bax & Company et al. *COBRA - MARKET INTELLIGENCE REPORT*. 2023. URL: <https://evmarketsreports.com/wp-content/uploads/database-1-1.pdf> (visited on 10/05/2024).
- [140] Hongxia Chen et al. 'Insight into wide temperature electrolyte based on lithiumdifluoro(oxalate)borate for high voltage lithium-ion batteries'. In: *Journal of Alloys and Compounds* 876 (2021),

- p. 159966. ISSN: 0925-8388. DOI: <https://doi.org/10.1016/j.jallcom.2021.159966>. URL: <https://www.sciencedirect.com/science/article/pii/S092583882101375X>.
- [141] B. Vikram Babu et al. ‘Structural and electrical properties of Li₄Ti₅O₁₂ anode material for lithium-ion batteries’. In: *Results in Physics* 9 (2018), pp. 284–289. ISSN: 2211-3797. DOI: <https://doi.org/10.1016/j.rinp.2018.02.050>. URL: <https://www.sciencedirect.com/science/article/pii/S2211379718301402>.
- [142] Xinghao Lu. ‘Characteristics and properties of anode materials for lithium-ion batteries’. In: *Applied and Computational Engineering* 61 (May 2024), pp. 108–116. DOI: 10.54254/2755-2721/61/20240937.
- [143] George Crabtree, Elizabeth Kocs and Lynn Trahey. ‘The energy-storage frontier: Lithium-ion batteries and beyond’. In: *MRS Bulletin* 40 (Dec. 2015), pp. 1067–1078. DOI: 10.1557/mrs.2015.259.
- [144] Thomas Nemeth et al. ‘Lithium titanate oxide battery cells for high-power automotive applications – Electro-thermal properties, aging behavior and cost considerations’. In: *Journal of Energy Storage* 31 (2020), p. 101656. ISSN: 2352-152X. DOI: <https://doi.org/10.1016/j.est.2020.101656>. URL: <https://www.sciencedirect.com/science/article/pii/S2352152X20314936>.
- [145] Arunabh Ghosh and Fouad Ghamouss. ‘Role of Electrolytes in the Stability and Safety of Lithium Titanate-Based Batteries’. In: *Frontiers in Materials* 7 (July 2020), p. 186. DOI: 10.3389/fmats.2020.00186.
- [146] Katja Kretschmer. ‘Phosphate-based cathode materials for rechargeable batteries’. PhD thesis. May 2018. DOI: 10.13140/RG.2.2.34340.32647.
- [147] Linda Jing et al. *Battery report 2023*. Tech. rep. Volta Foundation, 2023.
- [148] Duy Khanh Nguyen et al. ‘Rich essential properties of Si-doped graphene’. In: (2020). ISSN: 2313-0105. DOI: <https://doi.org/10.1038/s41598-020-68765-x>. URL: <https://www.nature.com/articles/s41598-020-68765-x#citeas> (visited on 16/05/2024).
- [149] Junbo Hou et al. ‘Materials and electrode engineering of high capacity anodes in lithium ion batteries’. In: *Journal of Power Sources* 450 (2020), p. 227697. ISSN: 0378-7753. DOI: <https://doi.org/10.1016/j.jpowsour.2019.227697>. URL: <https://www.sciencedirect.com/science/article/pii/S0378775319316908>.
- [150] J. Choi and D. Aurbach. ‘Promise and reality of post-lithium-ion batteries with high energy densities.’ In: *Nat Rev Mater* 1 (2016). DOI: <https://doi.org/10.1038/natrevmats.2016.13>.

- [151] Beyonder. *About Beyonder*. URL: <https://www.beyonder.no/facilities> (visited on 16/05/2024).
- [152] Sreehari K. Saju et al. ‘Hard carbon anode for lithium-, sodium-, and potassium-ion batteries: Advancement and future perspective’. In: *Cell Reports Physical Science* 5.3 (2024), p. 101851. ISSN: 2666-3864. DOI: <https://doi.org/10.1016/j.xcrp.2024.101851>. URL: <https://www.sciencedirect.com/science/article/pii/S2666386424000766>.
- [153] Xinwei Dou et al. ‘Hard carbons for sodium-ion batteries: Structure, analysis, sustainability, and electrochemistry’. In: *Materials Today* 23 (2019), pp. 87–104. ISSN: 1369-7021. DOI: <https://doi.org/10.1016/j.mattod.2018.12.040>. URL: <https://www.sciencedirect.com/science/article/pii/S1369702118310873>.
- [154] Hailei Zhao. ‘Lithium Titanate-Based Anode Materials’. In: vol. 172. June 2015, pp. 157–187. ISBN: 978-3-319-15457-2. DOI: 10.1007/978-3-319-15458-9_6.
- [155] Linda Jing et al. *Battery report 2022*. Tech. rep. Volta Foundation, 2022.
- [156] Jang-Yeon Hwang, Seung-Taek Myung and Yang-Kook Sun. ‘Sodium-ion batteries: present and future’. In: *Chemical Society Reviews* 46.12 (2017), pp. 3529–3614. DOI: 10.1039/C6CS00776G. URL: <https://pubs.rsc.org/en/content/articlehtml/2021/xx/c6cs00776g> (visited on 29/04/2024).
- [157] Mario Pagliaro and Francesco Meneguzzo. ‘Lithium battery reusing and recycling: A circular economy insight’. In: *Heliyon* 5.6 (2019), e01866. ISSN: 2405-8440. DOI: <https://doi.org/10.1016/j.heliyon.2019.e01866>. URL: <https://www.sciencedirect.com/science/article/pii/S2405844019347012> (visited on 29/04/2024).
- [158] Krishnakanth Sada, Joe Darga and Arumugam Manthiram. ‘Challenges and Prospects of Sodium-Ion and Potassium-Ion Batteries for Mass Production’. In: *Advanced Energy Materials* 13.39 (2023), p. 2302321. DOI: <https://doi.org/10.1002/aenm.202302321>. eprint: <https://onlinelibrary.wiley.com/doi/pdf/10.1002/aenm.202302321>. URL: <https://onlinelibrary.wiley.com/doi/abs/10.1002/aenm.202302321> (visited on 18/05/2024).
- [159] Da Deng. ‘Li-ion batteries: basics, progress, and challenges’. In: *Energy Science and Engineering*. Ed. by Tomas Käberger. Volume3, Issue5. Society of Chemical Industry and John Wiley & Sons Ltd, 2015, pp. 385–418. ISBN: 2050-0505. DOI: <https://doi.org/10.1002/ese3.95>. URL: <https://onlinelibrary.wiley.com/doi/full/10.1002/ese3.95> (visited on 20/02/2024).
- [160] Håvard Korneliussen. ‘Batterier’. In: NTNU, 2021. Chap. Notat 12.

- [161] Xiulin Fan and Chunsheng Wang. ‘High-voltage liquid electrolytes for Li batteries: progress and perspectives’. In: (2021). URL: <https://pubs.rsc.org/en/content/articlelanding/2021/cs/d1cs00450f> (visited on 10/05/2024).
- [162] Ping He et al. ‘Solid-State Electrolytes for Lithium-Ion Batteries: Fundamentals, Challenges and Perspectives’. In: (2019). URL: <https://link.springer.com/article/10.1007/s41918-019-00048-0> (visited on 10/05/2024).
- [163] Thomas Schmaltz et al. ‘Solid-State Battery Roadmap 2035+’. In: *Fraunhofer ISI* (2022). URL: <https://publica.fraunhofer.de/entities/publication/7be4b3d3-2844-42d9-b900-a19e1ee1ddea/details> (visited on 16/04/2024).
- [164] Alireza Haghpanah Jahromi and Sheikh Setareh. ‘Ionic liquids in green energy storage devices: lithium-ion batteries, supercapacitors, and solar cells’. In: (2024). URL: <https://link.springer.com/article/10.1007/s00706-024-03178-4> (visited on 10/05/2024).
- [165] Andrew Ulvestad. *A Brief Review of Current Lithium Ion Battery Technology and Potential Solid State Battery Technologies*. 2018. DOI: <https://doi.org/10.48550/arXiv.1803.04317>. arXiv: 1803.04317 [physics.app-ph]. URL: <https://arxiv.org/abs/1803.04317> (visited on 19/03/2024).
- [166] Trang Thi Vu et al. ‘Hybrid electrolytes for solid-state lithium batteries: Challenges, progress, and prospects’. In: *Energy Storage Materials* 61 (2023), p. 102876. ISSN: 2405-8297. DOI: <https://doi.org/10.1016/j.ensm.2023.102876>. URL: <https://www.sciencedirect.com/science/article/pii/S2405829723002556> (visited on 22/03/2024).
- [167] Yonglin Huang, Bowen Shao and Fudong Han. ‘Solid-State Batteries: An introduction’. In: *Department of Mechanical, Aerospace, and Nuclear Engineering, Rensselaer Polytechnic Institute* (June 2022). DOI: 10.1021/bk-2022-1413.ch001. URL: <https://pubs.acs.org/doi/full/10.1021/bk-2022-1413.ch001> (visited on 19/03/2024).
- [168] Theodosios Famprikis et al. ‘Fundamentals of inorganic solid-state electrolytes for batteries’. In: *Nature materials* 18 (2019), pp. 1278–1291. DOI: <https://doi.org/10.1038/s41563-019-0431-3>. URL: <https://www.nature.com/articles/s41563-019-0431-3> (visited on 13/05/2024).
- [169] Takahiro Kozawa et al. ‘Bulk-type all-solid-state batteries with mechanically prepared LiCoPO₄ composite cathodes’. In: *Journal of Solid State Electrochemistry* (2019). DOI: <https://doi.org/10.1007/s10008-019-04218-4>. URL: <https://link.springer.com/article/10.1007/s10008-019-04218-4> (visited on 10/05/2024).

- [170] Linchun He et al. ‘A new approach for synthesizing bulk-type all-solid-state lithium-ion batteries’. In: *J. Mater. Chem. A* 7 (16 2019), pp. 9748–9760. DOI: [10.1039/C8TA12375F](https://doi.org/10.1039/C8TA12375F). URL: <http://dx.doi.org/10.1039/C8TA12375F> (visited on 10/05/2024).
- [171] M. Tatsumisago and A. Hayashi. ‘19 - Chalcogenide glasses as electrolytes for batteries’. In: *Chalcogenide Glasses*. Ed. by Jean-Luc Adam and Xianghua Zhang. Woodhead Publishing, 2014, pp. 632–654. ISBN: 978-0-85709-345-5. DOI: <https://doi.org/10.1533/9780857093561.2.632>. URL: <https://www.sciencedirect.com/science/article/pii/B9780857093455500192> (visited on 10/05/2024).
- [172] Joscha Schnell et al. ‘All-solid-state lithium-ion and lithium metal batteries – paving the way to large-scale production’. In: *Journal of Power Sources* 382 (2018), pp. 160–175. ISSN: 0378-7753. DOI: <https://doi.org/10.1016/j.jpowsour.2018.02.062>. URL: <https://www.sciencedirect.com/science/article/pii/S0378775318301836> (visited on 19/04/2024).
- [173] Junfan Ding et al. ‘Integrated lithium metal anode protected by composite solid electrolyte film enables stable quasi-solid-state lithium metal batteries’. In: *Chinese Chemical Letters* 31.9 (2020), pp. 2339–2342. ISSN: 1001-8417. DOI: <https://doi.org/10.1016/j.cclet.2020.03.015>. URL: <https://www.sciencedirect.com/science/article/pii/S1001841720301340> (visited on 07/05/2024).
- [174] Xian-Xiang Zeng et al. ‘Lithiation-derived repellent toward lithium anode safeguard in quasi-solid batteries’. In: *Chem* 4.2 (2018), pp. 298–307. URL: [https://www.cell.com/chem/pdf/S2451-9294\(17\)30484-9.pdf](https://www.cell.com/chem/pdf/S2451-9294(17)30484-9.pdf) (visited on 07/05/2024).
- [175] Hui Yang and Nianqiang Wu. ‘Ionic conductivity and ion transport mechanisms of solid-state lithium-ion battery electrolytes: A review’. In: *Energy Science & Engineering* 10.5 (2022), pp. 1643–1671. DOI: <https://doi.org/10.1002/ese3.1163>. URL: <https://onlinelibrary.wiley.com/doi/full/10.1002/ese3.1163> (visited on 07/05/2024).
- [176] Kuirong Deng et al. ‘Single-ion conducting artificial solid electrolyte interphase layers for dendrite-free and highly stable lithium metal anodes’. In: *J. Mater. Chem. A* 7 (21 2019), pp. 13113–13119. DOI: [10.1039/C9TA02407G](https://doi.org/10.1039/C9TA02407G). URL: <http://dx.doi.org/10.1039/C9TA02407G> (visited on 15/04/2024).
- [177] Tobias Placke et al. ‘Lithium ion, lithium metal, and alternative rechargeable battery technologies: the odyssey for high energy density’. In: *Solid State Electrochemistry* (2017). DOI: <https://doi.org/10.1007/s10008-017-3610-7>. URL: <https://link.springer.com/article/10.1007/s10008-017-3610-7> (visited on 21/03/2024).

- [178] Zhi Chang et al. ‘A stable quasi-solid electrolyte improves the safe operation of highly efficient lithium-metal pouch cells in harsh environments’. In: *Nat Commun* (2022). DOI: <https://doi.org/10.1038/s41467-022-29118-6>. URL: <https://www.nature.com/articles/s41467-022-29118-6> (visited on 25/04/2024).
- [179] Peter Kurzweil and Klaus Brandt. ‘Chapter 3 - Overview of Rechargeable Lithium Battery Systems’. In: (2019). Ed. by Jürgen Garche and Klaus Brandt, pp. 47–82. DOI: <https://doi.org/10.1016/B978-0-444-63777-2.00003-7>. URL: <https://www.sciencedirect.com/science/article/pii/B9780444637772000037> (visited on 21/03/2024).
- [180] Sudeshna Sen et al. ‘The role of polymers in lithium solid-state batteries with inorganic solid electrolytes’. In: *J. Mater. Chem. A* 9 (35 2021), pp. 18701–18732. DOI: 10.1039/D1TA02796D. URL: <http://dx.doi.org/10.1039/D1TA02796D> (visited on 13/05/2024).
- [181] Alain Mauger et al. ‘Sulfide and Oxide Inorganic Solid Electrolytes for All-Solid-State Li Batteries: A Review’. In: (2020). DOI: <https://doi.org/10.3390/nano10081606>. URL: <https://www.mdpi.com/2079-4991/10/8/1606> (visited on 18/04/2024).
- [182] Pallab Barai et al. ‘Oxide-Based Solid-State Batteries: A Perspective on Composite Cathode Architecture’. In: *Nat Energy* (2022). DOI: <https://doi.org/10.1002/aenm.202201939>. URL: <https://onlinelibrary.wiley.com/doi/full/10.1002/aenm.202201939> (visited on 19/05/2024).
- [183] Shaojie Chen et al. ‘Sulfide solid electrolytes for all-solid-state lithium batteries: Structure, conductivity, stability and application’. In: *Energy Storage Materials* 14 (2018), pp. 58–74. ISSN: 2405-8297. DOI: <https://doi.org/10.1016/j.ensm.2018.02.020>. URL: <https://www.sciencedirect.com/science/article/pii/S2405829717306669> (visited on 09/05/2024).
- [184] YG. Lee, S. Fujiki and C. Jung. ‘High-energy long-cycling all-solid-state lithium metal batteries enabled by silver-carbon composite anodes’. In: *Nat Energy* (2020). DOI: <https://doi.org/10.1038/s41560-020-0575-z>. URL: <https://www.nature.com/articles/s41560-020-0575-z> (visited on 08/04/2024).
- [185] Xueying Yang et al. ‘The Critical Role of Fillers in Composite Polymer Electrolytes for Lithium Battery’. In: *Nano-Micro Letters* 75 (2023). DOI: <https://doi.org/10.1007/s40820-023-01051-3>. URL: <https://link.springer.com/article/10.1007/s40820-023-01051-3> (visited on 13/05/2024).
- [186] Duygu Karabelli, Kai Peter Birke and Max Weeber. ‘A Performance and Cost Overview of Selected Solid-State Electrolytes: Race between Polymer Electrolytes and Inorganic

- Sulfide Electrolytes’. In: *Batteries* 7.1 (2021). ISSN: 2313-0105. URL: <https://www.mdpi.com/2313-0105/7/1/18> (visited on 10/05/2024).
- [187] Joon Ching Juan et al. ‘A review of polymer electrolytes: fundamental, approaches and applications’. In: (2016). DOI: <https://doi.org/10.1007/s11581-016-1756-4>. URL: <https://link.springer.com/article/10.1007/s11581-016-1756-4#citeas> (visited on 18/04/2024).
- [188] Mingzhu Liu et al. ‘High-performance solid polymer electrolytes for lithium ion batteries based on sulfobetaine zwitterion and poly (ethylene oxide) modified polysiloxane’. In: *Journal of Alloys and Compounds* 742 (2018), pp. 619–628. ISSN: 0925-8388. DOI: <https://doi.org/10.1016/j.jallcom.2018.01.263>. URL: <https://www.sciencedirect.com/science/article/pii/S0925838818302718> (visited on 13/05/2024).
- [189] Electricity - Magnetism. *Advantages and Disadvantages of Lithium Polymer Batteries*. 2024. URL: <https://www.electricity-magnetism.org/electric-battery/advantages-and-disadvantages-of-lithium-polymer-batteries/> (visited on 24/03/2024).
- [190] K. Daems et al. ‘Advances in inorganic, polymer and composite electrolytes: Mechanisms of Lithium-ion transport and pathways to enhanced performance’. In: *Renewable and Sustainable Energy Reviews* 191 (2024), p. 114136. ISSN: 1364-0321. DOI: <https://doi.org/10.1016/j.rser.2023.114136>. URL: <https://www.sciencedirect.com/science/article/pii/S1364032123009942> (visited on 03/05/2024).
- [191] Yong Guo et al. ‘Solid-state lithium batteries: Safety and prospects’. In: *eScience* 2.2 (2022), pp. 138–163. ISSN: 2667-1417. DOI: <https://doi.org/10.1016/j.esci.2022.02.008>. URL: <https://www.sciencedirect.com/science/article/pii/S2667141722000209> (visited on 03/05/2024).
- [192] Heng Zhang et al. ‘Single lithium-ion conducting solid polymer electrolytes: advances and perspectives’. In: *Chem. Soc. Rev.* 46 (3 2017), pp. 797–815. DOI: 10.1039/C6CS00491A. URL: <http://dx.doi.org/10.1039/C6CS00491A> (visited on 15/04/2024).
- [193] Ziyu Song et al. ‘A reflection on polymer electrolytes for solid-state lithium metal batteries’. In: *Nature Communications* 14 (Aug. 2023). DOI: 10.1038/s41467-023-40609-y. URL: <https://www.nature.com/articles/s41467-023-40609-y>.
- [194] Meihuang Wang et al. ‘Surface positive-charged modification of inorganic fillers to optimize lithium ion conductive pathways in composite polymer electrolytes for lithium-metal batteries’. In: *Journal of Colloid and Interface Science* 630 (2023), pp. 634–644. ISSN: 0021-9797. DOI: <https://doi.org/10.1016/j.jcis.2022.10.137>. URL: <https://www.sciencedirect.com/science/article/pii/S0021979722019087> (visited on 09/05/2024).

- [195] Daxian Cao et al. ‘Processing Strategies to Improve Cell-Level Energy Density of Metal Sulfide Electrolyte-Based All-Solid-State Li Metal Batteries and Beyond’. In: *American Chemical Society* (Oct. 2020). DOI: <https://doi.org/10.1021/acsenergylett.0c01905>. URL: <https://pubs.acs.org/doi/10.1021/acsenergylett.0c01905> (visited on 19/04/2024).
- [196] Taro Inada et al. ‘Fabrications and properties of composite solid-state electrolytes’. In: *Solid State Ionics* 158.3 (2003), pp. 275–280. ISSN: 0167-2738. DOI: [https://doi.org/10.1016/S0167-2738\(02\)00889-5](https://doi.org/10.1016/S0167-2738(02)00889-5). URL: <https://www.sciencedirect.com/science/article/pii/S0167273802008895> (visited on 19/04/2024).
- [197] L. Lu and O. Ishiyama. ‘14 - Iron ore sintering’. In: *Iron Ore*. Ed. by Liming Lu. Woodhead Publishing, 2015, pp. 395–433. ISBN: 978-1-78242-156-6. DOI: <https://doi.org/10.1016/B978-1-78242-156-6.00014-9>. URL: <https://www.sciencedirect.com/science/article/pii/B9781782421566000149> (visited on 20/05/2024).
- [198] Heiner Heimes et al. ‘PRODUCTION OF ALL-SOLID-STATE BATTERY CELLS’. In: (Feb. 2019). URL: https://www.researchgate.net/publication/330902525_PRODUTION_OF_ALL-SOLID-STATE_BATTERY_CELLS (visited on 19/04/2024).
- [199] Zheng Liang et al. ‘Composite lithium metal anode by melt infusion of lithium into a 3D conducting scaffold with lithiophilic coating’. In: (Feb. 2016). DOI: <https://doi.org/10.1073/pnas.1518188113>. URL: <https://www.pnas.org/doi/full/10.1073/pnas.1518188113> (visited on 19/04/2024).
- [200] Lynsey Hart. ‘Sputtering: Process, Types and Uses’. In: (Sept. 2019). URL: <https://nanografi.com/blog/sputtering-process-types-and-uses/> (visited on 17/04/2024).
- [201] Kian Kerman et al. ‘Review—Practical Challenges Hindering the Development of Solid State Li Ion Batteries’. In: *Journal of The Electrochemical Society* 164 (2017). DOI: 10.1149/2.1571707jes. URL: <https://iopscience.iop.org/article/10.1149/2.1571707jes> (visited on 19/04/2024).
- [202] Wentao Yao et al. ‘Design Principle, Optimization Strategies, and Future Perspectives of Anode-Free Configurations for High-Energy Rechargeable Metal Batteries’. In: *Electrochemical Energy Reviews* 4 (July 2021). DOI: 10.1007/s41918-021-00106-6. URL: <https://link.springer.com/article/10.1007/s41918-021-00106-6> (visited on 18/05/2024).
- [203] Xiaofei Yang et al. ‘Recent advances and perspectives on thin electrolytes for high-energy-density solid-state lithium batteries’. In: *Energy & Environmental Science* 14 (2 2021),

- pp. 643–671. DOI: 10.1039/D0EE02714F. URL: <https://pubs.rsc.org/en/content/articlelanding/2021/ee/d0ee02714f> (visited on 19/04/2024).
- [204] K. Hatzell and Y. Zheng. ‘Prospects on large-scale manufacturing of solid state batteries’. In: *MRS Energy & Sustainability* 8 (2021), pp. 33–39. DOI: <https://doi.org/10.1557/s43581-021-00004-w>. URL: <https://link.springer.com/article/10.1557/s43581-021-00004-w> (visited on 19/04/2024).
- [205] Ulrik Grape. ‘Recovery Act – Solid State Batteries for Grid-Scale Energy Storage’. In: (2015). URL: https://www.energy.gov/sites/prod/files/2016/10/f34/Seeo_SolidStateBatteries_FTR_DE-0E0000223_0_April_2015.pdf (visited on 09/05/2024).
- [206] Shuaifeng Lou et al. ‘Interface issues and challenges in all-solid-state batteries: lithium, sodium, and beyond’. In: *Advanced Materials* 33.6 (2021), p. 2000721. DOI: <https://doi.org/10.1002/adma.202000721>. URL: <https://onlinelibrary.wiley.com/doi/full/10.1002/adma.202000721> (visited on 07/05/2024).
- [207] Ann Mari Svensson. *Personal communication*. Apr. 2024.
- [208] Silje Nornes Bryntesen et al. ‘Opportunities for the State-of-the-Art Production of LIB Electrodes—A Review’. In: *Energies* 14.5 (2021). ISSN: 1996-1073. DOI: 10.3390/en14051406. URL: <https://www.mdpi.com/1996-1073/14/5/1406> (visited on 12/04/2024).
- [209] Mihai Duduta et al. ‘Semi-Solid Lithium Rechargeable Flow Battery’. In: *Advanced Energy Materials* 1.4 (2011), pp. 511–516. DOI: <https://doi.org/10.1002/aenm.201100152>. eprint: <https://onlinelibrary.wiley.com/doi/pdf/10.1002/aenm.201100152>. URL: <https://onlinelibrary.wiley.com/doi/abs/10.1002/aenm.201100152> (visited on 15/04/2024).
- [210] Yuzhao Liu et al. ‘Development of quasi-solid-state anode-free high-energy lithium sulfide-based batteries’. In: *Nature Communications* 13 (July 2022). DOI: <https://doi.org/10.1038/s41467-022-32031-7>. URL: <https://www.nature.com/articles/s41467-022-32031-7> (visited on 26/04/2024).
- [211] Wookil Chae et al. ‘A Brief Review of Gel Polymer Electrolytes Using In Situ Polymerization for Lithium-ion Polymer Batteries’. In: *Polymers* 15.4 (2023). ISSN: 2073-4360. DOI: 10.3390/polym15040803. URL: <https://www.mdpi.com/2073-4360/15/4/803> (visited on 03/05/2024).
- [212] Jiajia Li et al. ‘Recent applications of ionic liquids in quasi-solid-state lithium metal batteries’. In: *Green Chemical Engineering* 2.3 (2021), pp. 253–265. ISSN: 2666-9528. DOI: <https://doi.org/10.1016/j.gce.2021.03.001>. URL: <https://www.sciencedirect.com/science/article/pii/S2666952821000169> (visited on 08/04/2024).

- [213] Minghua Chen et al. ‘Effectively Elevating Ceramic Fillers’ Dispersity in Gel Hybrid Electrolyte through Bridge-Linked Construction for High-Performance Lithium Metal Batteries’. In: *Batteries* 9.5 (2023). ISSN: 2313-0105. DOI: 10.3390/batteries9050270. URL: <https://www.mdpi.com/2313-0105/9/5/270> (visited on 14/05/2024).
- [214] Jiahua Ou, Gaoran Li and Zhongwei Chen. ‘Improved composite solid electrolyte through ionic liquid-assisted polymer phase for solid-state lithium ion batteries’. In: *Journal of the Electrochemical Society* 166.10 (2019). Cited by: 19, A1785–A1792. DOI: 10.1149/2.0401910jes. URL: <https://www.scopus.com/inward/record.uri?eid=2-s2.0-85073200621&doi=10.1149%2f2.0401910jes&partnerID=40&md5=a9e857395dd36c9c72ea7cc78d991cb8> (visited on 09/04/2024).
- [215] Jan-Paul Brinkmann et al. ‘Ceramic-in-Polymer Hybrid Electrolytes with Enhanced Electrochemical Performance’. In: *ACS Applied Materials & Interfaces* (2022). DOI: 10.1021/acsmi.2c13408. URL: <https://pubmed.ncbi.nlm.nih.gov/36409931/> (visited on 08/05/2024).
- [216] David Ayme-Perrot et al. ‘NMR Study of Lithium Transport in Liquid-Ceramic Hybrid Solid Composite Electrolytes’. In: *ACS Applied Materials & Interfaces* (2022). URL: <https://pubs.acs.org/doi/10.1021/acsmi.2c10666> (visited on 08/05/2024).
- [217] Jarosław Syzdek et al. ‘Ceramic-in-polymer versus polymer-in-ceramic polymeric electrolytes—A novel approach’. In: *Journal of Power Sources* 194.1 (2009), pp. 66–72. ISSN: 0378-7753. DOI: <https://doi.org/10.1016/j.jpowsour.2009.01.070>. URL: <https://www.sciencedirect.com/science/article/pii/S0378775309001748> (visited on 08/05/2024).
- [218] A. Basille, A. Bhatt and A. O’Mullane. ‘Stabilizing lithium metal using ionic liquids for long-lived batteries’. In: *Nat Commun* 7 (2016). DOI: <https://doi.org/10.1038/ncomms11794>. URL: <https://www.nature.com/articles/ncomms11794> (visited on 08/04/2024).
- [219] W. Li, E.M. Erickson and A. Manthiram. ‘High-nickel layered oxide cathodes for lithium-based automotive batteries’. In: *Nat Energy* 5 (2020), pp. 26–34. ISSN: 2214-9937. DOI: <https://doi.org/10.1038/s41560-019-0513-0>. URL: <https://www.nature.com/articles/s41560-019-0513-0> (visited on 30/04/2024).
- [220] BloombergNEF. ‘Lithium-Ion Battery Pack Prices Hit Record Low of \$139/kWh’. In: (26th Nov. 2023). URL: <https://about.bnef.com/blog/lithium-ion-battery-pack-prices-hit-record-low-of-139-kwh/> (visited on 03/05/2024).
- [221] Richard Schmuch et al. ‘Performance and cost of materials for lithium-based rechargeable automotive batteries’. In: *Nature Energy* (2018), pp. 267–278. DOI: <https://doi.org/10.1038/s41560-018-0513-0>

- 0.1038/s41560-018-0107-2. URL: <https://www.nature.com/articles/s41467-022-32031-7> (visited on 25/04/2024).
- [222] T. Hetteshheimer et al. ‘Lithium-Ion Battery Roadmap - Industrialization Perspectives toward 2030’. In: (2023). DOI: 10.24406/publica-2153. URL: https://www.isi.fraunhofer.de/content/dam/isi/dokumente/cct/2023/Fraunhofer-ISI_LIB-Roadmap-2023.pdf (visited on 06/05/2024).
- [223] Ghassan Zubi et al. ‘The lithium-ion battery: State of the art and future perspectives’. In: *Renewable and Sustainable Energy Reviews* 89 (2018), pp. 292–308. ISSN: 1364-0321. DOI: <https://doi.org/10.1016/j.rser.2018.03.002>. URL: <https://www.sciencedirect.com/science/article/pii/S1364032118300728> (visited on 15/04/2024).
- [224] A. Snowdon N. and Rai et al. *Battery Metals Watch: The end of the beginning.* 2022. URL: <https://www.goldmansachs.com/intelligence/pages/gs-research/battery-metals-watch-the-end-of-the-beginning/report.pdf> (visited on 25/04/2024).
- [225] IEA. *Global EV Outlook 2024*. 2024. URL: <https://www.iea.org/reports/global-ev-outlook-2024> (visited on 23/02/2024).
- [226] ‘Time for lithium-ion alternatives’. In: *Nat Energy* 7 (2022). DOI: <https://doi.org/10.1038/s41560-022-01073-y>. URL: <https://www.nature.com/articles/s41560-022-01073-y> (visited on 01/05/2024).
- [227] Steven Lee and Arumugam Manthiram. ‘Can Cobalt Be Eliminated from Lithium-Ion Batteries?’ In: *ACS Energy Letters* 7.9 (2022), pp. 3058–3063. DOI: 10.1021/acsenenergylett.2c01553. URL: <https://pubs.acs.org/doi/full/10.1021/acsenenergylett.2c01553> (visited on 01/05/2024).
- [228] U.S. Geological Survey. ‘Graphite (Natural)’. In: (2021). URL: <https://pubs.usgs.gov/periodicals/mcs2021/mcs2021-graphite.pdf> (visited on 01/05/2024).
- [229] John F. Slack, Bryn E. Kimball and Kim B. Shedd. ‘Cobalt’. In: *Critical mineral resources of the United States—Economic and environmental geology and prospects for future supply: U.S. Geological Survey Professional Paper 1802* (2017), F1–F40. DOI: <https://doi.org/10.3133/pp1802F>. URL: <https://pubs.usgs.gov/publication/pp1802F> (visited on 01/05/2024).
- [230] Nelson Bunyui Manjong et al. ‘A comparative assessment of value chain criticality of lithium-ion battery cells’. In: *Sustainable Materials and Technologies* 36 (2023), e00614. ISSN: 2214-9937. DOI: <https://doi.org/10.1016/j.susmat.2023.e00614>. URL: <https://www.sciencedirect.com/science/article/pii/S2214993723000490> (visited on 06/05/2024).

- [231] Shirin S. Zadeh Fei Meng James McNeice and Ahmad Ghahreman. ‘Review of Lithium Production and Recovery from Minerals, Brines, and Lithium-Ion Batteries’. In: *Mineral Processing and Extractive Metallurgy Review* 42.2 (2021), pp. 123–141. DOI: 10.1080/08827508.2019.1668387. eprint: <https://doi.org/10.1080/08827508.2019.1668387>. URL: <https://doi.org/10.1080/08827508.2019.1668387> (visited on 06/05/2024).
- [232] Youping Miao et al. ‘An overview of global power lithium-ion batteries and associated critical metal recycling’. In: *Journal of Hazardous Materials* 425 (2022), p. 127900. ISSN: 0304-3894. DOI: <https://doi.org/10.1016/j.jhazmat.2021.127900>. URL: <https://www.sciencedirect.com/science/article/pii/S0304389421028697> (visited on 01/05/2024).
- [233] Dana L. Thompson et al. ‘The importance of design in lithium ion battery recycling – a critical review’. In: *The Royal Society of Chemistry* 22 (2020), pp. 7585–7603. DOI: 10.1039/D0GC02745F. URL: <https://pubs.rsc.org/en/content/articlehtml/2020/gc/d0gc02745f> (visited on 02/05/2024).
- [234] Krystyna Giza, Beata Pospiech and Jerzy Gęga. ‘Future Technologies for Recycling Spent Lithium-Ion Batteries (LIBs) from Electric Vehicles—Overview of Latest Trends and Challenges’. In: *Energies* 16.15 (2023). ISSN: 1996-1073. DOI: 10.3390/en16155777. URL: <https://www.mdpi.com/1996-1073/16/15/5777> (visited on 02/05/2024).
- [235] Zachary J. Baum et al. ‘Lithium-Ion Battery Recycling-Overview of Techniques and Trends’. In: *ACS Energy Letters* 7.2 (2022), pp. 712–719. DOI: 10.1021/acsenergylett.1c02602. URL: <https://pubs.acs.org/doi/full/10.1021/acsenergylett.1c02602> (visited on 01/05/2024).
- [236] Jiangfeng Mao et al. ‘Toward practical lithium-ion battery recycling: adding value, tackling circularity and recycling-oriented design’. In: *Energy & Environmental Science* 15 (2022), pp. 2732–2752. DOI: 10.1039/D2EE00162D. URL: <https://pubs.rsc.org/en/content/articlehtml/2022/ee/d2ee00162d> (visited on 02/05/2024).
- [237] Bin Huang et al. ‘Recycling of lithium-ion batteries: Recent advances and perspectives’. In: *Journal of Power Sources* 399 (2018), pp. 274–286. ISSN: 0378-7753. DOI: <https://doi.org/10.1016/j.jpowsour.2018.07.116>. URL: <https://www.sciencedirect.com/science/article/pii/S0378775318308498> (visited on 01/05/2024).
- [238] Wędrychowicz M et al. ‘Recovery of Non-Ferrous Metals from PCBs Scrap by Liquefaction from Lead’. In: *Materials (Basel)* (Mar. 2022). DOI: 10.3390/ma15062089. URL: <https://www.ncbi.nlm.nih.gov/pmc/articles/PMC8953818/> (visited on 02/05/2024).

- [239] H. Rallo et al. 'Battery dismantling centre in Europe: A centralized vs decentralized analysis'. In: *Resources, Conservation & Recycling Advances* 15 (2022), p. 200087. ISSN: 2667-3789. DOI: <https://doi.org/10.1016/j.rcradv.2022.200087>. URL: <https://www.sciencedirect.com/science/article/pii/S2667378922000256> (visited on 01/05/2024).
- [240] Xin Sun et al. 'Life cycle assessment of lithium nickel cobalt manganese oxide (NCM) batteries for electric passenger vehicles'. In: *Journal of Cleaner Production* 273 (2020), p. 123006. ISSN: 0959-6526. DOI: <https://doi.org/10.1016/j.jclepro.2020.123006>. URL: <https://www.sciencedirect.com/science/article/pii/S0959652620330511> (visited on 01/05/2024).
- [241] David da Silva Vasconcelos et al. 'Circular Recycling Strategies for LFP Batteries: A Review Focusing on Hydrometallurgy Sustainable Processing'. In: *Metals* 13.3 (2023). ISSN: 2075-4701. DOI: [10.3390/met13030543](https://doi.org/10.3390/met13030543). URL: <https://www.mdpi.com/2075-4701/13/3/543> (visited on 18/05/2024).

A KI deklarasjon

Deklarasjon om KI-hjelpemidler

Har det i utarbeidingen av denne rapporten blitt anvendt KI-baserte hjelpemidler?

Nei

Ja

Hvis ja: spesifiser type av verktøy og bruksområde under.

Tekst

Stavekontroll. Er deler av teksten kontrollert av:
Grammarly, Ginger, Grammarbot, LanguageTool, ProWritingAid, Sapling, Trinkai.ai eller lignende verktøy?

Tekstgenerering. Er deler av teksten generert av:
ChatGPT, GrammarlyGO, Copy.AI, WordAi, WriteSonic, Jasper, Simplified, Rytr eller lignende verktøy?

Skriveassistanse. Er en eller flere av ideene eller fremgangsmåtene i oppgaven foreslått av:
ChatGPT, Google Bard, Bing chat, YouChat eller lignende verktøy?

Hvis ja til anvendelse av et tekstverktøy - spesifiser bruken her:

Grammarly, chatGPT, Builbot og DeepL er brukt som stavekontroll og for å finne synonymer. Elicit er brukt som søkemonitor

Kode og algoritmer

Programmeringsassistanse. Er deler av koden/algoritmene som i) fremtrer direkte i rapporten eller ii) har blitt anvendt for produksjon av resultater slik som figurer, tabeller eller tallverdier blitt generert av: *GitHub Copilot, CodeGPT, Google Codey/Studio Bot, Replit Ghostwriter, Amazon CodeWhisperer, GPT Engineer, ChatGPT, Google Bard* eller lignende verktøy?

Hvis ja til anvendelse av et programmeringsverktøy - spesifiser bruken her:

Bilder og figurer

Bildegenerering. Er ett eller flere av bildene/figurene i rapporten blitt generert av:
Hvis ja til anvendelse av et bildeverktøy, spesifiser bruken her:

Andre KI verktøy. har andre typer av verktøy blitt anvendt? Hvis ja spesifiser bruken her:

Jeg er kjent med NTNUs regelverk: *Det er ikke tillatt å generere besvarelse ved hjelp av kunstig intelligens og levere den helt eller delvis som egen besvarelse.* Jeg har derfor redegjort for all anvendelse av kunstig intelligens enten i) direkte i rapporten eller ii) i dette skjemaet

Underskrift/ Dato/ Sted

Amin Babiker, Eiv Høynd, Maja Færøed Reknes, Magnus Vøllea / 22.05.24 / NTNU Gløshaugen